Ph.D. Dissertation

"INCREASING RENEWABLE ENERGY POTENTIAL OF LANDFILL GAS
BY ELECTROCATALYTIC CONVERSION OF CARBON DIOXIDE TO METHANE AT
LOW TEMPERATURE."

By

ASMA AKTER RONY

To be presented to the Faculty of the Graduate School of

The University of Texas at Arlington in Partial Fulfillment

of the Requirements

for the Degree of

DOCTOR OF PHILOSOPHY

THE UNIVERSITY OF TEXAS AT ARLINGTON

December 2023

Acknowledgments

Table of Contents

List of Tables

List of Figures

Increasing Renewable Energy Potential of Landfill Gas by Electrocatalytic Conversion of Carbon Dioxide to Methane at Low Temperature

Asma Akter Rony, Dr. Melanie L. Sattler, The University of Texas at Arlington

Abstract**:**

The conversion of carbon dioxide into methane at a low temperature has great potential to reduce current international environmental issues like global warming and will create new sources of renewable energy. The overall goal of this research is to increase renewable energy production from landfill gas using an unconventional process – electrocatalytic methanation of carbon dioxide – which has not been implemented for landfill gas yet. The electrocatalytic methanation follows the Waseda process, which applies an electric field in the presence of a Ruthenium-supported cerium oxide (CeO_2) catalyst. The specific objectives of this research were:

1. To explore the impact of independent variables (time, power, heat application, catalyst preparation method, electric field type, degradation of catalyst over time, performance of reactivated used catalyst) on the conversion of carbon dioxide (CO_2) to methane (CH_4) using synthetic landfill gas, as well as test the process at room temperature.

2. To test the Waseda method on real landfill gas, using the values of Objective 1 that showed maximum CO_2 to CH_4 conversion, and

3. To conduct a life cycle environmental and cost analysis for the conversion of CO_2 in landfill gas to CH_4, using the Waseda process.

Ruthenium-supported cerium oxide (CeO_2) catalyst was prepared by the impregnation method. Landfill gas, hydrogen gas, and argon gas were passed through the catalyst bed in a quartz glass tube in a ratio of 1: 1.09: 1.87, with an electric field imposed by two copper electrodes.

Experiments were conducted to vary the parameters listed in Obj. 1. During the experiment for Objective 2, 54.53 W was applied to impose a strong electric field in the presence of 0.33 gm of catalyst evenly spread on the catalyst bed. A life cycle environmental analysis was conducted using Sustainable Minds software (ISO 14025) to estimate the total environmental impact and carbon footprint by life cycle stages of the process, including raw materials acquisition, use, transportation, and end of life. A life cycle cost analysis using present worth and a 2% interest rate was done for a 20-year lifetime [Macrotrend, 2020].

The methane concentration increased by 34. 5% in the presence of the catalyst and electric field (199.9V and 0.183A) in the baseline experiment over the initial measured methane concentration of the inlet (sample) gas. The impact of different power (25 V to 240 V) was analyzed, and the maximum wattage applied for this experiment was 54.53 W, which increased methane conversion 3% over the baseline experiment. However, applied heat in the presence of the EF did not improve the methane conversion. The method of catalyst preparation did not impact the conversion significantly. Using a non-uniform electric field reduced the conversion compared to a uniform electric field.

For Objective 2, it was found that electrocatalysis increased the methane fraction of real landfill gas by up to 43% compared to the initial inlet gas composition measured.

The overall environmental impact of the lab-scale Waseda process is -51.5 mPts and -20.4 kg CO_2-equivalents per kg of methane generated. A millipoint (mPt) is 1 1/1000th of the annual environmental load (i.e. entire production/consumption activities in the economy) that one person in the US produces. In Sustainable Minds, this assumes that hydropower (the form of renewable energy with the lowest environmental impact and CO_2 footprint in Sustainable Minds) is used to

provide electricity needed for the Waseda process, and that the methane generated is used to generate power that replaces power from the standard US grid. Using the lab-scale apparatus, this assumption is necessary for the process to yield environmental benefits. An industrial-scale version of the equipment would have lesser environmental and CO_2 impact per kg of methane generated, due to efficiencies of scale.

The total cost of the process was estimated to be \$13.99/kg of methane. The cost of producing 1 kWh of electrical energy from the methane generated was estimated to be \$3.21. This cost would be reduced considerably if the small lab-scale apparatus were scaled up to commercial size.

Chapter 1
Introduction

1.1 The need for alternatives to fossil natural gas

After serving for 4.5 billion years, the world's dry natural gas reserve is running out of stock. The world's remaining proven dry natural gas reserve is 6923 trillion cubic feet (Tcf) and will last for 52 years if the current consumption rate (48 cubic feet per capita per day) does not change and no more new sources are found [Worldometers, 2017]. Figure 1.1 below shows the world's natural gas consumption in Million Cubic Feet (MMcf) over time. The world's population is growing at a rate of 1.12 % and that is leading to a higher consumption rate of natural dry gas reserves [Worldometers, 2017].
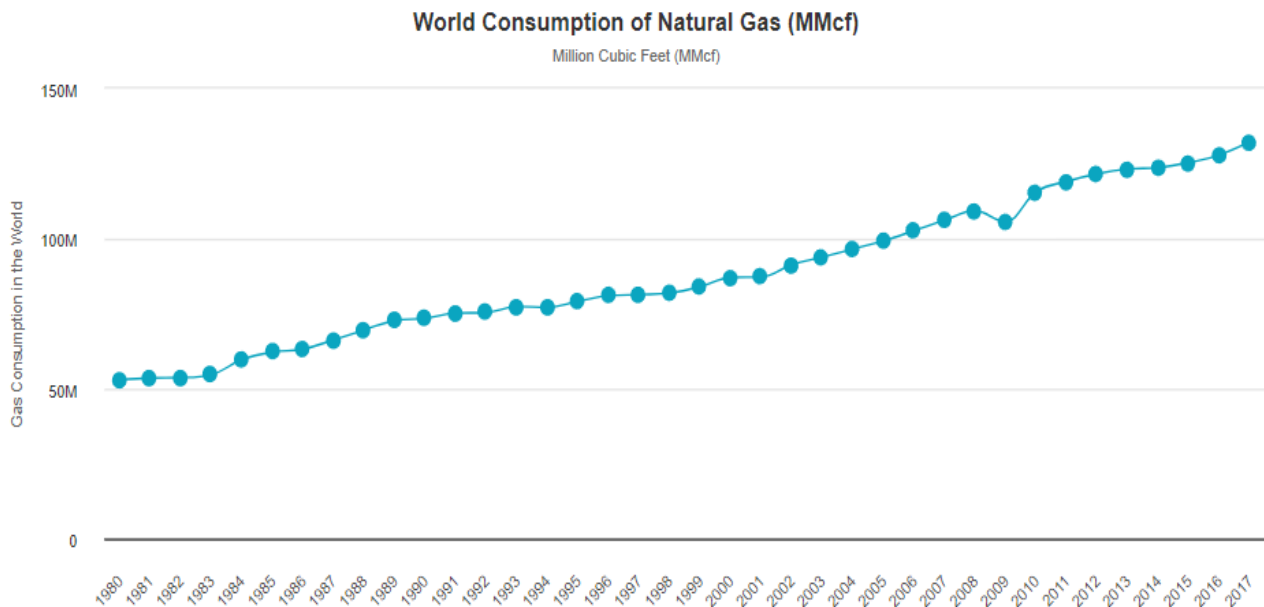
Figure 1.1: History of World's Natural Gas Consumption [Worldometers, 2017]

The United States ranks 4th position in terms of natural gas reserves and owns 5.3% of the total gas reserve of the world. The total proven US natural gas reserve is 34.52 Tcf, which is anticipated to last almost 83 years based on the current per capita consumption rate [EIA, 2023].

Table 1-1: U.S. proven reserves of crude oil, crude oil and lease condensate, and total natural gas [EIA, 2020-21].

	Crude oil billion barrels	Crude oil and lease condensate billion barrels	Total natural gas trillion cubic feet
U.S. proved reserves as of December 31, 2021	35.8	38.2	473.3
Extensions and discoveries	5.7	6.3	67.6
Net revisions	1.6	2.3	100.0
Net adjustments, sales, and acquisitions	1.8	1.8	22.6
Estimated production	-3.8	-4.1	-38.1
Net additions to U.S. proved reserves	5.3	6.2	152.1
U.S. proved reserves as of December 31, 2021	41.2	44.4	625.4
Percentage change in U.S. proved reserves	14.8%	16.2%	32.1%

Figure 1.2: U.S. proven reserves of crude oil, crude oil and lease condensate, and total natural gas [EIA, 2020-21]

There is a large volume of unproven natural gas reserves which are also called technically recoverable resources (TRR), that could possibly be producible in the future. The existing exploration and production technologies can be used to increase the amount of natural dry gas reserves. However, the unknown locations of those TRRs make any future extraction very uncertain and time-consuming. The world has 52 years left to find new alternatives to natural gas

to continue the smooth use of natural gas. The rising price of gas indicates that it is time to reduce the speed of consumption of our natural resources.

1.2 Landfills: a source of renewable biogas/methane

Various sources of renewable natural gas can replace the dwindling reserves of fossil natural gas. One such source of renewable natural gas/biogas is landfills. A landfill (schematic shown in Figure 1.3) is a waste repository specially designed by engineers, where all the environmental impacts of open waste disposal have been addressed. This modern way of disposing of waste can reduce air, water, and soil pollution from Volatile Organic Compounds (VOCs), including phenols and solvents, and heavy metals. Among different types of landfills, Municipal Solid Waste Landfills (MSWLFs) are designed to receive and treat non-hazardous such as household and/ or commercial solid waste, nonhazardous sludge, conditionally exempt small quantity generator waste, and industrial nonhazardous solid waste [U.S. EPA, 2023]. Anaerobic (without oxygen) and some aerobic (in the presence of oxygen) biodegradation of organic waste in landfills is a source of greenhouse gas emissions into the environment.
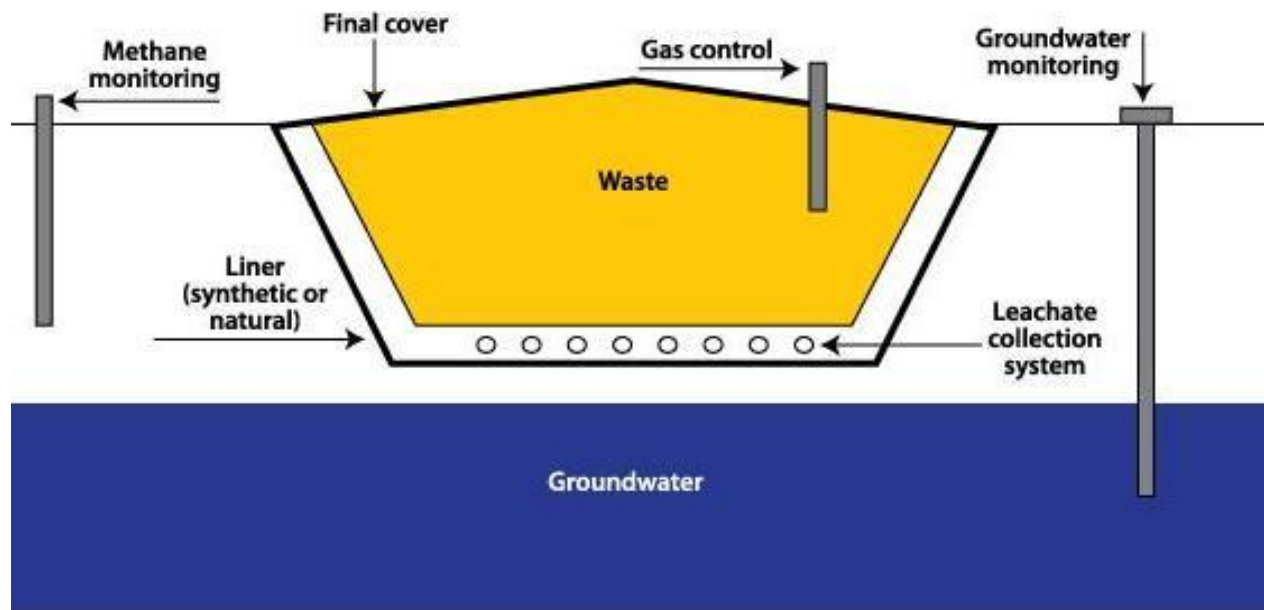
Figure 1.3: Schematic of a landfill

Landfill gas is composed of around 40 to 60% methane and 40 to 60% carbon dioxide According to EPA (2020) shown in Figure 1.4 below, MSWLFs are the third largest human-related source of methane emissions, accounting for 14.5% of the total methane emissions in the US. Landfill gas also contains a few more gases (e.g., nitrogen, oxygen, ammonia, sulfides, hydrogen, and other gases) but the total amount of other gases is less than 1%.
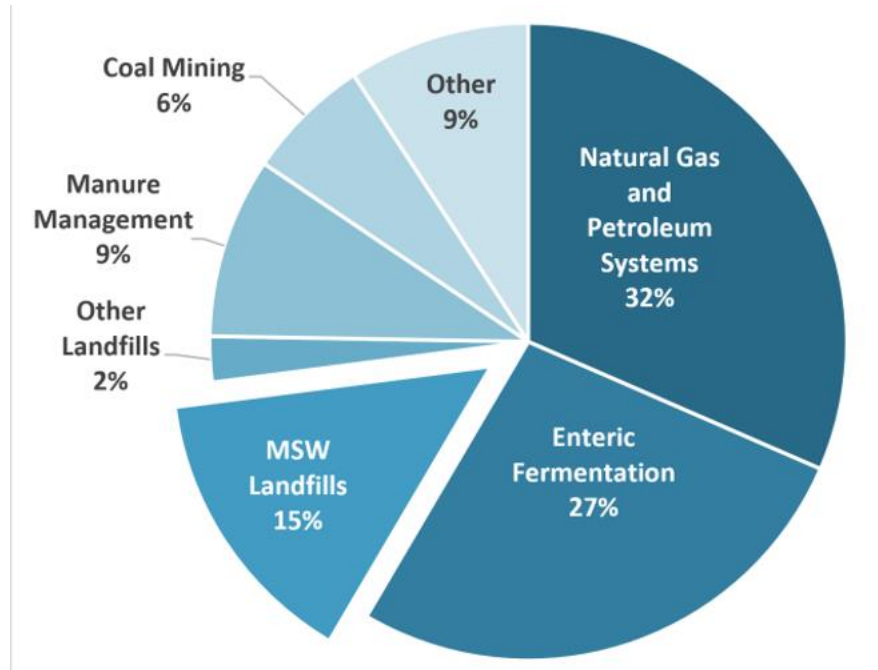
Figure 1.4: U.S Methane Emissions by Source [U.S. EPA, 2020]

Methane, which is the largest constituent of natural gas and a major constituent of landfill gas as well, can be burned as a renewable fuel for ovens, turbines, automobiles, kilns, and more. The energy content of landfill gas could be increased by converting the carbon dioxide gas into methane as well.

1.3 Importance of capturing and using methane from landfills

There are a few gases that can trap heat in the atmosphere and eventually cause an increase in the overall temperature. These are called greenhouse gases because they absorb radiant energy that would be emitted out to space, and instead reemit it toward the earth's surface, as shown in Fig. 1.5. Water vapor (H_2O), carbon dioxide (CO_2), methane (CH_4), ozone (O_3), and nitrous oxide (N_2O) are the primary greenhouse gases. They are naturally occurring in the atmosphere and cause

a natural greenhouse effect, without which the Earth's average temperature would be almost 58°F less than the current average if there were no greenhouse gases [NASA, 2023].

The problem has been that due primarily to burning of fossil fuels, the level of greenhouse gases in the atmosphere is far above naturally occurring levels, trapping additional heat. Because of the rising temperature of Earth's surface and atmosphere, the globe is already having measurable effects like water shortages, increased fire threats, drought, weed and pest invasions, intense storm damage and salt invasion, and many more. Methane is a more potent greenhouse gas than carbon dioxide, with the ability to capture 28-36 times the amount of heat ver. Hence, capturing and using the methane generated by landfills is critically important, so that it does not exacerbate climate change.
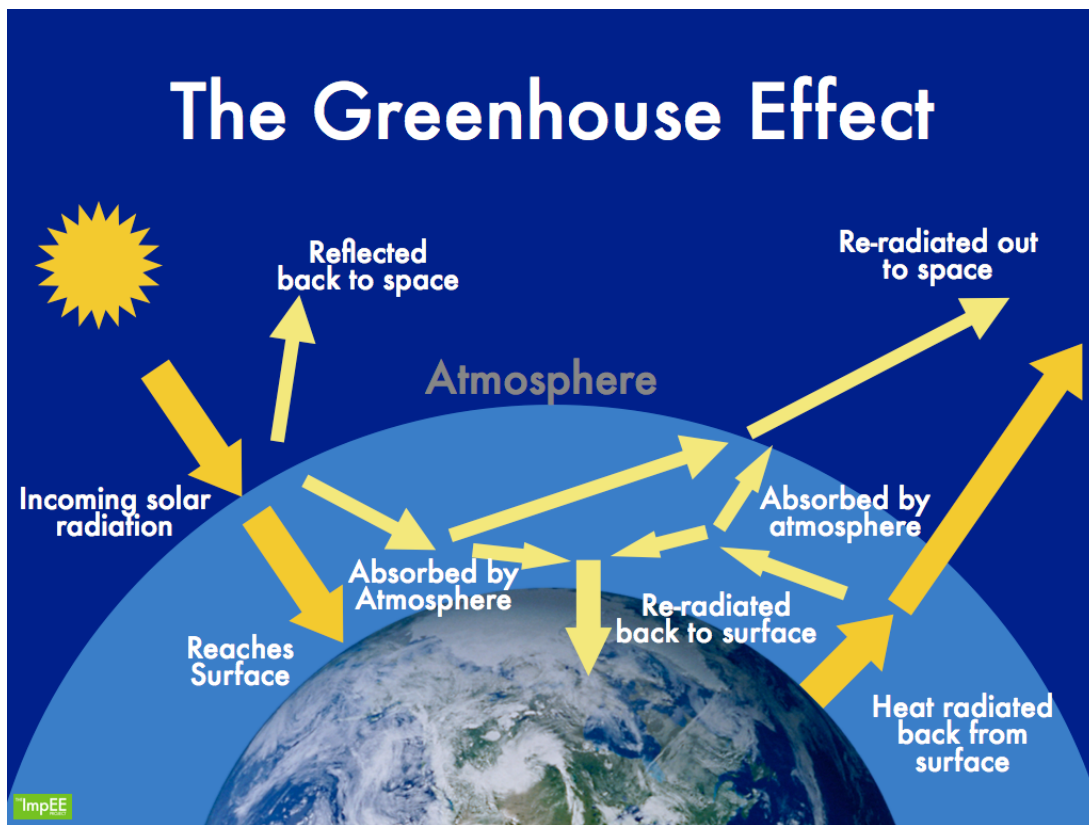
Figure 1.5: The Greenhouse Effect [Environment clean generations, 2011]

1.4 Increasing renewable energy from landfills by converting carbon dioxide to methane

Converting carbon dioxide emitted from landfills into methane will create more renewable fuel and decrease the pressure of using fossil natural gas as fuel. Typical conversion of carbon dioxide to methane requires a high temperature of 300°C to 400°C and a high pressure (3Mpa for an optimal conversion). The process is called Sabatier reaction, or Sabatier process, where a nickel catalyst is used, as shown in Eq. 1. Providing temperatures of 400°C requires fuel, which counters the purpose of creating methane as fuel, and is costly.

$$CO_2 + 4\,H_2 \xrightarrow[\text{Pressure + Catalyst}]{400°C} CH_4 + 2\,H_2O \qquad \Delta H = 165.0 \text{ kJ/mol} \text{ --------(1)}$$
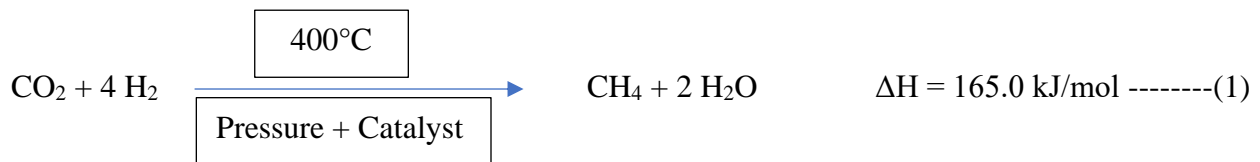
Catalytic methanation of carbon dioxide at a low temperature is challenging. However, breaking the C-O bond and hydrogenation can be done in the presence of an electric field and metal catalysts at a low temperature and room pressure.

An improvement on the Sabatier process was developed by a team of Waseda University scientists in February 2020, by applying an electric field to provide energy for the reaction to occur at low temperature (Yamada, 2020). If the application of the electric field was powered by renewable energy (e.g., solar, wind, or hydropower), there would be no fossil fuel energy consumption. The advantage of using renewable energy to convert carbon dioxide to methane, overusing renewable energy directly, is that methane, the main constituent of natural gas, can similarly be used in natural-gas powered vehicles and appliances.

This low temperature methanation process could be applied to increase the methane content of landfill gas and anaerobic digester gas. Research is needed to analyze the impact of process

variables such as time, power, temperature, catalyst preparation method, electric field type, degradation of catalyst over time, performance of reactivated used catalyst.

1.5 Overall goal of research and objectives

The overall goal of this research is to increase renewable energy production from landfills by converting carbon dioxide in landfill gas to methane using a low-temperature Waseda process. Specific objectives of this research are:

1. Explore the impact of independent variables (time, power, temperature, catalyst preparation method, electric field's type, degradation of catalyst over time, performance of reactivated used catalyst) of the Waseda process on the conversion of carbon dioxide in synthetic landfill gas to methane. Determine reaction rate and methane percent before and after the reaction. Also, test the process at room temperature.

2. Using the best values of process variables determined in Obj. 1, test the Waseda process with real landfill gas.

3. Conduct an energy balance and life cycle environmental and economic analyses of the Waseda process.

1.6 Organization of Dissertation

The rest of the dissertation is organized into a series of five chapters followed by appendices.

Chapter 2 presents a literature review of carbon dioxide conversion into different potential sources of energy e.g., methane, methanol, and carbon monoxide. This chapter also will discuss available data resources.

Chapter 3 illustrates the project methodology. This section includes the experimental design of a lab based electrocatalytic hydrogenation of carbon dioxide. Also, it summarizes the measurement methods including units being used. It gives an idea of how the data were prepared, reported, and analyzed.

Chapter 4 discusses in detail the experimental results of all three objectives obtained and compares them with the existing literature.

Chapter 5 summarizes the main conclusions from the current research work and provides some recommendations for future direction of study.

The appendices include raw data table, graphs, and output files of statistical analysis.

Chapter 2
Literature Review

This chapter provides more information concerning landfills as a source of biogas for renewable energy, methods to increase carbon dioxide conversion to fuel (such as methane), and climate change and the importance of capturing methane from landfills.

2.1 Waste Management Methods and Production of Biogas for Renewable Energy:

2.1.1 Background

Sustainable solid waste management and engineering studies analyze and enable several ways of managing solid waste without compromising the needs of future generations. However, the scenario of solid waste disposal was not always pleasing. People in Athens used to take their household waste to a nearby disposal

Figure 2.1: Unplanned waste dumpsite

area in around 5000 B.C. but there were no proper waste dumping guidelines. Thousands of years passed without any proper method of dealing with human-made waste. The first garbage collection system was started in the Roman Empire, when the waste was simply dumped in a large pit and forgotten, and it led to a major issue by the 1700s. The gas produced from the biodegradation of organic waste, chemicals, non-biodegradable portion of the wastes, and the produced leachate

contaminated all the forms of our environment. Ground water, lakes, seas, air, soil, wildlife, and agriculture started the journey of being polluted.

The 'age of sanitation' started in the early 1800s; however, the idea of modern waste management emerged after 1890s. In the beginning of 20th century, almost all the cities of the United States offered garbage collection system. Landfills and incinerators were introduced to dispose of household waste. Water and ocean dumping were common, too. The rise of the chemical age, explosions in population growth, and increasing appetites have increased waste production rates, waste types and contaminants significantly over the decade. Although landfills are a popular waste disposal system, they still can impair the environment by polluting the groundwater and the air: landfill liners and covers are not 100% efficient, and some water and air pollutants are still emitted. Modern engineers are innovating advanced technologies to mitigate the overall environmental pollution with advanced gas and leachate collection systems.

Recently, engineers have updated the basic design of a landfill by adding synthetic polyethylene as a landfill liner and cover component. As a liner it helps to prevent leachate from seeping into the soil and groundwater, while as a cover component, it helps to reduce the amount of water that gets into the landfill and prevents waste from being exposed to the air and prevents methane from leaking to the atmosphere. Polyethylene is a versatile material that is flexible, strong, highly dense, impermeable, and resistant to corrosion making it a better choice for using in landfills. It also traps produced Greenhouse Gases (GHG) inside the landfill, so the gas does not pollute the air. On the other hand, the captured gas can be collected and used as a renewable energy source. The proportion of waste type (paper, food, plastics, sludge, etc.) plays a very crucial role in the gas production rate and concentration of certain gases.

2.1.2 Composition of waste in landfills in the US

Municipal Solid Waste Management is a priority for local governments, the State, and the country itself. This management includes several methods such as: waste reduction by recycling/reusing and composting with/without energy recovery, and landfilling. Some methods are more environmentally beneficial than others. The effectiveness and the method of MSW management depend on the total waste production and composition of the waste stream in a certain area. The total solid waste generation and per capita waste generation in the United States have an increasing trend since 1960. The total solid waste generated from the United States municipality in 2018 was 292.4 million U.S. short tons reported by the U.S. EPA in 2018 shown in Figure 2.2 below.
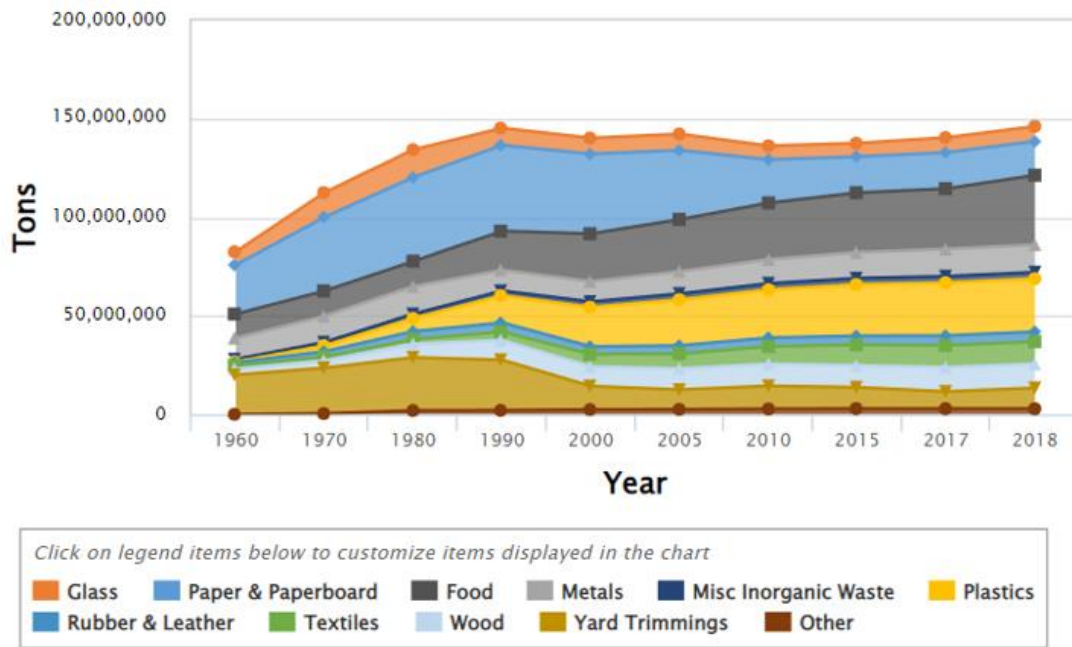
Figure 2.2: Total Solid Waste Generation in the US (1960 to 2018) [U.S. EPA, 2018]

More than 50% of the total solid waste generated (146 million tons) was landfilled that includes organic waste (food, paper, plastics, wood, rubber, textiles), inorganic wastes, glass, metals, and some miscellaneous waste. The highest percentage of categorized waste generated in 2018 was paper and paperboard and accounted for 23.1%. Food waste comprised another significant category with 21.6%. Along with other organic waste (Only the organic wastes produce CO2 and methane), food and paper waste escalate the methane generation during the biodegradation process in the landfill [U.S. EPA, 2018]. Figure 2.3 below represents the total solid waste landfilled in the United States by material in 2018.
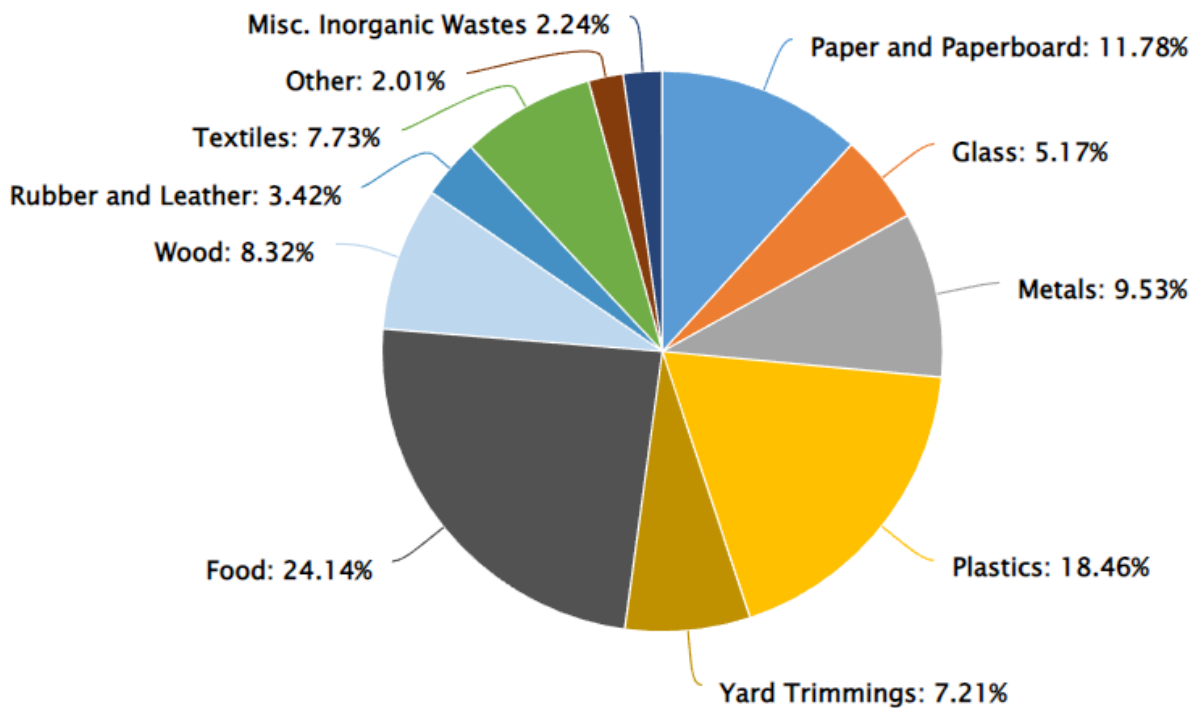
Figure 2.3: Total MSW Landfill by Material [U.S. EPA, 2018].

2.1.3 Gas generation in a landfill over time

Figure: 2.6 included below shows the methane and carbon dioxide production over time in a landfill. The x-axis of the graph represents time, measured in days, and the y-axis represents the amount of gas generated, measured in liters per dry kg-yr.

At the beginning of the graph methane production is quite low and carbon dioxide is high, as the waste is still fresh and has not decomposed much yet. Also, oxygen is present. Over time, the process becomes anaerobic (no oxygen) that is a necessary condition for methanogens to populate and produce methane. The production of both methane and carbon dioxide increases over time as the waste continues to break down and decompose. As the graph progresses, the production of methane overtakes carbon dioxide production, reaching a peak at around 69 days after the waste was deposited in the landfill. After this point, the production of both gases will gradually decline. Overall, Figure: 2.4 is an important tool for understanding the long-term effects of landfills on the environment, and for developing strategies to manage their impact.
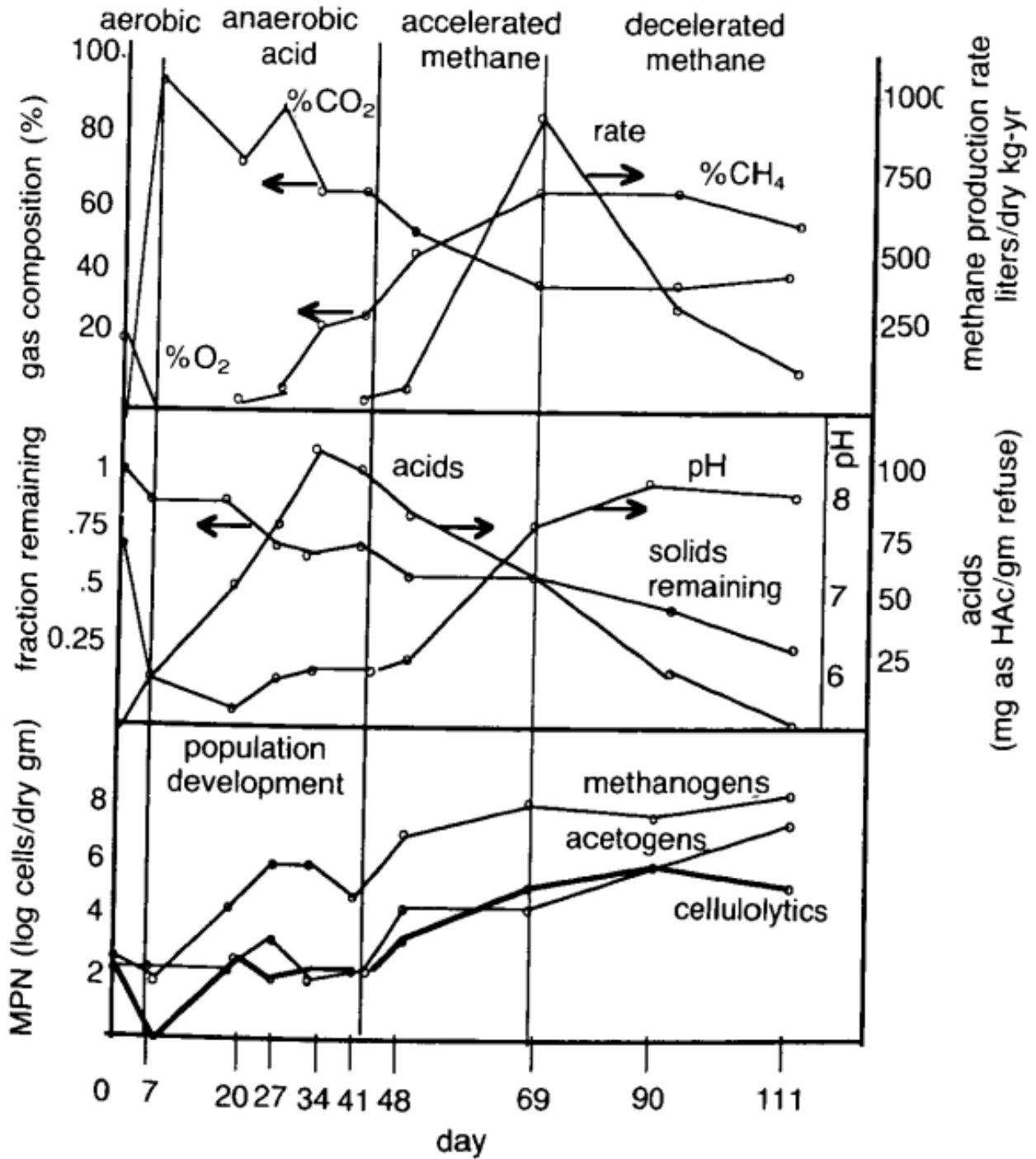
Figure 2.4: Anaerobic digestion process: waste decomposition, gas generation, and microorganism formation over time.

2.1.4 Anaerobic Digesters

An anaerobic digester is a technology used for organic waste management and the production of biogas. It works by breaking down organic matter such as food waste, agricultural waste, or sewage sludge in the absence of oxygen. This process creates biogas which is a mixture of methane and carbon dioxide that can be used as a source of renewable energy as shown in Figure 2.5 below. Anaerobic digestion reduces the amount of waste sent to landfills, decreases greenhouse gas emissions, and generates a nutrient-rich byproduct that can be used as fertilizer. This Electrocatalysis could be used in anaerobic digester gas to convert carbon dioxide into methane in higher composition.
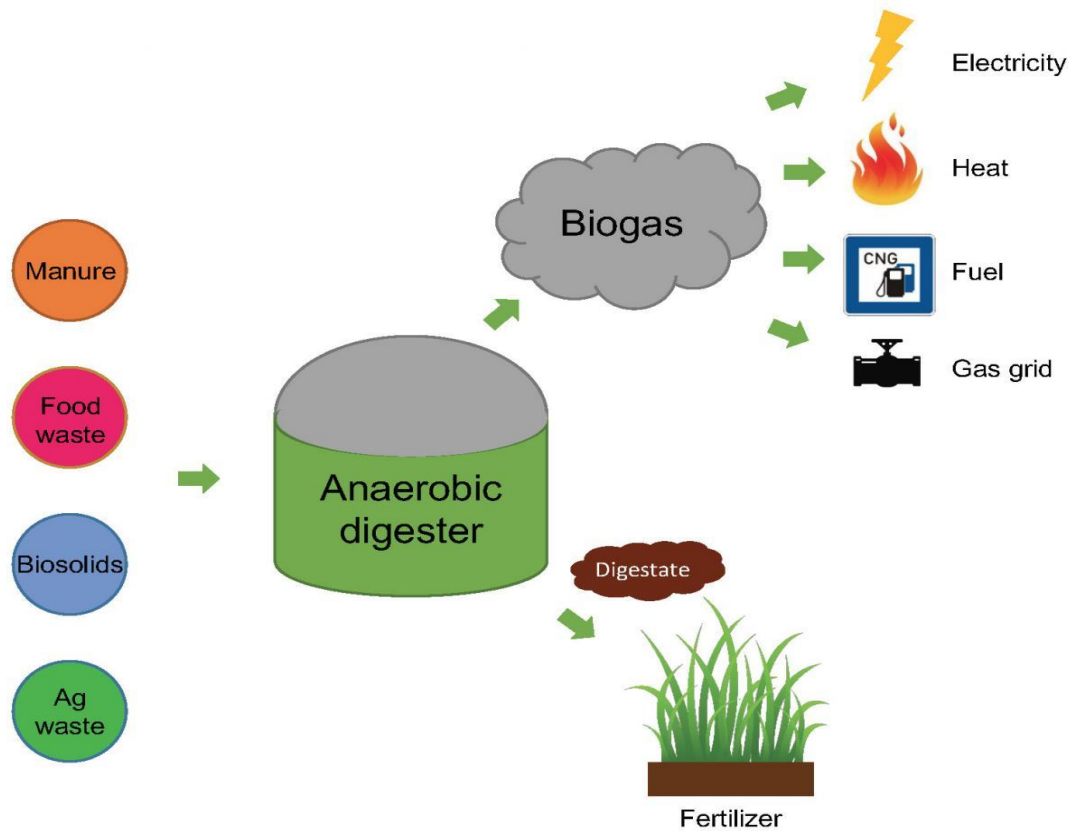
Figure 2.5: Schematic of an anaerobic digester, Ohio State University, 2018

Glucose, a simple carbohydrate, has been used in the equations below to demonstrate the degradation of aerobic and anaerobic processes in solid waste decomposition and energy production. Anaerobic degradation produces higher methane than aerobic processes.

Anaerobic degradation with the presence of oxygen and moisture would proceed according to:

$$C_6H_{12}O_6 + H_2O \rightarrow 3CH_4 + 3CO_2 \qquad (\Delta H = -145 \text{ kJ/mol}) \text{ ---------------(2)}$$

Aerobic degradation of glucose in the presence of oxygen would proceed according to:

$$C_6H_{12}O_6 + 6O_2 \rightarrow 6CO_2 + 6H_2O \text{ (l)} \qquad (\Delta H = -2815.8 \text{ kJ/mol}) \text{ ------------(3)}$$

2.1.5 Waste Management Hierarchy

The most preferable waste management strategy is to produce less waste, based on the U.S. EPA waste management hierarchy (shown in Figure 2.6). Even if we produce less waste, there will always be some amount of waste we will be producing daily. Reusing and recycling the materials can help reduce overall waste accumulation. Some of the
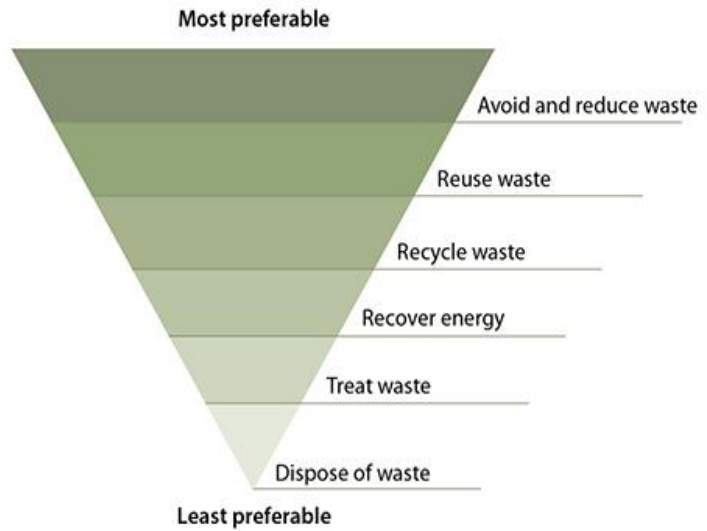
Figure 2.6: U.S. EPA's Waste Management Hierarchy, [U.S. EPA, 2022]

waste will still be unrecyclable. Recovering energy from unusable and unrecyclable waste can help meet a significant portion of daily energy needs. Before disposing of the waste at an authorized

disposal site, the waste can be treated to reduce contaminants. After disposing of the waste, running, and maintaining the site by following established rules and regulations is important.

When we send waste to a Materials Recovery Facility (MRF), the waste goes through several procedures like hand sorting, air classifier, eddy separator, electrostatic separation, optical sorting, and/or magnetic separation to be separated. This MRF process is time-consuming and expensive; an alternative is collecting the waste in separate containers shown in Figure: 2.7 below.

Figure 2.7: Waste collection system based on waste type [Shutterstock, 2023]

2.1.6 Comparing the compositions of landfill gas, digester gas, and natural gas.

Landfills and anaerobic digesters are the sources of biogas that consist of high-potential renewable energy sources. However, the composition of different gases is different in natural gas, biogas, and landfill gas. Table 2-1 shows a comparison of these three different gas compositions.

The data of landfill gas composition was collected from US EPA 2023, anaerobic digester gas composition data was from the National Institute of Health (NIH) 2020, and the natural gas composition data was collected from the Dutton Institute- Penn State, 2004.

Table 2-1: The compositions of landfill gas, digester gas, and natural gas

Gas source	Methane	Carbon dioxide	Nitrogen	Oxygen	Hydrogen	Other gases (trace level)
Landfill gas	45% to 60%	40% to 60%	< 1%	< 1%	< 1%	ammonia, sulfides, carbon monoxide, and nonmethane organic compounds (NMOCs): trichloroethylene, benzene, and vinyl chloride.
Anaerobic digester	50% to 75%	25% to 50%	2-8%	< 1%	< 1%	Carbon monoxide and Hydrogen sulfide
Natural gas	> 75%	<2-3%	<3%	1%	N/A	Butane, Pentane, Hydrogen sulfide, Helium, Ethane (3-8%), Propane (1-2%)

Note: gas composition can vary depending on the source and location and the number above is approximate range.

Converting the carbon dioxide portion into methane will lead to a higher methane content and more renewable. Scientists have been trying to convert carbon dioxide into more useful liquids (e.g., methanol) and/or gases (e.g., methane), and/or solids (e.g., bicarbonate) for years. They have been successful in many cases. However, the conversion of carbon dioxide to methane requires high temperatures and pressure that are costly for large-scale industrial setups. Alternative reaction paths will save money.

The composition of natural gas at the wellhead mainly contains methane. In liquid natural gas, other hydrocarbons such as ethane, propane, butane, pentane, hydrogen sulfides, carbon dioxide, nitrogen, and helium. The percent composition can vary based on the location of extracted gas. The methane percent of natural gas can be as low as 65% [Penn State College of Earth and Mineral Science, FSC 432, 2022]. In Table 2-2 below, components of natural gas in three different locations (Canada, Kansas, and Texas) are provided as an example of location-based gas composition. According to the Penn State College of Earth and Mineral Science FSC 432, the nitrogen content in the natural gas of Texas can be as high as 25.6% and the helium content can be as high as 1.8%.

Table 2-2: Location based natural gas composition. Penn State College of Earth and Mineral Science, FSC 432, 2022.

Components/Location	Canada	Kansas	Texas
Methane	77.1	73.0	65.8
Ethane	6.6	6.3	3.8
Propane	3.1	3.7	1.7
Butane	2.0	1.4	0.8
Pentane	3.0	0.6	0.5
Hydrogen Sulfide	3.3	0.0	0.0
Carbon dioxide	1.7	0.0	0.0
Nitrogen	3.2	14.7	25.6
Helium	0.0	0.5	1.8

2.2 Historic and Future Emissions of Carbon Dioxide, and Conversion of Carbon Dioxide to Useful Products

2.2.1 Historical and Future Emissions of Atmospheric Carbon Dioxide

NOAA's (The National Oceanic and Atmospheric Administration) Global Monitoring Lab, Mauna Loa Observatory in Hawaii has analyzed the average global atmospheric carbon dioxide concentration (shown in Figure 2.8 and Figure 2.9 below), finding that it was the highest in 2021 over a 63-year time span. The increasing trend in carbon dioxide concentration is mainly due to the incomplete combustion of fossil fuels like coal and oil. The global concentration of atmospheric carbon dioxide has tripled from roughly 0.8 to 2.4 ppm (ppm = parts per million) because humans are adding more carbon dioxide into the atmosphere than natural processes (like photosynthesis) can remove [NOAA, 2022].
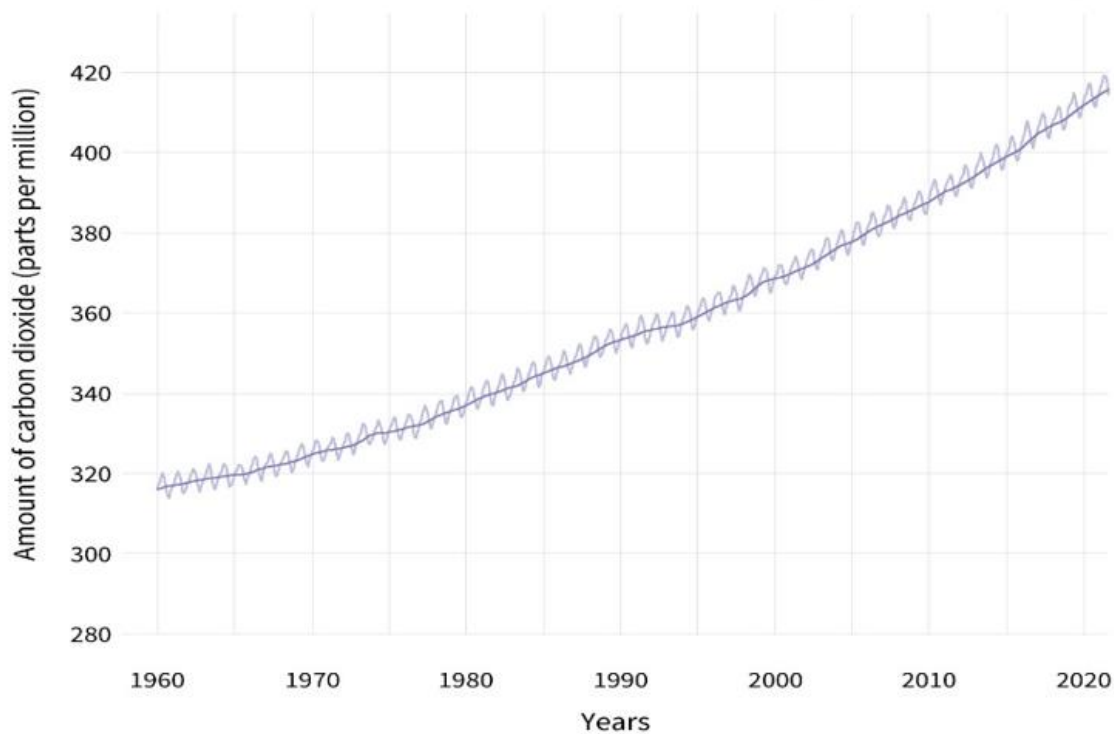
Figure 2.8: Atmospheric carbon dioxide (1960 to 2020) measured in Mauna Loa Observatory, [NOAA, 2022]

Industrialization and the invention of new technologies like cars, refrigerators, and air conditioning are significant in terms of releasing GHGs into the atmosphere. On top of that, new technologies are being discovered and developed almost every day and atmospheric carbon dioxide will continue to increase. By the end of this century, the estimated future atmospheric carbon dioxide emissions could be more than 125 billion tons per year. Scientists are trying to reduce the total CO_2 emissions and/or convert carbon dioxide into valuable products such as methane, methanol, or other useful gases/liquids.

Past and future carbon dioxide emissions (billions of tons/year)

Past and future atmospheric carbon dioxide (parts per million)

Socioeconomic pathways

very high emissions → *very low emissions*

SSP5-8.5   SSP3-7.0   SSP2-4.5   SSP1-2.6   SSP1-1.9

NOAA Climate.gov, adapted from IPCC AR6 Technical Summary, Figure TS.4
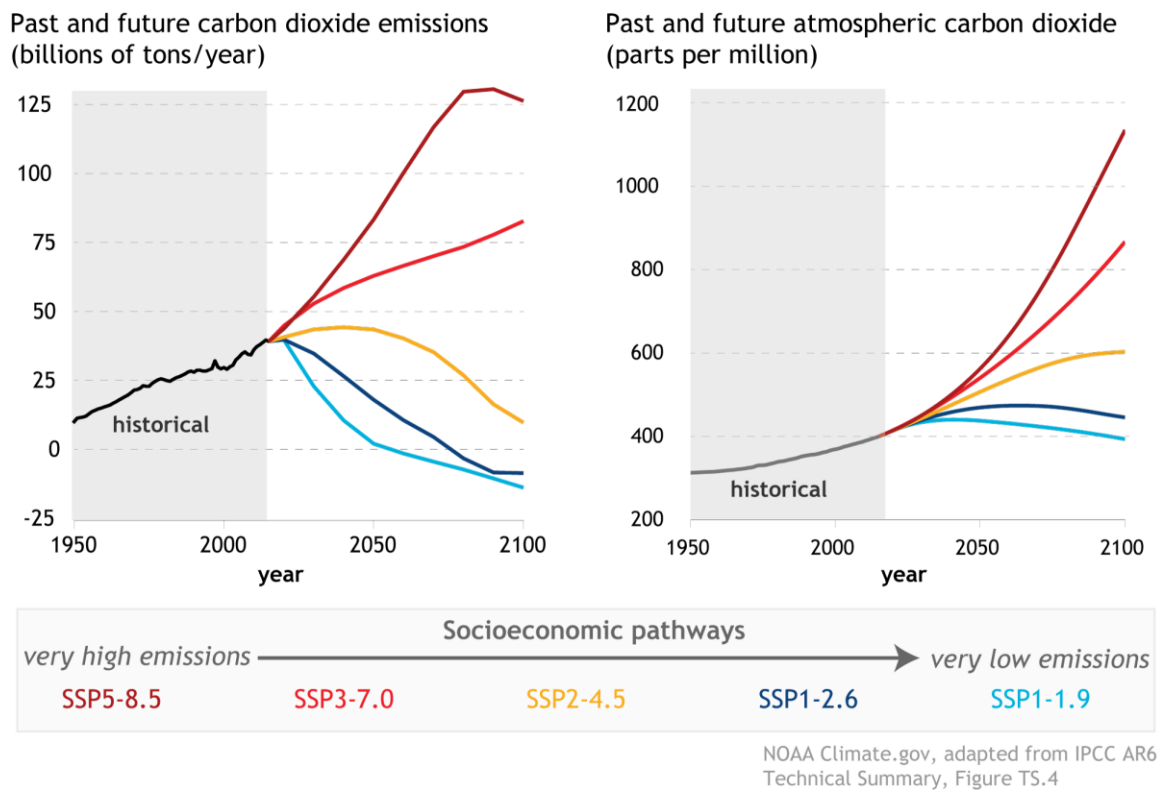
Figure 2.9: Estimated past and future carbon dioxide [NOAA, 2022]

Historical environmental information observation and analysis does not provide suitable estimation and assessment of future climate change-related risks which mainly depend on the pattern of social development, global engagement in environmental protection, political willingness, and technological advancement. Climate information modeling helps decision-makers to understand the future risks of climate change and adapt accordingly. Shared Socio-economic Pathways (SSPs) are the scenarios that describe the distinctive nature of future development pathways for human societies. Figure 2.10 below describes different SSPs and the challenges associated with them.

In Shared Socio-economic Pathways, SSP 1 refers to a sustainable social development where future estimated emissions would be less, and thus survival will be less challenging. On the other hand, SSP 5 indicates higher fossil fuel consumption and elevated emissions to the environment that increase challenges to mitigate. If the current development remains consistent, that indicates the future development in the middle of the road in Shared Socio-economic Pathways.
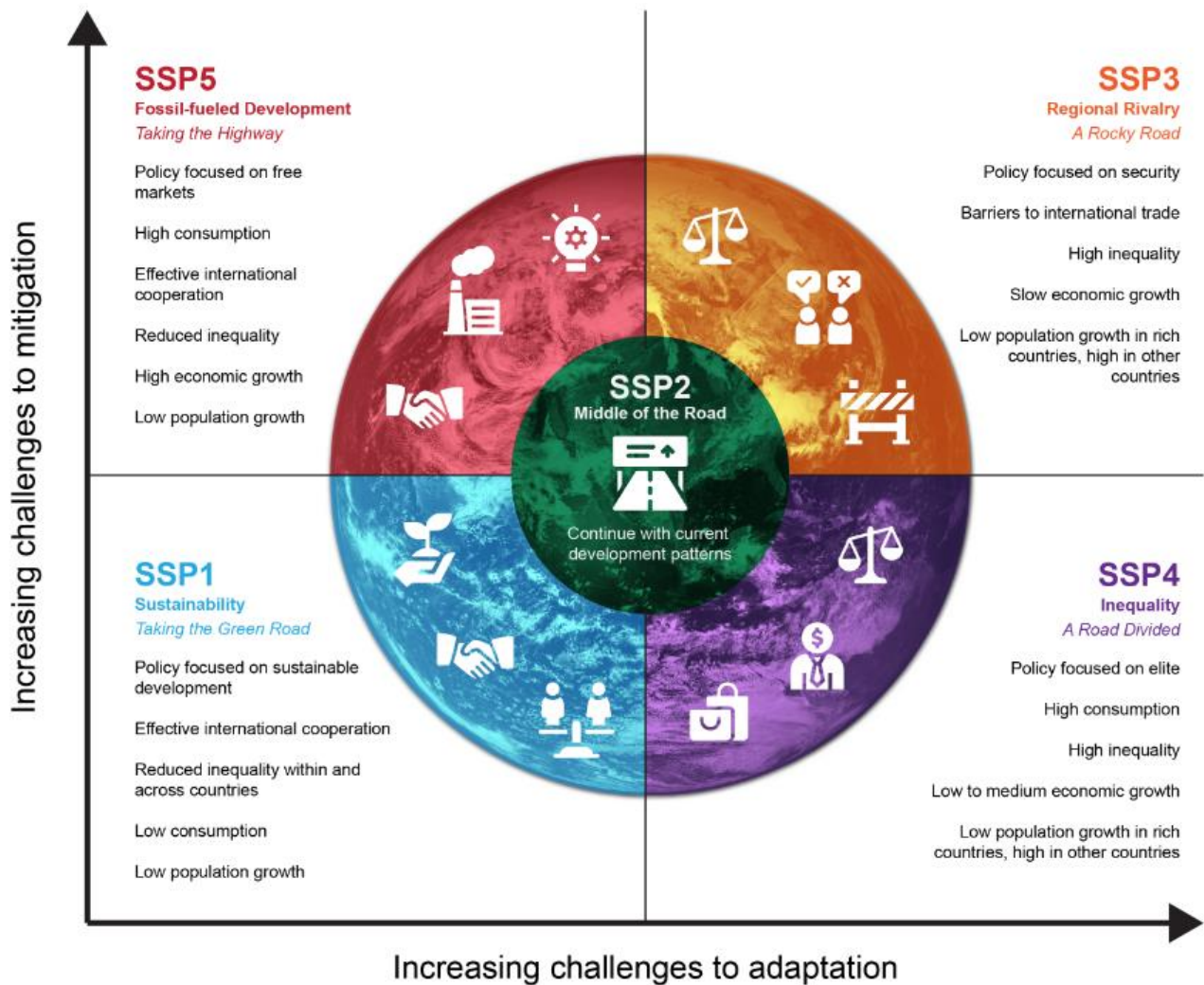
Figure 2.10: Different SSPs vs. the challenges associated with them.

Figure 2.11 shows the estimated global surface temperature change in future years based on the different Shared Socio-economic Pathways (SSPs) scenarios.
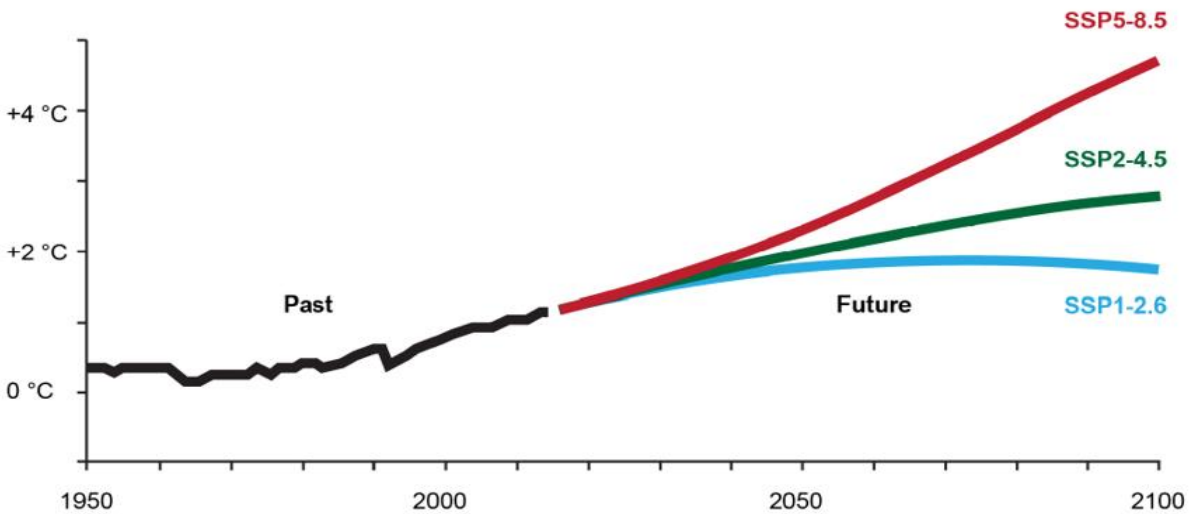
Figure 2.11: Global surface temperature change based on SSPs [climate data, Canada, 2023]

2.2.2 Conversion of carbon dioxide to useful products

Repurposing and utilizing CO_2 will reduce its contribution to global warming. Some of the mercantile and direct potential uses of CO_2 include metal fabrication, refrigerants, fire extinguishing, food and beverage manufacturing, commodity products, rocks, plastics, concretes, bicarbonates, renewable energy sources, and helping plants to grow in greenhouses. In pharmaceuticals, some specialty products with biological activity are also created from carbon dioxide.

Even considering the direct uses of carbon dioxide, the amount we produce and release into the atmosphere is significant and needs unconventional pathways to find diverse new applications. This relatively small and comparatively unreactive gas can be turned into rocks (e.g., $CaCO_3$), cement, carbon fiber through algae, insulation foam for housing, and fuel (e.g., methane) [The Institution of Engineering and Technology (IET), 2019]. Converting CO_2 into useful products such as methanol, ethanol and methane is a current topic amongst science enthusiasts. However, CO_2 itself cannot be burned as fuel because the carbon atom is already in the most oxidized state (+4). Burning involves combining a fuel with oxygen; the oxygen oxidizes the carbon atom in the fuel, releasing heat.

In terms of the energy balance, it may turn out that more energy will need to be used to convert CO_2 to methane than will be obtained by burning the methane. The form of energy as methane, however, is sometimes preferred over solar or wind power. Methane can be used as a storage medium for solar and wind power, which are variable. Also, natural gas (70% methane) can be used to power vehicles and appliances; currently few vehicles or appliances operate directly from solar power.

The process of converting carbon dioxide to methane can also be done using renewable energy (e.g., solar or wind power); otherwise, net fossil fuel will be used. Even if we use fossil fuel, this conversion is still environmentally beneficial as methane is a more potent greenhouse gas.

There are a few processes available to convert carbon dioxide into methane. These processes vary in their mechanism and efficiency. The advantages and disadvantages of different conversion processes are listed in Table 2-3 below.

Table 2-3: Different methods of converting CO_2 into CH_4.

No	Name of the method	Process	Advantages	Disadvantages
01	Methanation with catalyst	The process involves reacting carbon dioxide with hydrogen over a catalyst to produce methane.	• High efficiency, • Scalability, • The ability to produce pure methane.	• High temperatures and pressure • catalyst needed.
02	Biological methanation	This process uses microorganisms (Archaea) to convert carbon dioxide to methane typically in anaerobic conditions.	• Using renewable sources • Taking advantage of waste products • Producing high quality methane	• It can take longer than other methods. • Sensitive to pH • Sensitive temperature.
03	Methane synthesis via carbon electrolysis	this process uses an electric current to convert carbon dioxide into methane	• Low temperatures • No catalyst required	• Still experimental process. • Needs further development. • not yet scalable or efficient

04	Nano-photometric model	This process uses a small sphere called a metal-organic framework to trap carbon dioxide, then irradiates it to turn its molecules into methane.	• Low temperatures • No catalyst required	• Still experimental processes • Need further development. • Not yet scalable or efficient

2.2.2.1 Sabatier Reaction

The "Sabatier reaction" was discovered by a Chemistry Noble prize winner Paul Sabatier and was considered the game changer in converting carbon dioxide into methane in the late 19th century (1897). The reaction mechanism of Sabatier reaction follows the first method - Methanation with catalyst, - listed in Table 2-3 above. Due to the high activation energy of the reactant, high temperatures and pressures are required for this small and usually unreactive molecule (CO_2) to activate. As a result, even after the Sabatier process was developed, the industrial use of CO_2 as an energy-producing feedstock was restricted and unpopular. New ideas for minimizing the temperature and pressure barrier were studied and some researchers have applied electricity and sunlight to overcome the activation energy barrier. The results are promising but not 100% favorable yet [The Institution of Engineering and Technology (IET), 2019].

If the application of the electric field in the Sabatier process were powered by solar energy, there would be no fossil fuel energy consumption. The advantage of using solar energy to convert carbon dioxide to methane, overusing solar energy directly, lies in the application. Methane is the main constituent of natural gas and can similarly be used in natural-gas powered vehicles and appliances.

2.2.2.2 Reaction Mechanism for Sabatier Reaction

CO_2 molecules are weak electrophiles with a δ^+ carbon center as the electrons in CO_2 bonds are more attracted to oxygen than carbon due to oxygen's higher electronegativity. In presence of the catalysts and an electric field, the reactant gas molecule (CO_2) gets attached to the catalyst surface by chemical adsorption; known as chemisorption and creates more chemically reactive intermediates. Due to the higher chemical reactivity, the intermediates split into ions and move the reaction forward. The catalyst used is ruthenium acetylacetonate, a coordination compound of a ligand, called acetylacetonate ($O_2C_5H_7^-$) and Ruthenium (Ru^{3+}). Figure 2.12 below shows how catalysts help form products at a lower activation energy [Zhang and Chemtalk].
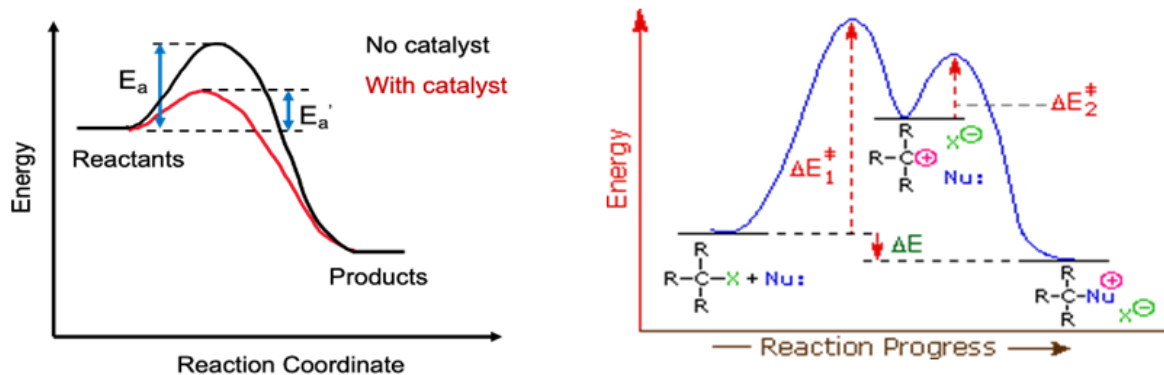
Figure 2.12: Activation energy vs reaction rate with and without catalyst; Zhang and Chemtalk, 2023

The ions produced in the reaction chamber due to catalytic activity are shown below:

$$H_2 \xrightarrow{\text{Ru(acac)}_3 \text{ \& electric field}} 2H^+ \qquad \text{---(7)}$$

$$CO_2 \xrightarrow{\boxed{Ru(acac)_3 \text{ \& electric field}}} C^{4+} + O^{2-} \quad \text{---(8)}$$

C^{4+} reacts with H^+ and produces CH_4 shown in the equation below: The catalyst remains unchanged after reaction.

$$CO_2(g) + 8H^+(g) + 8e^- \rightarrow CH_4(g) + 2H_2O(g) \text{ ---(9)}$$
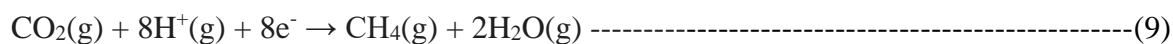
2.2.2.3 Previous Research Using Electrocatalytic conversion of CO_2 to CH_4: Yamada, 2020

Yamada et al. (2020) of Waseda University published a research paper on "Low-Temperature Conversion of Carbon Dioxide to Methane in an Electric field." They applied an unconventional reaction system called electrocatalysis. The activation of CO_2 at a low temperature with the presence of a direct current (DC) electric field and a catalyst bed supported by stainless steel electrodes has previously been demonstrated by them also. For this specific research, they used nickel, ruthenium, copper, cobalt, and iron supported by CeO_2 to prepare catalysts by impregnation method (1), as shown in Figure 2.13. The impregnation method of catalyst preparation has several steps such as stirring, evaporating, drying, keeping the catalyst in a reducing atmosphere to activate, and passing through a sieve (75 µm) for a particular particle size.
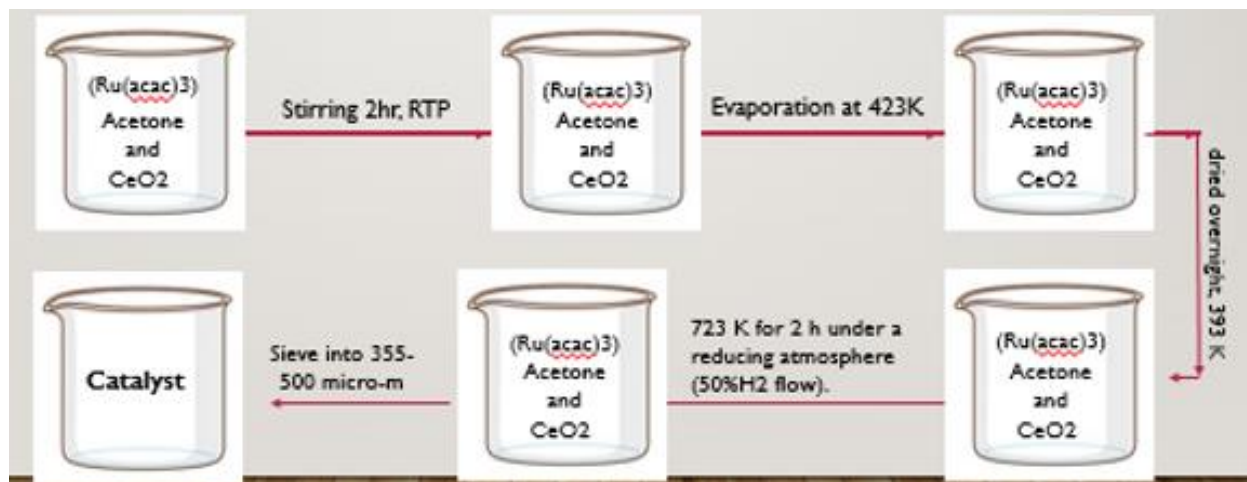
Figure 2.13: Impregnation method (1) of catalyst preparation [Yamada, 2020]

A fixed bed flow-type reactor made of a quartz glass tube was used for the activity test. The electric field was imposed by two stainless steel electrodes at the top and bottom of the catalyst bed. The catalyst (80 to 100 mg) was reduced in presence of hydrogen and argon (1:3) at 723 K. A DC power supply was connected, and a 5.0 mA current was imposed on the catalyst bed. 150 V was stable without any plasma discharge during the activity test. Feed gases were Hydrogen and carbon dioxide with a carrier (noble gas) argon in a ratio of 4:1:5. Argon gas was used as an inert gas that prevented chemical degradation of the reactant, carried the reactant gases in the reaction chamber, and reduced chances of fire from sparks. The other two gases are the reactant gases: Hydrogen gas reduces CO_2 into CH_4 in the reaction chamber. Two different gas flow rates were used:100 SCCM for the screening test and 200 SCCM for the other tests. A Porapak N packet column was used to analyze carbon monoxide, methane and carbon dioxide used in this experiment in a GC-FID. All the water vapor produced during the reaction was collected through condescension by putting a cold trap outside of the gas outlet. Carbon dioxide conversion, methane selectivity and CO_2 consumption rate were calculated by the following equations.

CO_2 conversion (%) = {($F_{CO, out} + F_{CH_4, out}$) / $F_{CO_2, in}$} × 100 ---------------------(4)

CH$_4$ selectivity (%) = {(FCH$_{4, out}$) / (FCO$_{, out}$ + FCH$_{4, out}$)} × 100   ---------------------(5)

CO$_2$ consumption rate r = FCO$_{, out}$ + FCH$_{4, out}$ ---------------------(6)

They also used an FC-IR Spectrophotometer, MCT-M detector, and a zinc selenide (ZnSe) window to determine *in-situ* DRIFTS (diffuse reflectance infrared Fourier transform spectroscopy) measurements that clarifies the reaction mechanism further in presence of an electric field. DRIFTS measurement works by detecting the motion of particle/atom based on light absorbance of an assigned carbonyl group. By analyzing the signals generated by a sensor/detector, the position, velocity, and other properties of the particle or atom can be calculated. The catalyst was charged with Teflon in a DRIFTS cell and used. After the reduction of the catalyst in H$_2$ flow at 573K for 2 hours, they purged the catalyst in airflow for 30 minutes. All the background spectra were recorded at 343K (EF) and 493 K (no EF) under Argon gas at 15 SCCM. The resolution of spectra was 4cm^{-1}, and 20 scans were recorded at 5.0 mA and 0.20kV. The presence of electric field proceeds CO$_2$ methanation in both low and high coordinated Ru sites without CO being adsorbed on the Ru surface.

The activity test showed that Ru, Ni, and Co supported catalysts that increased methane production. The highest methane selectivity and carbon dioxide conversion were recorded using 5wt%Ru/CeO$_2$. The particle size of the catalyst plays a vital role in CO$_2$ to methane conversion, along with Ru loading. Isolated Ru and a temperature higher than 570K lead to formation of CO rather than methane. Imposing an electric field lowers the need for a high temperature for methanation compared to no electric field. The variables they considered and analyzed were temperature, electric field, time, effects of partial pressure, and the reaction pathways [Yamada, 2020].

2.2.2.4 Previous Research Electrocatalytic conversion of CO_2 to CH_4: Manabe, (2016)

Manabe et al. (2016) published a scientific report on "Surface protonic promotes catalysis" that explained catalytic steam reforming of methane in the presence of an electric field. Kinetic analysis in that research paper demonstrated the synergetic effect between an electric field and catalytic activity. Over 1wt% of Pd-supported cerium dioxide was effective to drive the reaction forward at a lower temperature (473 K) by lowering the activation energy to one-third of the apparent activation energy. The surface of the catalyst plays an important role in proton conduction that eventually activates methane at a lower temperature even though methane is a small, almost unreactive molecule.

$$CH_4 + 2H_2O \rightarrow CO2 + 4H_2 \qquad \Delta H°_{298} = 164 \text{ KJ mol}^{-1} \text{--------------------------------(iv)}$$
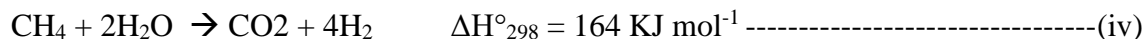
Application of electric field while performing electro-reforming (EF) reduces the reaction temperature even more, apparently to 423K.

The catalytic activity was stable for over a 6-hour time. The results were analyzed after the first five minutes of applying the electricity with a steady flow point. After *operando*-DRIFTS measurements and kinetic investigations, a higher product (methane) formation rate was observed. The catalyst preparation method was impregnation, and the steps are shown in the flow chart (Figure 2.14) below:
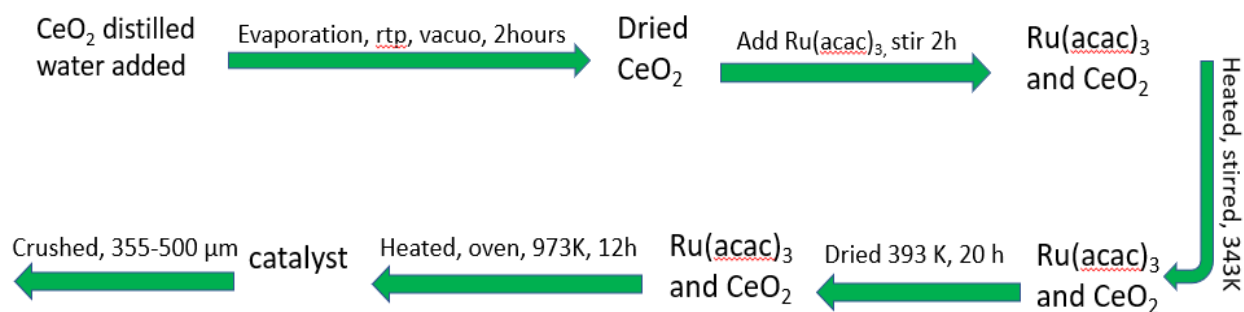
Figure 2.14: Impregnation method (2) of catalyst preparation [Manabe, 2016]

The activity test was done in a cylindrical quartz glass tube (6mm, id) where two stainless steel electrodes were inserted with a spark gap of 1.1 mm. An oscilloscope was used to measure the imposed current and the response voltage waves, and a thermocouple was used to measure the catalyst bed temperature while the reaction was running. The catalyst weight was 80 mg, and the catalyst bed height was 1.6 mm. The total flow rate was 120 SCCM for the supply gas. A DC power supply was used to impose a current of 5 mA. Methane formation was calculated by the ratio of the input and output moles of carbon atoms in reactant and product species. The reaction rate was correspondent to the sum of the products (CO, CO_2) flow rate.

Operando-DRIFTS measurements were done to illustrate the adsorbed elements on catalysts with or without EF using an FT-IR, an MCT detector and a diffuse reflectance infrared Fourier transform spectroscopy reactor cell. The Operando-DRIFTS activity evaluations were done by using a GC-FID. The catalyst characterization was done by the dispersion ratio and particle diameter of the Pd catalyst using a CO pulse. The phase and morphology of the catalyst for AC impedance were analyzed by X-ray diffraction and scanning electron microscopy [Manabe, 2016].

2.2.2.5 The purpose of this research

Neither the Waseda nor Manabe processes were applied for producing renewable energy from landfill gas before. In both processes, the temperature applied was higher than 340°K, which is costly. Testing the process in room temperature and pressure to lower cost and applying this low-temperature CO_2 to CH_4 conversion in landfill gas would create potential sources for renewable energy. This research will systematically explore how various variables impact the process, which has not been done before. Also, a life cycle analysis and a cost analysis will be done in this research that was not included in the previous research on the Waseda process.

2.3 Methane trend in the environment and the importance of its capture and use

2.3.1 History: Atmospheric Methane

Methane is one of the most dominant greenhouse gases present in the Earth's atmosphere. Since pre-industrial times, the atmospheric methane concentration of the globe has risen by a factor of 2.6. Methane mole fraction rose from 1600 ppb to 2000 ppb (ppb is parts per billion) from 1984 to 2004 (Figure 2.15), representing the maximum value in approximately 800,000 years.

Over a 20-year period, methane traps 84 times more heat per mass unit than carbon dioxide (CO_2), which is known as the "20-year global warming potential." When accounting for aerosol interactions, methane is 105 times more effective in global warming [AGAGE, 2023]. Among the natural sources of atmospheric methane, methanogenesis (when anaerobic microorganisms break down organic waste and produce methane) is one of the most common. This process produces methane mainly in aquatic ecosystems and ruminant animals. Other natural

sources of atmospheric methane are wetlands (167 Tg of CH$_4$/ year), melting permafrost, plants (62–236 Tg a^{-1} of methane), methane clathrates, and so on.
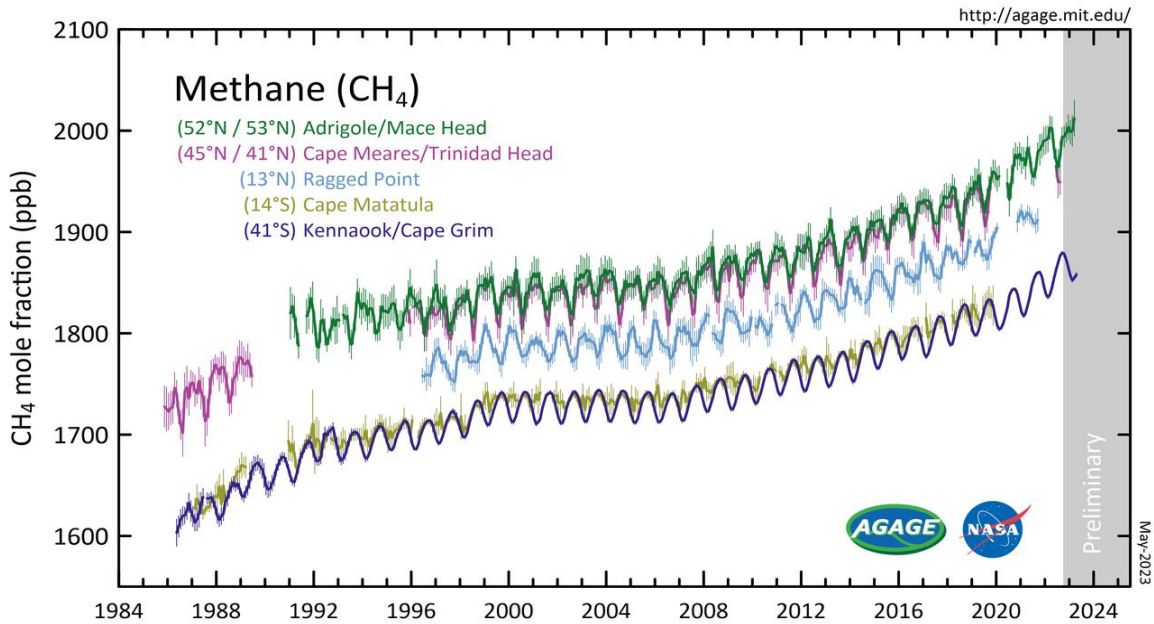
Figure 2.15: Atmospheric methane (1984 to 2024) [AGAGE, 2023]

Plants do not produce methane as an end-product or by-product of metabolism, they release unused methane by transpiration from absorbed water if the water contains any methane. Rice plants diffuse methane into the atmosphere during anaerobic decomposition. Dead seagrasses also release methane. On the other hand, methane is not only a potent greenhouse gas but also a very useful fuel. Capturing and utilizing methane rather than emitting it into the atmosphere is of current interest because it helps in both ways: mitigating the atmospheric methane concentration and can be used as fuel.

2.3.2 Collecting Methane

New research published by Stanford-led researchers has shown that removing 3-years' worth of human-emitted methane will reduce the temperature by 0.21°C (32.38 °F) and will prevent 50,000 premature deaths annually by the year 2050. However, methane removal technologies are not available yet, and it will take time, effort, and investment to develop practically effective technologies [Stanford Earth Matters Magazine, 2021]. Scientists are focusing on finding a practical way of extracting the existing atmospheric methane even though some argue that it is not worth time and investment, as methane stays in the atmosphere for 10-12 years. Most methane removal methods require air and catalyst at the same time. One effective and fast methane removal method is photocatalytic oxidation with hydroxyl radicals in the presence of chlorine that acts as a catalyst and sunlight. Another is spreading sea water aerosols added to iron (acts as a catalyst) into the atmosphere. Now scientists are emphasizing enhancing this natural process that involves seawater aerosols [Science Business, 2021].

MIT researchers have found a way of controlling methane emissions along with removing them from the atmosphere by using a type of clay called Zeolite treated with a small amount of copper [MIT, 2022]. Zeolite is a naturally abundant clay that oxidizes methane to carbon dioxide. As of now, there are no fully developed technologies or methods available to extract methane from the environment. Utilizing methane rather than releasing it into the atmosphere will be a game changer as it is a source reduction approach to the problem.

The difficulties of extracting methane from the atmosphere include the scarcity of the gas present in the air. Methane is 200 times less abundant than carbon dioxide. Capturing a lot of air,

processing it, and extracting methane will also require a significant amount of energy. This gas has a low boiling point, which makes converting it to liquid more difficult.

Methane tends to be more concentrated in sources like landfills, livestock waste, and fossil fuel production facilities and less dense than carbon dioxide. So, it is easier to capture methane in large quantities using equipment like gas pipeline compressors and storage tanks. Overall, capturing methane and carbon dioxide both is difficult.

Chapter 3
Methodology

3.1 Laboratory Set-up

The flow-type reactor was created (shown in Figure 3.1 and Figure 3.2 below) in a quartz glass tube that has a low thermal expansion coefficient (average $5.0 \times 10^{-7}/ °C$) and a high melting point (2000° F), by following Yamada (2020). The tube is cylindrical with a diameter of 25 mm (0.98 in) and a length of 304.8 mm (12 in). A support stand and a clamp were used to hold the quartz tube vertically. Two rubber stoppers that can withstand temperatures up to 570° F for 20 minutes were used to create the inlet and outlet for the reactor. On the top rubber stopper, a semi-flexible Teflon tube (temperature tolerance of up to 600° F and pressure tolerance of 160 psi at 72° F) was inserted.
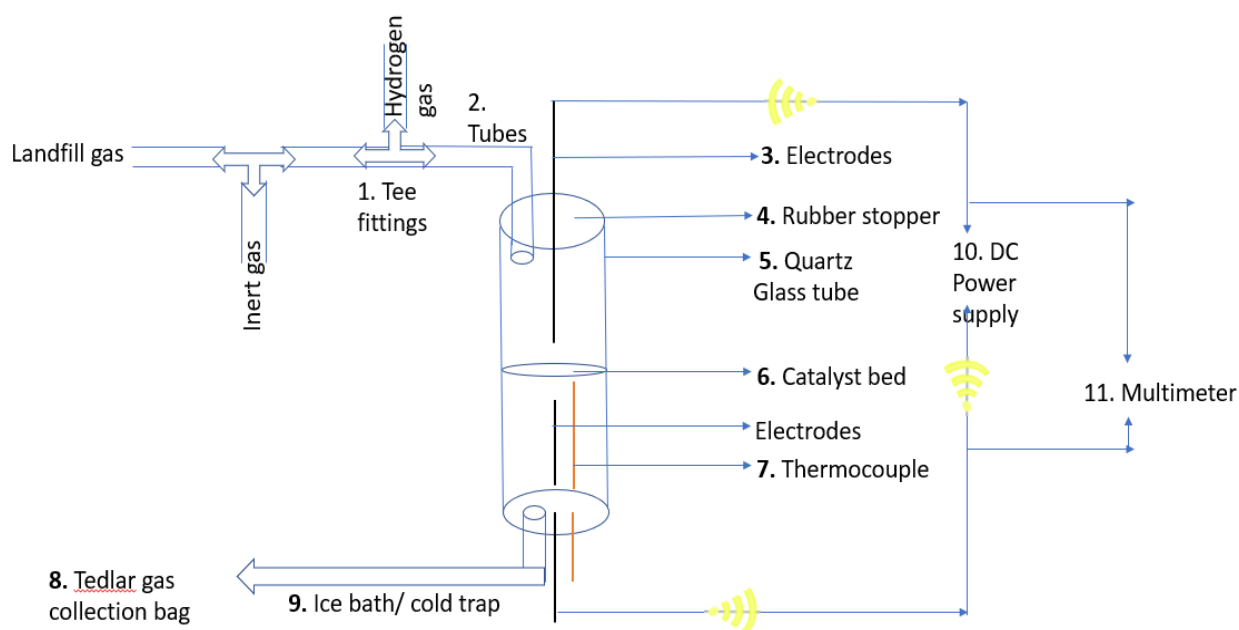
Figure 3.1: Flow diagram of the laboratory setup.

The tube was connected to a synthetic landfill gas cylinder (CO_2: CH_4 =1:1), argon gas cylinder, and hydrogen gas cylinder. All these three gas cylinders are from Matheson Tri-gas and are ultra-high purity gas. Synthetic landfill gas contains 50% methane, which is a flammable gas at high concentrations, and 50% carbon dioxide. Argon gas was used as an inert gas to reduce any chance of explosion and fire in case of any spark from the electrodes. This gas also prevents any degradation of the reactant from unwanted chemical reactions as well as acts as a heat transfer agent. Argon gas has a thermal conductivity, k of 0.16 (Btu/hr ^{o}F) [Engineeringtoolbox, 2023]. Hydrogen is another reactant gas supplied to the reaction chamber that reduces CO_2 into CH_4.

A copper electrode (2mm OD) was inserted into the reactor through the top rubber stopper. The bottom rubber stopper also had a copper electrode of the same outer diameter along with a quarter-inch plastic tube (gas outlet).

Figure 3.2: Laboratory setup.

A K-type thermocouple probe with 2mm outer diameter was inserted into the bottom rubber stopper to measure the catalyst bed temperature. The K-type thermocouple was connected to an E-Z Probe General Purpose Pyrometer (EZK-C) by EDL-INC shown in Figure 3.3 that can measure temperature in the range of -35°C to 985°C or -30°F to 1800°F.
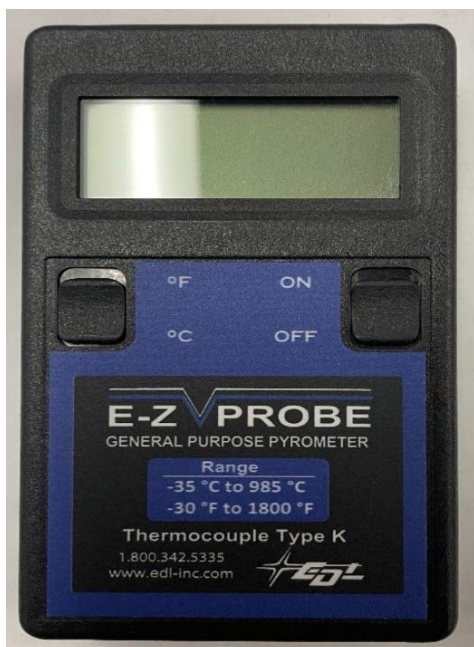
Figure 3.3: E-Z Probe General Purpose Pyrometer (EZK-C)

To measure the actual voltage (V) and current (A) passing through the copper electrodes, a multimeter was used manufactured by EXTECH voltage detector (EX330) by Extech shown in Figure 3.4 below. Even though the copper electrodes have low resistance, there might be less electricity passing through the system because of the variability of spark gap between two electrodes. The spark gas was kept constant for better and reliable data analysis.

Figure 3.4: EXTECH voltage detector EX330

Electrodes were connected to two DC power supplies in parallel mode (JESVERTY SPS-12003 0-120V 0-3A) shown in Figure 3.5 below to obtain higher voltage output. The maximum voltage passed through the system was measured at 240V and the maximum current passed through the system was measured at 0.2161 A. The total power (W) calculated was 51.864 W.
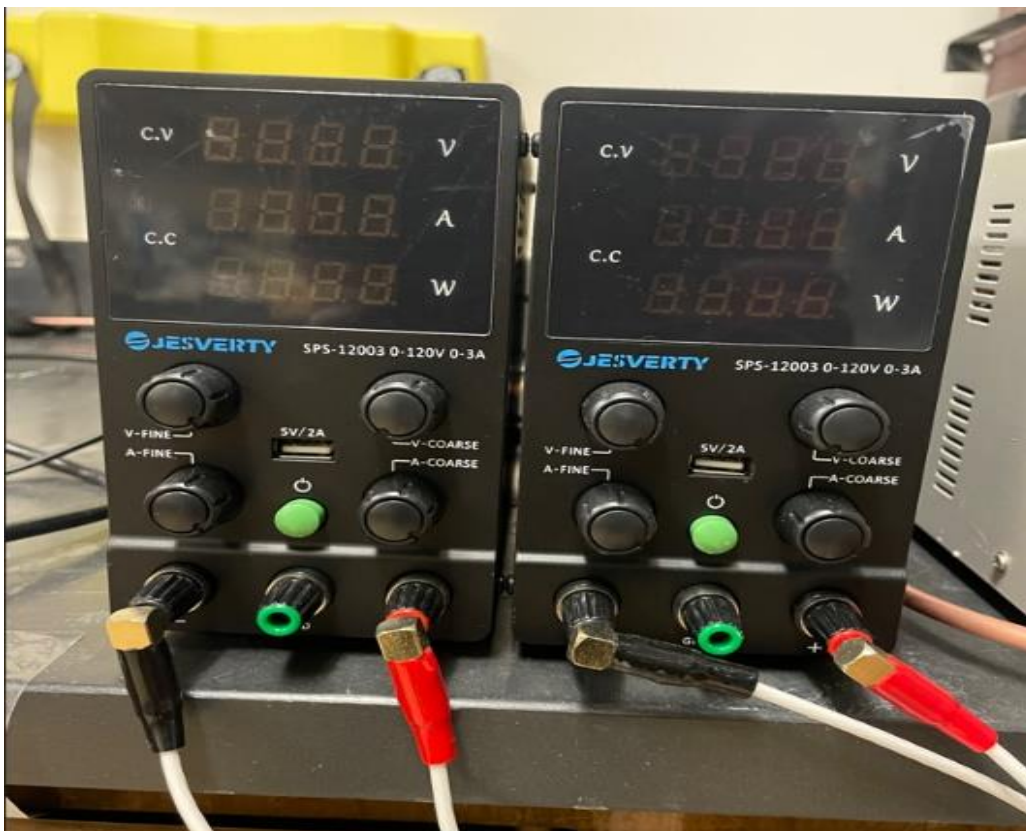
Figure 3.5: DC power supplies in parallel mode (JESVERTY SPS-12003)

The gas flow rate and pressure were observed and controlled by Matheson rotameters 1000 series with a flow range of 10 to 130 standard cubic centimeters per minute (SCCM). All three gas cylinders were connected to separate gas flow meters (Matheson FM 1000) shown in Figure 3.6 for precise readings and controlling the different gas flow rate independently.

Figure 3.6: Matheson Rotameter 1000 series

For external temperature input, another DC power supply (Mastech HY3003D-3 shown in Figure 3.7) was connected to a heating pad (Shown in Figure 3.8) that was wrapped around the catalyst bed from the outside of the quartz glass tube. The temperature measured (inside the tube) was on the catalyst bed was 90°C while the temperature on the heating pad (outside of the quartz glass tube) was 196 °C. The temperature difference measured was because of the insulating properties of the quartz glass. The highest temperature measured by the pyrometer thermocouple on the catalyst bed was 90 °C. The heating pads were Film Heater Adhesive Polyimide pad with a dimension of 25mmx50mm.

Figure 3.7: Mastech DC power supply (HY3003D-3)

Figure 3.8: Film Heater Adhesive Polyimide pad

The catalyst bed was made from acid resistant silica wool for furnace that has a temperature tolerance of up to 2000° F, 0.78 Btu heat Flow Rate at 800° F, and density of 10 lbs./cu. ft. The catalyst bed temperature was measured by an E-Z prob type k thermocouple.

The catalyst bed was supported by two thermoplastic supports created in the UTA 3D printing lab shown in Figure 3.9. These specially 3D-designed supports (2, one on top and one on the bottom of the catalyst bed) also help the electrodes to stay in the center of the reactor and create a uniform electric field. The spark gap was measured and kept between 1.00 to 1.50 mm for all the experiments.
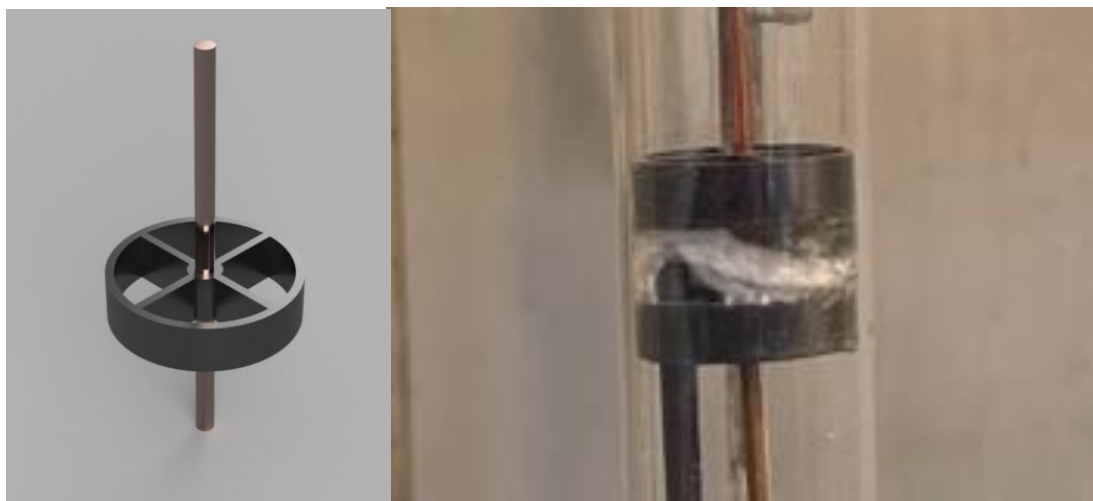
Figure 3.9: Catalyst bed support created in UTA 3D Printing lab

The outlet plastic tube was coiled and placed in a cold bath shown in Figure 3.10 below to release any heat produced and carried by the produced gas. This tube has two outlets. One was used for cleaning the tube by passing argon gas to the hood. Another outlet was connected to a 1-L Tedlar bag, where the produced gas was collected for Gas chromatographic (GC) analysis.

Figure 3.10: Cold trap for the outlet gas

The Gas Chromatographic (GC) analysis was done by SRI model SRI8610C with FID detector, shown in Figure 3.11 below. The GC column separates methane and carbon dioxide for quantification purposes. In an actual system at a landfill, remaining carbon dioxide would need to be separated from methane for end uses requiring a high concentration of methane (e.g. pipeline natural gas). However, since these technologies are already well developed and did not need to be researched, their use was beyond the scope of this experiment.
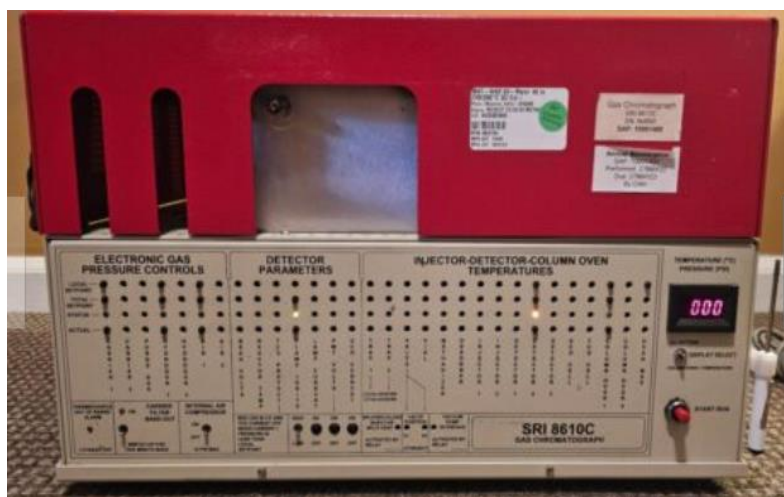
Figure 3.11: Gas Chromatograph, SRI8610C

3.2 Catalyst Preparation: Impregnation method 1 (Yamada 2020)

Ruthenium-supported cerium (IV) oxide was prepared by the impregnation method [Yamada, 2022]. All the necessary equipment such as beakers, magnetic stirrer, ceramic boat, and spatula were washed with soap and lukewarm water and then rinsed with alcohol and dried before use. To prepare 5 wt% $Ru(acac)_3$ supported CeO_2, the following steps were followed: The molar mass CeO_2 or cerium (IV) oxide = 172.115 g/mol and molar mass of ruthenium acetylacetonate $Ru(acac)_3$ = 398.39 g/mol.

Step 1: 0.5 g $Ru(acac)_3$ was dissolved in 9.5 ml of acetone.

Step 2: 1 g CeO_2 was added to the previous mixture (Step 1)

Step 3: Stirred the mixture of CeO_2, acetone and $Ru(acac)_3$ for 2 hours at 423 K (150°C)

Figure 3.12: Catalyst preparation: stirring and heating.

Step 4: Obtained powder was dried overnight at 393 K (120°C) shown in Figure 3.13 below:

Figure 3.13**:** Dried catalyst ready for heat treatment

Step 5: Dried powder was reduced in a ceramic boat using a 50 % hydrogen flow in a tube furnace (Thermo Scientific Lindberg Blue M) at 723K (448°C) for 2 hours shown in Figure 3.14 and Figure 3.15 below. The total flow rate of hydrogen and argon gas was 100 SCCM. The total flow rate should be less than 200 SCCM to avoid impact of cold airflow on the heated quartz tube.

Figure 3.14: Tube furnace: Heat treatment of the catalyst

Figure 3.15: Catalyst after heat treatment

Step 6: The catalyst after heat treatment was ground in a clean dish by pestle. The particle size of the catalyst was 75 microns.

3.3 Catalyst Preparation: Impregnation method 2 (Manabe 2016)

Another typical impregnation method [Manabe, 2016] was followed to determine if the catalyst preparation method has any impact on the product formation rate. All the necessary equipment such as Buchner flask, funnel, beaker, magnetic stirrer, and spatula were washed with soap and lukewarm water and then rinsed with alcohol and dried before use. To prepare 5 wt% $Ru(acac)_3$ supported CeO_2, the following steps were followed:

Step 1: 0.5 g $Ru(acac)_3$ was dissolved in 9.5 ml of distilled water and 1 g CeO_2 was added to the mixture.

Step 2: The mixture was evaporated at room temperature and pressure in vacuo (shown in Figure 3.16) for 2 hours.

Figure 3.16: Set up of vacuo.

Step 3: The mixture of CeO_2, water and $Ru(acac)_3$ was heated for 2 hours at 343 K (69.85°C).

Step 4: The mixture of CeO_2, water and $Ru(acac)_3$ was dried for 20 hours at 393 K (119.85°C) on a hot plate shown in the Figure 3.17 below.

Figure 3.17: Dried catalyst

Step 5: The mixture of CeO_2, water and $Ru(acac)_3$ was heated for 12 hours in a muffle furnace at 973 K (119.85°C) in a muffle furnace shown in the Figure 3.18 below.

Figure 3.18: Catalyst after heat treatment

Step 6: The catalyst was crushed using the same evaporating dish by a pastel and sieved into 75 μm sieve.

3.4 Catalyst Characterization:

The catalyst characterization will answer the following question:

What is the elemental composition, surface area, and pore size distribution before and after catalyst use?

Table 3-1 below summarizes the catalyst characterization parameters, methods, and instruments used in the process.

Table 3-1: Catalyst characterization methods and instruments

Material Characterized	Parameter	Method of Characterization	Instrument
New and used catalyst. 5 wt% Ru(acac)$_3$ supported CeO$_2$	Visual	Field Emission Scanning Electron Microscope (FE-SEM)	Hitachi S-3000N FE-SEM
	Particle size	Sieve Analysis	Sieve 75 microns
	Elemental Composition	Energy Dispersive Spectroscopy (EDS)	Hitachi S-3000N FE-SEM

The advanced technology of Field Emission Scanning Electron Microscope (FE-SEM) provides high resolution, electrostatically less distorted microscopic imaging by maintaining accurate brightness and a stable current in the beam. Energy Dispersive Spectroscopy (EDS) determines the elemental composition and relative abundance of the catalyst sample by analyzing the intensity distribution of distinct X-ray signals produced by the electron beam imposed on the catalyst surface.

3.5 Experiments to address Obj. 1: Explore the impact of independent variables (time, power, temperature, catalyst preparation method, electric field's type, degradation of catalyst over time, performance of reactivated used catalyst) on synthetic landfill gas.

For experiments to address Objective 1, synthetic landfill gas was used for several reasons:

- It was difficult to collect real landfill gas in larger quantities because of the low pressure of the landfill gas in the gas wells.

- Synthetic landfill gas has a known concentration of CH_4 and CO_2 and does not have other impurities which may interfere in the reaction.

Table 3-3 presents an overview of the experiments conducted to address Obj. 1, along with the research questions, hypotheses, and results. Additional information about the sets of experiments is summarized in the sections below.

Table 3-2: Experiment sets conducted.

Set	Experimental set name	Variables	Research Question	Hypothesis	Explanation of Hypothesis
i	Baseline with voltage at room temperature and pressure	Time (min)	Is there any methane conversion applying 36.66 W of power over	There will be methane conversion in measurable times at room temperature.	Applying 36.66 W will create an electric field on the catalyst bed that would be strong enough to

			time with catalyst, no heat applied?		overcome the activation energy barrier for the reaction.
ii	Impact of power	Power (W)	How does power (W varies) impact the conversion?	Higher the voltage, the faster the methane conversion.	Higher power creates a stronger electric field, which would increase the reaction rate.
iii	Impact of Temperature/appl ied heat	Temperature (C)	Does the percent conversion change with applied external heat?	The reaction rate will differ from the baseline experiment.	External heat with an imposed EF would excite the reactants to form products more quickly. However, applying two different types of energy might have overstimulating effect on the molecules, leading to a decrease in the product formation rate.
iv	Impact of Catalyst	Catalyst prepared in	Does the method of preparing catalyst have	There will be no impact of how the catalyst was prepared.	Although the preparation method is different, the chemical compound is the same, so the

	preparation method	two different methods	any impact on the reaction rate?		reaction rate will not be impacted
v	Impact of electric field type	Electric field type	How does the shape of the applied electric field impact the conversion?	There will be different methane rates for different types of electric field.	The strength of a uniform EF and the strength of an interrupted EF will be different; the impact of EF type will be analyzed.
vi	Degradation of Catalyst over time	Time	Was the catalyst poisoned/did the quality of the catalyst degrade due to reaction?	The presence of CO and H_2O might poison the catalyst and degrade catalyst's performance.	Using the same catalyst for a long might degrade the catalytic activity due to moisture, silica, and some poisonous elements (S) present in the reactant gases.
vii	Reactivating the Catalyst	Catalyst	Is there any change in reaction rate after reactivation of the used catalyst?	The product formation rate might be a little slower for reactivated catalyst.	Used catalyst may have moisture and silica reducing the effectiveness of the catalyst.

Note: After Experiment number 1, values of the constants are the same unless the variables are varied.

3.5.1 Baseline Experiments

The standard Sabatier reaction requires high temperature and pressure for carbon dioxide to methane conversion. This research uses an electric field in presence of metal catalyst to conduct the reaction without high temperature and pressure. The baseline experiment answered the basic question of whether there is any reaction/ catalytic activity when an electric field is applied in presence of the catalyst, without applying external heat or pressure.

In the baseline experiments, the combined gas flow rate of landfill gas, hydrogen gas, and argon gas was 200 SCCM. Three Matheson rotameters (calibrated to air) were used to measure and control the gas flow rate from reactant gas cylinders. The gas flow rate of argon, hydrogen, and landfill gas was calculated by using Matheson factor table flow rate calculations. The flow rate for argon gas was 117.5 SCCM, hydrogen was 21.09 SCCM and landfill gas was 19.83 SCCM. One flow rate sample calculation for H_2 gas is shown below:

The combined gas flow is 200 SCCM and the ratios are landfill: hydrogen: argon $= 1: 4: 5$. The specific flow rate for hydrogen $= (\frac{4}{1+4+5}) * 200$ SCCM $= (\frac{4}{10}) * 200$ SCCM $= 80$ SCCM. As the flowmeters were calibrated to air, H_2 factor 3.793 was used to calculate the flow rate for hydrogen gas. The flow rate of hydrogen gas $= \frac{required\ flow\ rate\ of\ hydrogen,\ SCCM}{methason\ hydrogen\ factor} = \frac{80}{3.793} = 21.09$ SCCM.

The voltage (V) and current (A) measured in the multimeter were 199.99 v and 0.1834 A respectively. The total power (W) calculated by using the formula, Power $= V \times A$, was 36.66 watts. The catalyst bed temperature was 24 °C measured by the pyrometer. There were no changes in catalyst bed temperature during this experiment. The catalyst (0.5wt%Ru/CeO2) weight was

0.33g evenly spread on the catalyst bed. The total time (T) of the experiments was 1 hour and the produced gas was collected every 10 minutes in a Tedlar gas collection bag.

A 20-µg gas sample from the Tedlar gas collection bag was injected by a needle injector in a gas chromatograph (GC FID, Porapack N Column) and the area for both methane and carbon dioxide were recorded from the calibration. By using the recorded area from GC, methane fraction (%) and methane mass (µg) were calculated. The ratio between methane and carbon dioxide area was also calculated. The time (min) was the only variable in the baseline experiment, others were constants.

3.5.2 Impact of Power

Applying voltage creates an electric field on the catalyst bed that excites the molecules and lowers the activation barrier. The strengths of the electric field are different for different voltage and have impacts on the reaction rate. To investigate the impacts of different voltages, a range of voltages was applied. The hypothesis behind this experiment is "The higher the voltage, the greater the methane conversion rate". Specific voltages applied were 174.4v, 192.3v, 210.3v, 224.5v, and 240v. The total power imposed from those voltages were 28.18w, 33.94w, 40.36w, 45.73w, and 51.86w. Other parameters such as temperature, pressure, catalyst amount, catalyst preparation method, time, were constant.

3.5.3 Impact of Temperature

Temperature can change catalytic activities by exciting the molecules that help lower the activation barrier. This research investigated the impact of temperature on the product formation rate in the presence of both an electric field and catalyst to answer the research hypothesis: there will be an increase in methane concentration after reaction with external heat application.

A DC power supply (Mastech HY3003D-3) was used to apply external temperature by using a heating pad attached to the quartz glass tube, around the catalyst bed. The temperature measured inside the tube, on the catalyst bed was 90°C, while the temperature on the heating pad, outside of the quartz glass tube, was 196°C. The temperature difference measured was because of the insulating properties of the quartz glass. The highest temperature measured by the pyrometer thermocouple on the catalyst bed was 90 °C. Further investigation has been done by applying different varieties of temperatures.

In the presence of an electric field, a range of different temperatures was applied to study the methane conversion from carbon dioxide. To create the electric field, a voltage of 174 V and a current of 0.1616 A were applied. The total power was constant at 28.1 W for all the experiments. The variable of this experiment is temperatures which was applied by using heating pads connected to a separate DC power supply.

3.5.4 Impact of Catalyst Preparation Method

To analyze the effectiveness of catalyst prepared by two different methods, this experiment was designed. Both methods are called impregnation; however, the process differs from one another.

Two different methods of impregnation have been followed to prepare the catalyst [Yamada, 2020 and Manabe, 2016] to see if the method of preparing catalyst has any impact on the reaction rate and/ or product formation rate. The hypothesis behind this research is there will be no impact on the catalyst performance based on how the catalyst was being prepared. In one method, a muffle furnace was used for catalyst reduction, while the other method used a tube furnace was used. During the heat treatment of the catalyst 50% reducing environment was created inside the tube. Other factors such as time, temperature, voltage, ampere, gas flow rate, amount of the catalyst used, and so on were held constant.

3.5.5 Impact of Electric Field Type

In the baseline experiment, the electric field was kept constant by applying a specific voltage. A uniform electric field was created and the distance between two electrodes (spark gap) was constant too. If the magnitude of the electric field E is:

$$E = -\frac{\Delta V}{d}$$ ---(v)

where ΔV is the potential voltage difference between the copper electrodes and d is the distance separating the electrodes.

Changing the electrode type shown in Figure 3.19 below created ununiform electric field had impacts on the conversion process. To change the electric field type, a new pair of electrodes had been built, where a circular section of copper mesh was surrounded by copper wire and connected to copper electrodes. The copper mesh created a different type of electric field in the reaction chamber during the conversion process. The electric field was the only variable in this reaction and others were kept constant.

59
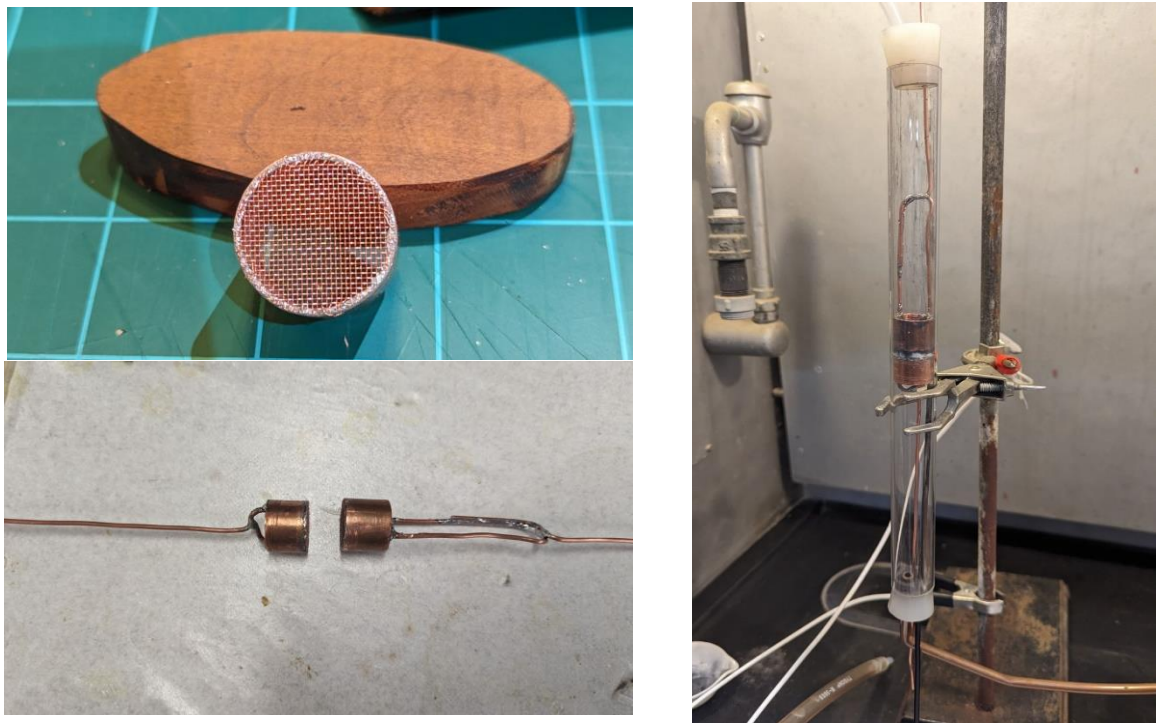
Figure 3.19: Set-up to produce a non-uniform electric field

3.5.6 Degradation of catalyst after use

During this electrocatalytic dry formation of methane, synthetic and real landfill gas will be used. Even though synthetic landfill gas does not contain any elements other than methane and carbon dioxide, the real landfill gas contains sulfur, that can poison the catalyst over time. Carbon monoxide is one of the byproducts of this reaction, that can poison the catalyst too. In addition, the strength of the electric field is not always the same due to the different voltages applied; that might impact the efficiency of catalysts over time. To identify whether the activity of the catalyst was changed during the experiment due to the imposed electric field over time, this experiment has been designed.

The highest amount of Power, 52 watts, has been applied to impose the strongest electric field. This power was constant along with other constants during the experiment. The experiment was run for a longer time than other experiments. In a 90-minutes time frame, 9 samples after reaction

will be collected every 10 minutes. The standard deviation of those three data points were calculated and recorded as well.

3.5.7 Reactivating the Catalyst

The products in this electrocatalysis process include methane, carbon dioxide, carbon monoxide and water vapor. The boiling points of the above-mentioned products are listed below.

Table 3-3: Boiling points of the produced gases.

Compound	Boiling point °F	Boiling point °C
Methane (CH_4)	-258.9	-161.6
Carbon dioxide (CO_2)	-109.2	-78.46
Carbon monoxide (CO)	-312.7	-191.5
Water vapor (H_2O)	212	100

The catalyst was collected after reaction mechanically (hand sorting from the bed) was sieved into 75 microns sieve to separate the silica and recovered by heating the catalyst in an oven at 100°C temperature for 2 hours to get rid of any moisture or water vapor. Other products were already in gaseous form and expected not to be bonded to the catalyst. Further catalyst characterization has been done to investigate the catalyst purity before and after the reaction, as described in the section below.

Catalysts are supposed to remain chemically unchanged after any reaction by definition. However, catalysts decay over a long period. To analyze the impact of moisture, silica, and other gases in

the reaction chamber, this experiment has been designed. This experiment aims to reactivate 0.33gm of the used catalyst and reuse them.

An experiment was conducted with the reactivated catalyst to determine whether the reactivated catalyst gave a different methane concentration after the reaction than the new catalyst or not. The variable for this reaction was time and the concentration of produced methane gas was analyzed every 10 minutes. Other parameters mentioned in Table 3-3 were held constant. The mean value of three data points has been taken and presented in a graph. This graph was compared to the baseline reaction to find if the methane concentration after has changed or not.

3.6 Methods to address Objective 2: Using the best values of process variables determined in Obj. 1, test the Waseda process with real landfill gas.

At room temperature and pressure and 54 W power was used to impose the strongest electric field in the presence of 0.33 gm fresh catalyst for optimal efficiency of the catalyst determined in obj. 1. The most effective electric field type analyzed in objective 1 was a uniform electric field had 37% increase in methane fraction. Two copper electrodes of 2 mm OD were used to create the uniform electric field for this experiment, that yield the maximum amount of methane. The Aircheck sampler pump (model: 224-PCXR8) shown in Figure 3.20 below was used to supply real landfill gas from the Tedlar gas collection bag to the reaction chamber. This experiment has provided information on whether this electrocatalytic conversion of CO_2 is efficient in real-life scenarios where the landfill gas contains contaminants that could poison the catalysts. The

concentration of H_2S and initial methane concentration present in the real landfill gas was measured by using Landtec Gem 5000.

Figure 3.20: Aircheck gas sampler pump

3.7 Objective 3: Conduct a life cycle environmental and economic analyses of the Waseda process, as applied to landfill gas.

For sustainable development, assessing the environmental and economic impact of any product or process from "cradle to grave" helps us make better decisions. In life cycle assessment (LCA), every stage of a product or process's lifecycle is considered including raw material extraction, processing, and manufacturing, transportation, use and end of life (Fig. 3.21).
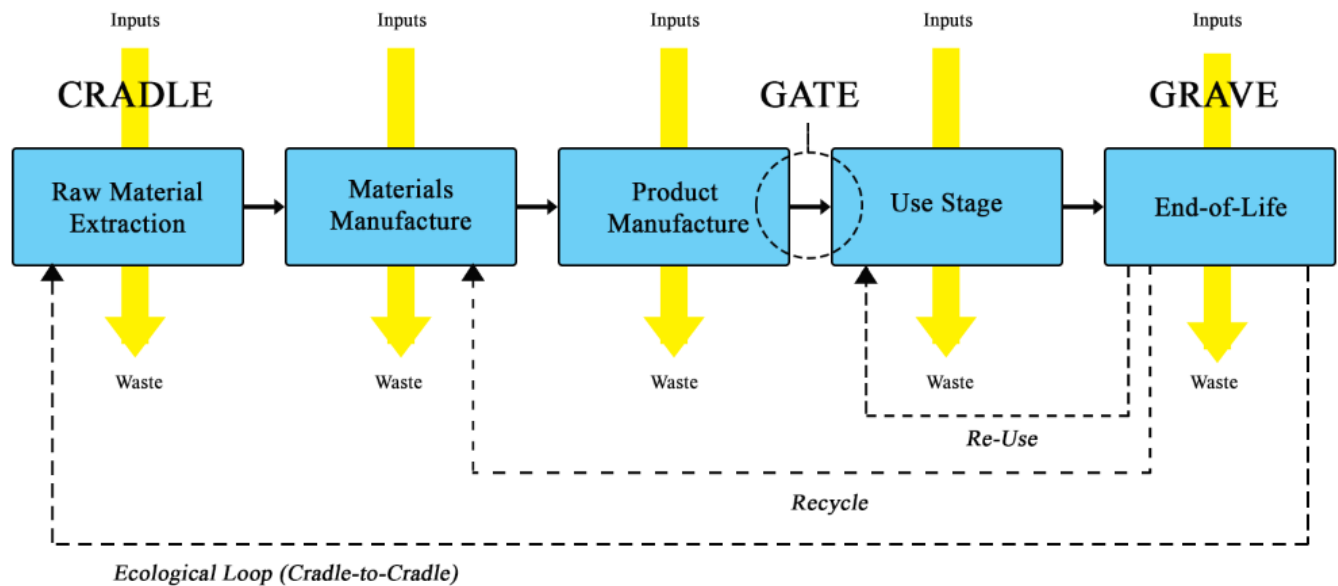
Figure 3.21: Stages of Life Cycle Analysis

LCA was done using Sustainable Minds; a cloud-based Life Cycle Assessment software (ISO 14025) that estimates, analyzes, and compares products' performance to improve the product development process [Sustainable Minds]. This software analyzes ecological damage by considering carbon emissions, acidification, ecotoxicity, ozone depletion and eutrophication. Other environmental releases such as smoke, carcinogens, and non-carcinogens and the human health damage due to this environmental release are considered.

The lab-scale version of the equipment for conducting the Waseda process was modeled in Sustainable Minds. An industrial-scale version of the equipment would have less environmental impact per kg of methane generated, but we did not have information about the parts needed for an industrial-scale system. The functional unit of the estimated environmental impacts was chosen as per kg of methane generated. The lifetime was chosen to be 20 years, as a standard lifetime,

since the Waseda process is in the research stage and no data is available on actual lifetimes. Inputs into Sustainable Minds for the different stages of the life cycle are summarized below:

3.7.1 Manufacturing

For the Manufacturing stage of the System Bill of Materials (SBOM), the 14 components of the lab-scale system for conducting the Waseda process were input as shown in Table 3-4 and Figure 3.22. Replacements for 11 of the items were assumed to be bought together at the beginning of the project, as it is convenient to purchase them in bulk quantity. 3 items (Thermocouple, DC power supply, and flow meters) were assumed to be bought again at year 10 due to their 10-year lifespan. The mass of replacement items was included in the System Bill of Materials input.

Table 3-4: Estimated replacement time of components of the lab-scale Waseda process

Item no	Item name	Replacement time	Reference
1	Plastic Tube	10 years	The guardian.com
2	Rubber stoppers	7 years	Stangnet.com
3	Quartz glass	10 years	Wastewatercenter.com
4	Thermocouple	10 years	Homedepot.com
5	DC power supply	10 years	Bravoelectro.com
6	Pyrometer	10 years	Wika.us
7	AAA batteries	4 months	Energizer.com
8	Heating pads	5 years	Amazon .com

Concept overview	System BOM	Results

▶ Manufacturing   Use   End of life   Transportation

Add a Part +   Add Sub-Assembly +   Import BOM +

Name	Material/Process	Qty	Amt	Unit	mPts	CO₂ eq. kg	MS	Part ID
Tee fittings *Measured, 12 gm*	Thermoplastic polyurethan	1	0.026	lb	4.12×10^{-3}	0.0386	E	
Tube for hydrogen *Measured weight = 0.60 lb or 270*	Thermoplastic polyurethan	1	0.6	lb	0.0951	0.890	E	
Copper Electrodes *Measured 25 g*	Copper, secondary, from e	1	0.055	lb	1.01×10^{-4}	2.85×10^{-3}	E	
Rubber Stopper *Measured 708 gm total, each 12.(*	Polybutadiene Rubber	1	1.56	lb	0.158	2.76	E	
Quartz Glass Tube *Measured 80 gm.*	Glass-packaging, white	1	0.18	lb	3.97×10^{-3}	0.0578	E	
Silica Catalyst Bed *Measured total = 114 g = 0.25132*	Silica sand	1	0.25	lb	1.42×10^{-4}	2.65×10^{-3}	E	
Thermocouple *Measured 45 gm.*	Steel, electric, chromium s	1	0.099	lb	0.264	0.246	E	
Tedlar gas collection bag *20 g each, 10 of them, 200 g= 0.4*	Polyvinylchloride, PVC	1	0.445	lb	0.0314	0.398	E	
Pyrometer *Measured 150 gm * 2 = 300 gm =*	Polypropylene, PP	1	0.661	lb	0.0394	0.589	E	
Multimeter and wire *Measured, 331 gm*	Polypropylene, PP	1	0.73	lb	0.0436	0.651	E	
Heating pads *Measured, 10 gm*	Nylon 66	1	0.02	lb	3.85×10^{-3}	0.0725	E	
DC power supply *Estimated, 1.3 Kg each * 6 = 7.8 ł*	Polyvinylchloride, PVC	1	17.19	lb	1.21	15.4	E	
Flow meters *Estimated 1 lb*	Polyvinylchloride, PVC	1	1	lb	0.0705	0.894	E	
AAA bateries *Estimated*	Aluminium, secondary, fror	1	1	lb	0.116	0.689	E	
Ruthenium(III) acetylacetona *Ruthenium(III) acetylacetonate, 1;*	Chemicals organic	1	0.002205	lb	1.49×10^{-4}	1.96×10^{-3}	E	
Cerium (IV) oxide *Cerium (IV) oxide, 10 gm = 0.022*	Cerium concentrate, 60% (	1	0.022046	lb	0.0164	0.0852	E	
Manufacturing total					**2.06**	**22.7**	**E**	

Figure 3.22: Inputs for the manufacturing phase of the environmental LCA for the lab-scale Waseda process

3.7.2 Use

In the use phase, it is assumed that there will not be any use of water as the system does not require cleaning. The highest amount of methane was produced during the impact of the power experiment when the reactor ran for 1 hour. The maximum voltage used was 240.2 V and the ampere used was 0.23 A recorded from the multimeter reading. Total wattage was 54.53 W. Now, $kWh = \frac{W \times Hourts}{1000}$

$= \frac{54.53 \times 1\ hr}{1000} = 0.05453$ kWh. Assuming the system will be running for 24 hours/day and 365 days a year, for 20 years., the power use for 20 years = 0.05453 kWh × 24 ×356 × 20 years = 9553.66 kWh. Hydropower and solar power were compared as sources of energy to power the Waseda process.

Copy of Electrocatalytic conversion of carbon dioxide > Concepts > **Carbon dioxide to methane conversion - Hydro**

Concept overview	System BOM	Results

Manufacturing	▶ Use	End of life	Transportation

Learn mor
System BC
Use stage
Consumab

Name	Consumables/water/power	Amt	Unit	mPts	CO₂ eq. kg	MS	
📁 Consumables				0	0		
No consumables have been added to this SBOM.							
📁 Water use				0	0		
No water use has been added to this SBOM.							
− 📁 Power use				5.47	50.8	E	
📄 Power Calculated	Hydro power, at reservoir power plan 9553.66	kWh	5.47	50.8	E		
Use total				**5.47**	**50.8**	**E**	

Figure 3.23: Inputs for the use phase of the environmental LCA for the lab-scale Waseda process

Emission savings from methane energy produced by the Waseda process were estimated, assuming the power displaced comes from the regular US power grid, as shown in Fig. 3.24 below. Total methane mass produced in the power reaction, assuming that the laboratory apparatus operates 24 hours a day for 20 years and using the highest amount of methane produced from the lab experiments, is 274.77 kg. 1 kg of methane when burned produces 53,940 kJ of energy [World-neuclear.org]. Assuming an average turbine efficiency of 29% [Reference], the amount of electricity that could be generated is 1195.25 kWh. Although more hydropower energy was needed to produce the methane (9554 kWh) than was produced by burning the renewable methane (1195 kWh), methane can be used to power vehicles and appliances, which cannot be powered directly using hydropower. Additional research is needed to reduce the amount of energy needed

Name	Consumables/water/power	Amt	Unit	mPts	CO_2 eq. kg
📁 Consumables				0	0
No consumables have been added to this SBOM.					
📁 Water use				0	0
No water use has been added to this SBOM.					
− 📁 Power use				59.5	1.01×10^3
📄 Power	Electricity, 120 V, US	1195.25	kWh	59.5	1.01×10^3
	Use total			59.5	1.01×10^3

Figure 3.24: Inputs to use phase for estimating emission savings from burning methane generated

68

to generate the methane. Scaling the process up from lab scale to field scale would provide some reduction of energy used per mass of methane generated, due to efficiencies of scale.

3.7.3 End of life:

In the end-of-life stage, it was assumed that every item used in this experiment is recyclable and will be recycled after 20 years. There was no net emission in this stage because Sustainable Minds allocates emissions associated with recycling to the new product that is made from the recycled material.

3.7.4 Transportation

It was assumed that all the necessary items were purchased locally within a radius of 100 miles. A combination truck with an average fuel mix (assuming 100% diesel and 0% gasoline) chosen for the transportation of the raw materials.

3.8 Life cycle cost analysis

A life cycle cost analysis was conducted in dollars per kg of methane produced to provide insight into the financial feasibility of the project for initial setup, maintenance costs (parts replacement), and operating cost (electricity) for a standard lifetime of 20 years. Several items/materials such as plastic tubes, tee fittings, AAA batteries, rubber stoppers, glass tubes, and silica wool bed were considered to be bought in bulk quantity at the project initiation, so their value is already in present worth. Thermocouples, DC power supplies, and Pyrometers were bought in Year 10 and the cost of these purchases was converted into present worth at an interest rate of 2% [Macrotrend, 2020].

Chapter 4
Results and Discussion

4.1) Catalyst Characterization

The topography and elemental composition of the catalysts were analyzed respectively by the Field Emission Scanning Electron Microscope (FE-SEM) and Energy Dispersive Spectroscopy (EDS) by using Hitachi S-3000N. The captured images were used to visualize the microstructure of catalysts from several magnifications. Three different catalyst samples listed below were analyzed:

a) Sample a: catalyst prepared in a muffle furnace following the method of Manabe (2016).

b) Sample b: catalyst prepared in a tube furnace following the method of Yamada (2020).

c) Sample c: used catalyst.

4.1.1 FE-SEM Results:

Figure 4.1 below shows the FE-SEM topography or microstructure of the catalyst prepared in a muffle furnace following the method of Manabe (2016) at two different magnifications (200 µm at left and 30 µm at right). The lighter portions in those images resemble particles with charge, implying the conductive nature of particles.
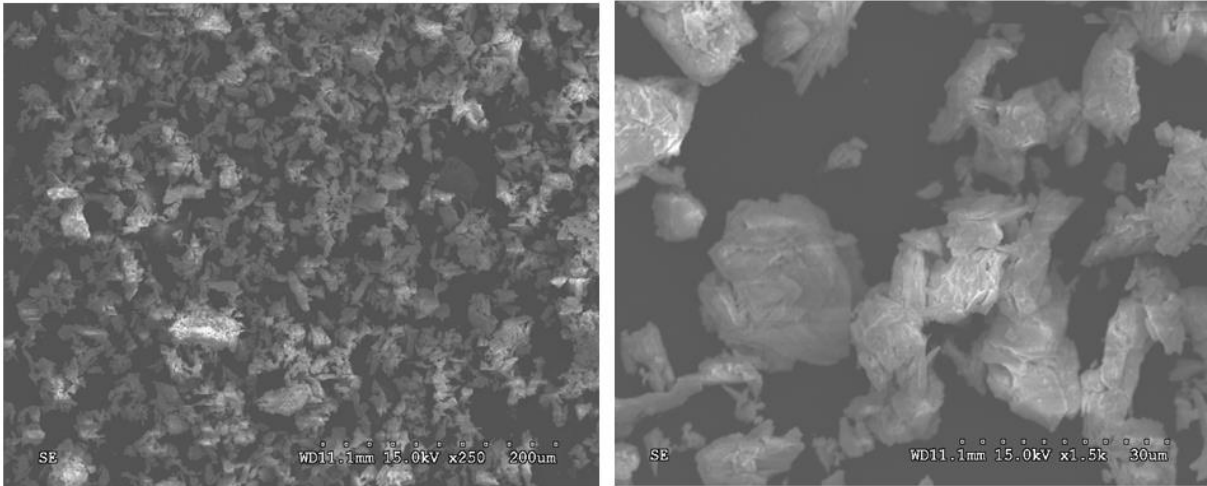
Figure 4.1: SEM analysis for the catalyst prepared in a muffle furnace following the method of Manabe (2016).

Figure 4.2 shows SEM analysis for the catalyst prepared in a tube furnace following the method of Yamada (2020) at two magnifications (50 µm and 30 µm). From visual observation, the lighter portion/ conductivity seemed similar. The particle size of the samples also looked similar: both had a combination of different size particles, with none of the particles larger than 75 microns. The microstructure of the samples looked similar as well, with no clusters detected. Clusters can reduce the performance of catalyst due to less active surface area.
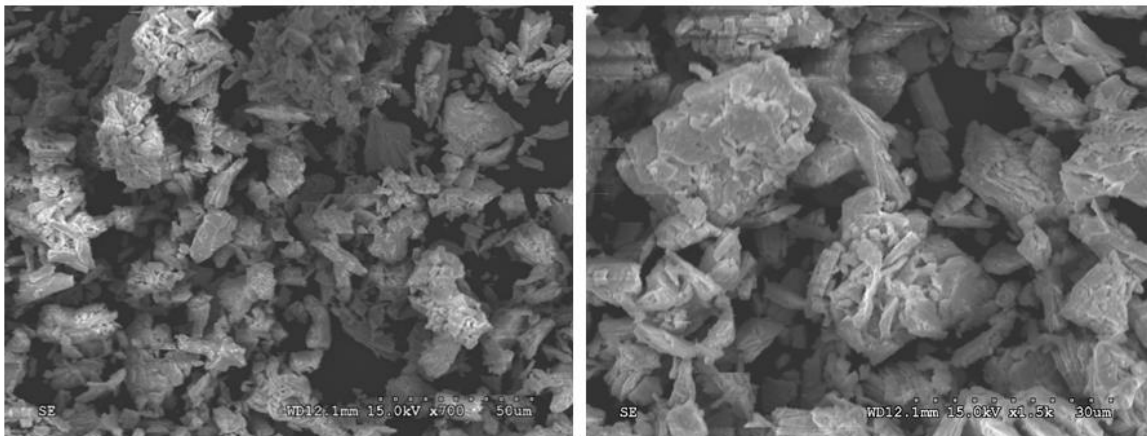
Figure 4.2: SEM analysis for the catalyst prepared in a tube furnace following the method of Yamada (2020).

Figure 4.3 shows SEM analysis for the used catalyst prepared in a tube furnace following the method of Yamada (2020), with a magnification scale of 500 µm and 30. The conductivity, particle size, and microstructure generally look similar to that of the fresh catalyst. However, the used catalyst also has elements present that look like thin hair, presumably silica from the catalyst bed attached to the used catalyst.
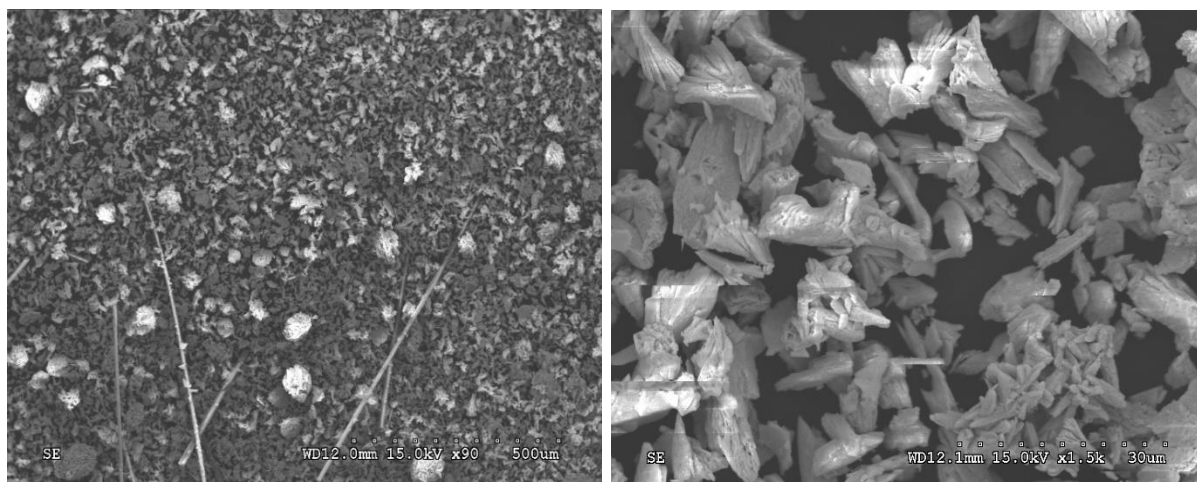
Figure 4.3: SEM analysis for the used catalyst prepared following the method of Yamada (2020)

4.1.2 Energy Dispersive Spectroscopy (EDS) results

Figure 4.4 below shows the Energy Dispersive Spectroscopy (EDS) results for the catalyst sample prepared in a muffle furnace. The elements present in the catalyst were ruthenium, oxygen, cerium, and carbon, which were all expected because they were used in catalyst preparation. No impurities were found. Figure 4.5 below shows EDS results for catalyst sample b, prepared in a tube furnace following the process of Yamada 2020. The elements were the same as the catalyst prepared in the muffle furnace. Even though the method was different, $0.5wt\%Ru/CeO_2$ was prepared in both

cases. Thus, the expected elements (ruthenium, oxygen, cerium, and carbon) were detected through

EDS. No other elements/impurities were detected.
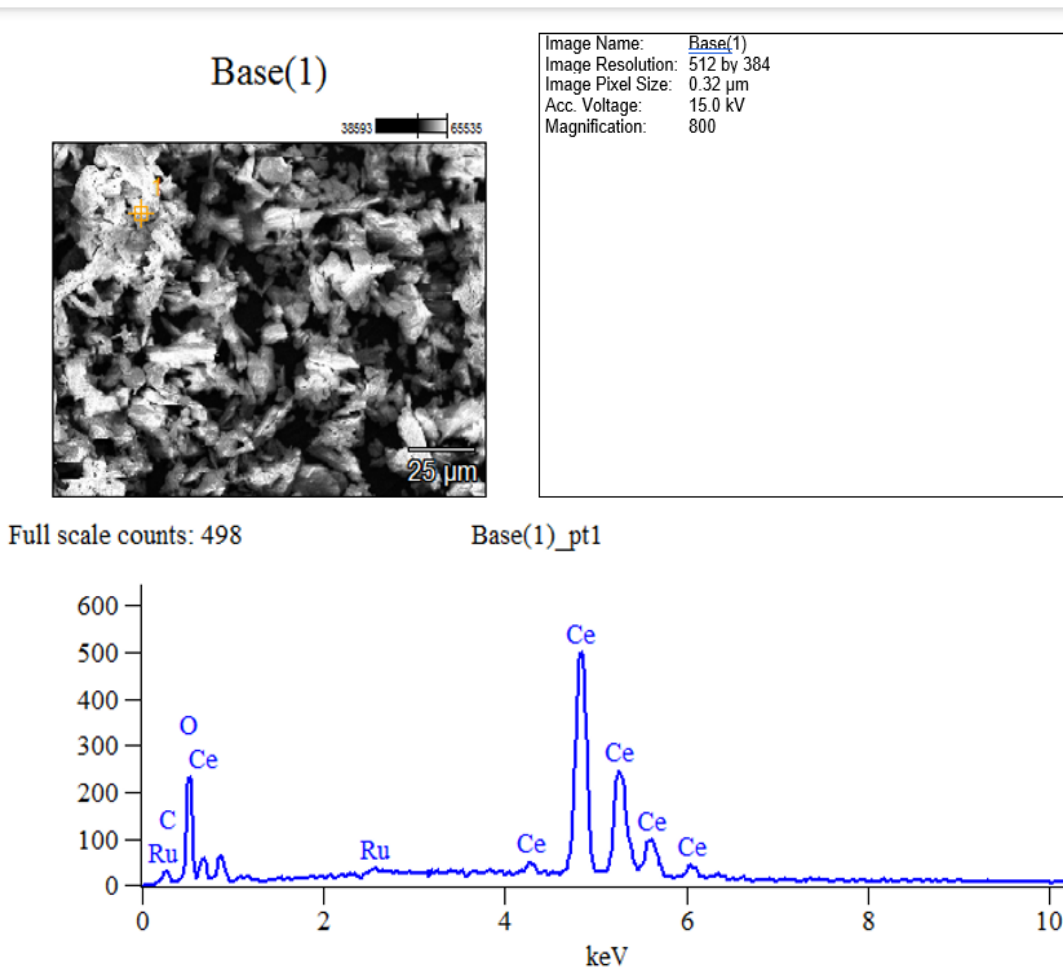
Figure 4.4: EDS analysis for the catalyst prepared in a muffle furnace following the

method of Manabe (2016).
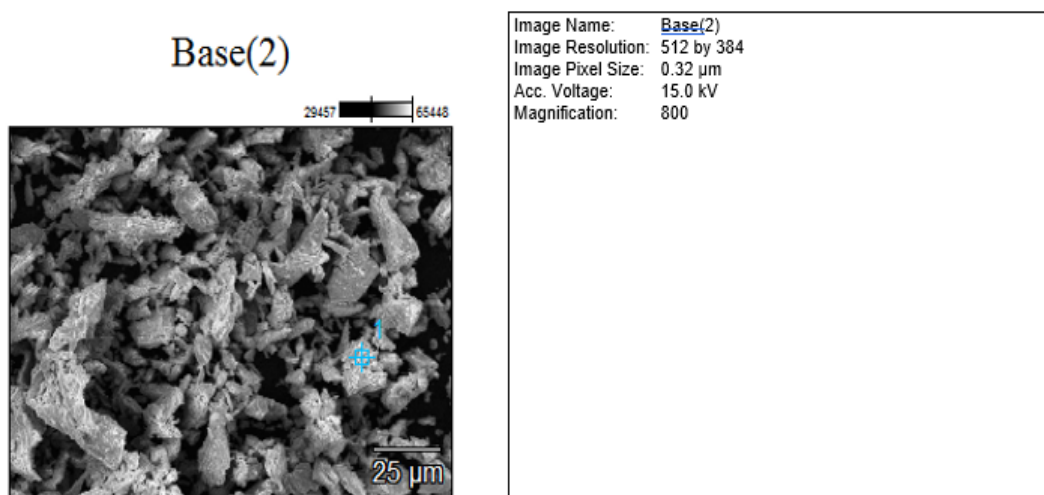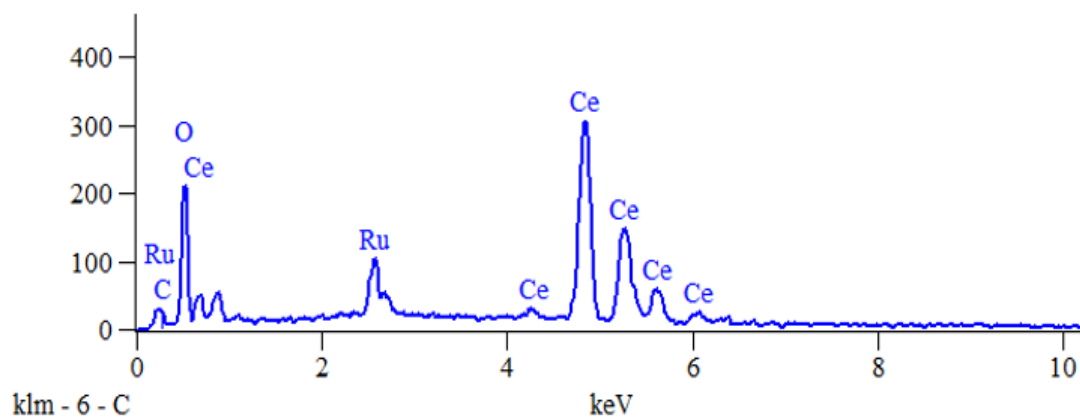
Figure 4.5: EDS analysis for the catalyst prepared in a tube furnace following the method of Yamada (2020).

Figure 4.6 below shows the Energy Dispersive Spectroscopy (EDS) results for the used catalyst. The presence of silica was confirmed, as suspected from the SEM analysis, along with oxygen, cerium, and carbon. A peak at around 2.5 keV indicates ruthenium, although it is not labeled.
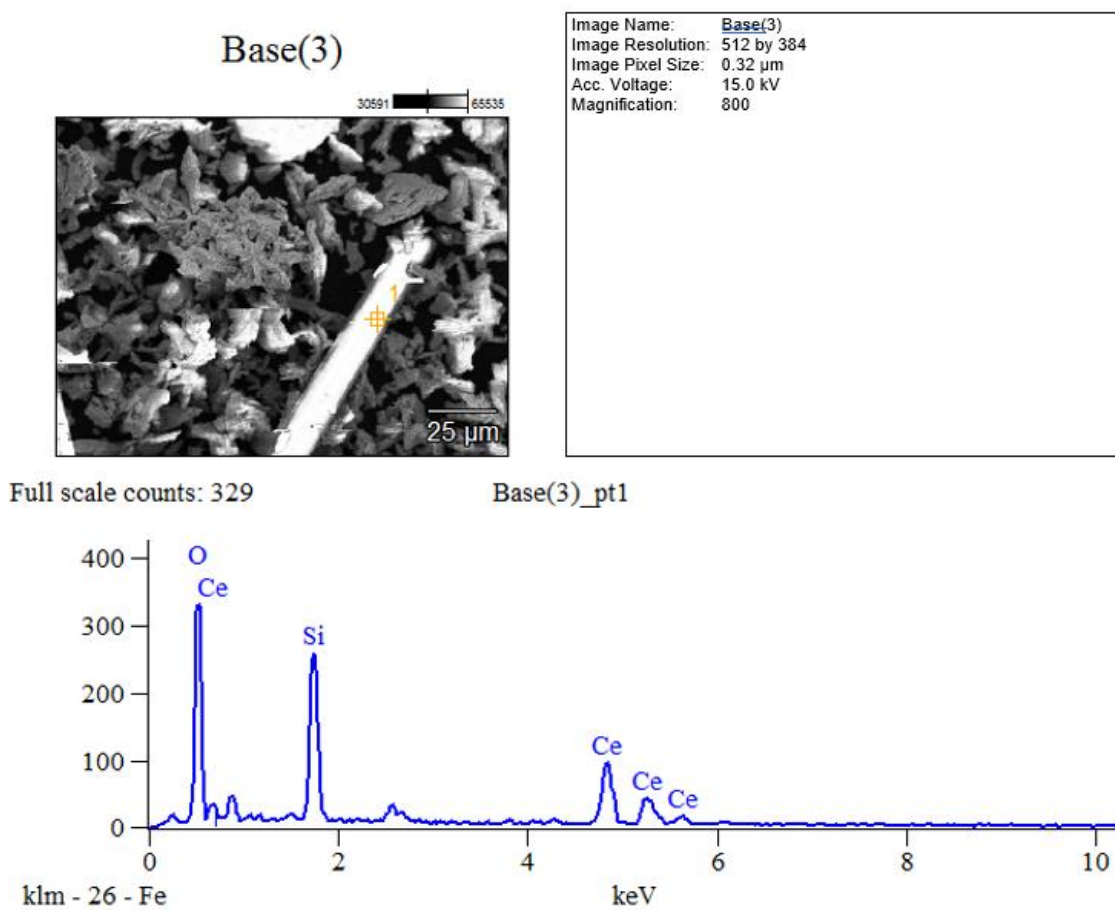
Figure 4.6: EDS analysis for used catalyst prepared following the method of Yamada (2020)

Table 4-1 compares the EDS composition results for the 3 samples. In the used catalyst, silica was detected that was attached to the catalyst from the silica wool bed. The weight percents for the other elements differ among samples a, b, and c because the EDS values are for a single data point on the catalyst surface and do not account for average composition.

Table 4-1: Catalyst composition comparison

	Wt.% O_2	Wt.% Ce	Wt.% C	Wt.% Ru	Wt.% Si
Sample a: catalyst prepared in a muffle furnace following the method of Manabe (2016)	18.64	72.55	0.01	8.80	0.0
Sample b: catalyst prepared in a tube furnace following the method of Yamada (2020)	7.45	84.76	0.70	7.09	0.0
Sample c: used catalyst prepared in a tube furnace following the method of Yamada (2020)	23.37	59.43	0.0	7.82	9.37

Figure 4.7 shows the visual difference (color) between the catalyst prepared in a muffle furnace tube furnace (left) and a muffle furnace (right). The chemical composition in both samples is the same based on the catalyst characterization. The reason for this visual color difference is unknown and needs further investigations in the future.
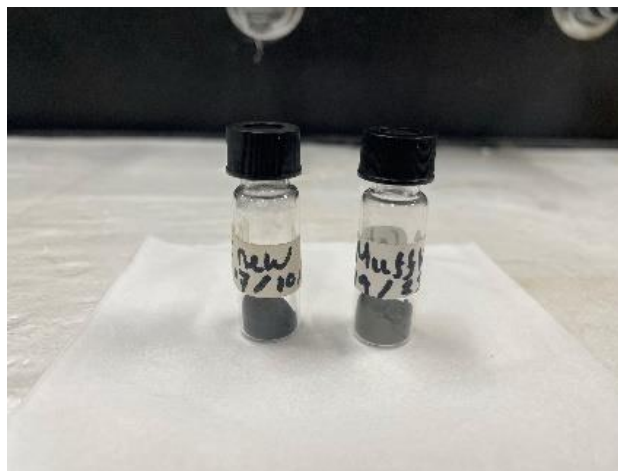
Figure 4.7: Visual difference of catalyst samples prepared following the method of Yamada (left) and Manabe (right)

4.2 Results of Obj. 1: Explore the impact of independent variables (time, power, temperature, catalyst preparation method, electric field's type, degradation of catalyst over time, performance of reactivated used catalyst) on synthetic landfill gas.

For the baseline experiment (4.2.1) and the degradation of catalyst over time (4.2.6) duplicates and their averages were taken for graphical illustration. Triplicates and their averages were used for the rest of the experiments below. The standard deviation of those date points has also been calculated and presented in the graph of each experiment.

4.2.1 Baseline Experiment: room temperature and pressure, 36.7 W power, no added heat, fresh catalyst prepared 0.33 gm, uniform electric field.

Figure 4.8 below shows the average methane fraction vs. time for the baseline reaction. The initial average fraction was measured from a combined gas flow (200 SCCM) of synthetic landfill gas, argon, and hydrogen gas that was flowing in the inlet before the electric field was imposed. The initial fraction of methane was measured using the GC. This measured methane fraction was less

77

than the synthetic landfill gas methane fraction (0.5) since the argon and hydrogen diluted the landfill gas fraction. As shown in Figure 4.8, an increased methane concentration was recorded throughout the experiment compared to the initial concentration of 0.092, with the increase ranging from 0.2 to 35%. The increase in methane concentration was significant at 10 and 20 minutes with a confidence level of 90 and 94% respectively based on a student's T-Test. The highest methane fraction was recorded as 0.123 at around 20 minutes, which represented a 35% increase in methane over the initial concentration. After 20 minutes, there was a decreasing trend in the conversion process, possibly due to reactants and water vapor produced during the reaction not desorbing and occupying active surface area of the catalyst. The increase in methane concentration at 30, 40 50 and 60 minutes is less significant (confidence level is in a range of 53% to 59%).
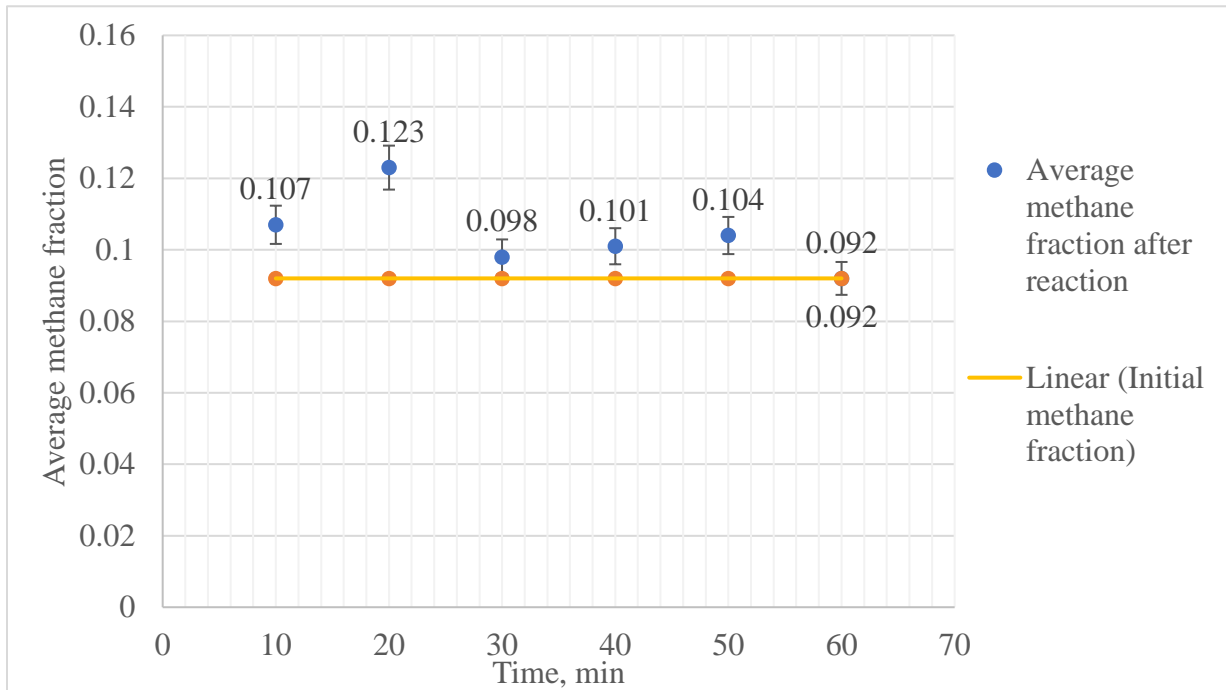
Figure 4.8: Methane fraction over time for the baseline experiment

4.2.2 Impact of power: room temperature and pressure, no added heat, fresh catalyst prepared 0.33 gm, uniform electric field.

In this experiment, the impact of different powers (W) was analyzed. Other parameters such as temperature, gas flow rates, catalyst, catalyst weight, spark gap, and time were kept constant. As zero volts do not impose any electric field (EF), the initial power for this experiment was set at 28.34 W and the maximum power applied was 54.53 W (thus, the horizontal axis of Figure 4.9 does not start at 0.0 W). The initial methane fraction in this experiment was 0.081, which is slightly different than the baseline initial methane fraction, possibly due to the use of a different syringe for the GC.

The strength of an electric field is directly proportional to the power applied; 54.53 W imposed the strongest electric field. It was hypothesized that a strong EF would provide energy to overcome the activation barrier of CO_2 and thus increase the methane conversion rate. The methane fraction of the gas collected at 54.53 watts was the highest and accounts for a 37.16% increase. The R^2 value for the regression line shown in Fig. 4.9 is 0.0185, however, which represents no correlation between power applied and methane fraction. A Q.TEST, however, showed that the data point 0.104 at 47.84 W was an outlier. After removing this point, the R^2 value increased to 0.94, as shown in Figure 4.10, This indicates that increasing the power did increase the methane conversion rate.
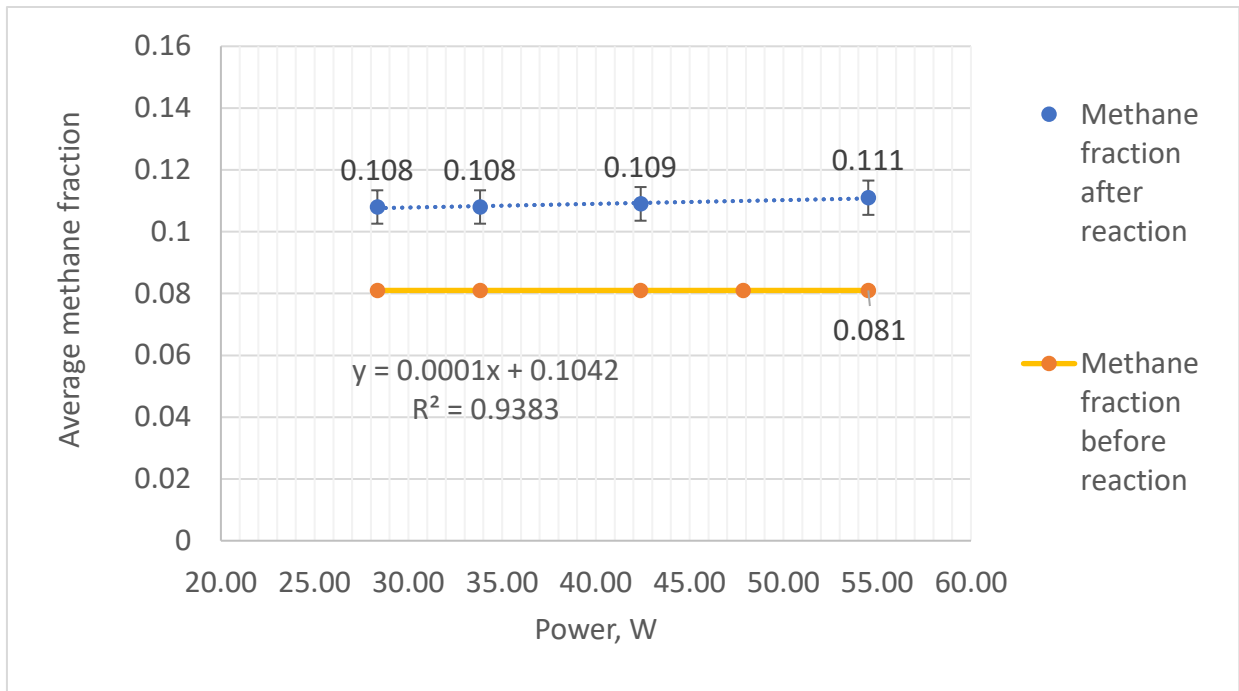
Figure 4.10: Methane fraction vs. power applied
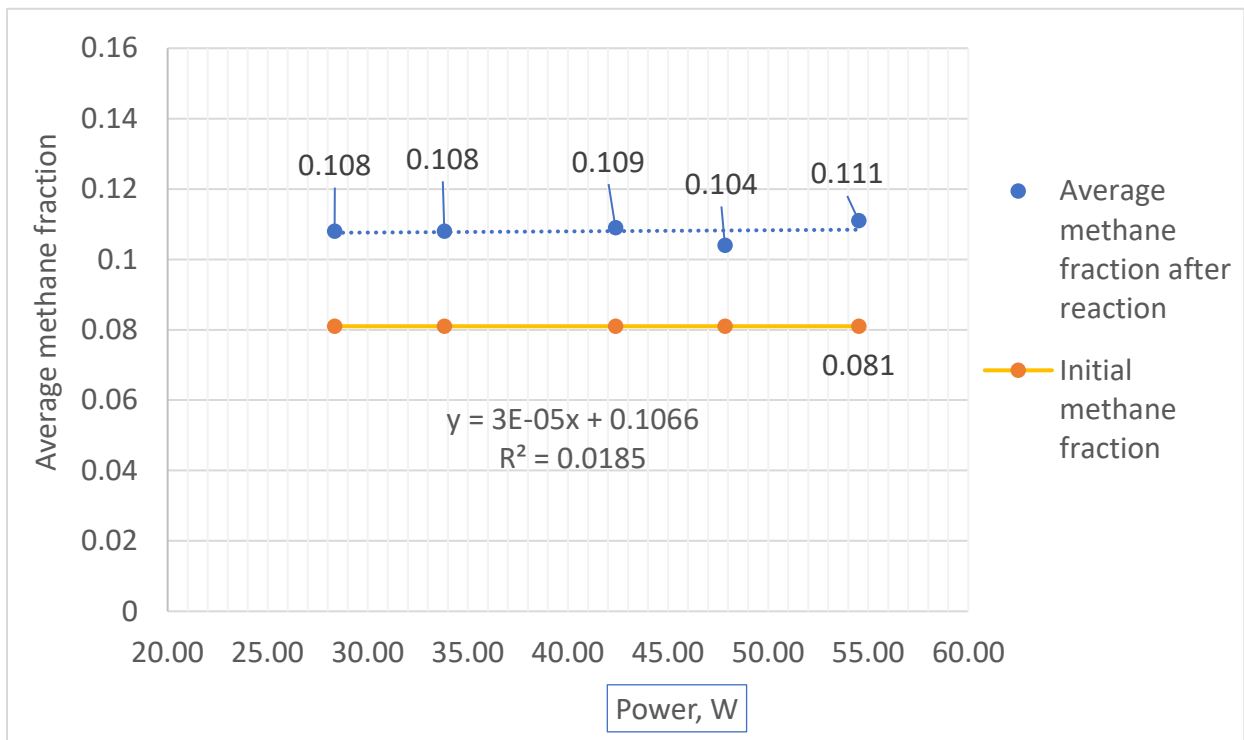
Figure 4.9: Methane fraction vs. power applied

4.2.3 Impact of applied temperature in the presence of an electric field (EF): 1 atmospheric pressure, fresh catalyst prepared 0.33 gm, uniform electric field.

In this experiment, the impact of applied heat in presence of an electric field was analyzed. Other parameters such as temperature, gas flow rates, catalyst, catalyst weight, spark gap, and time were kept constant. Figure 4.11 below shows the average methane fraction recorded before and after applying EF and heat together. The highest increase in methane concentration was around 7.0%. Given the error bars, it is difficult to conclude that there was a substantial change in the initial concentration due to the addition of heat. This is likely due to the fact that gaining extra energy from two separate energy sources (heat and EF) may overexcite the molecules, preventing them from attaching together as a product. A T-Test was performed to analyze whether the difference in methane concentration before and after electrocatalysis in presence of heat and EF was significant or not. For most of the data points it was not significant, as the confidence level was not higher than 70% except at 100°C and 140°C (at 140°C, fraction was actually lower).
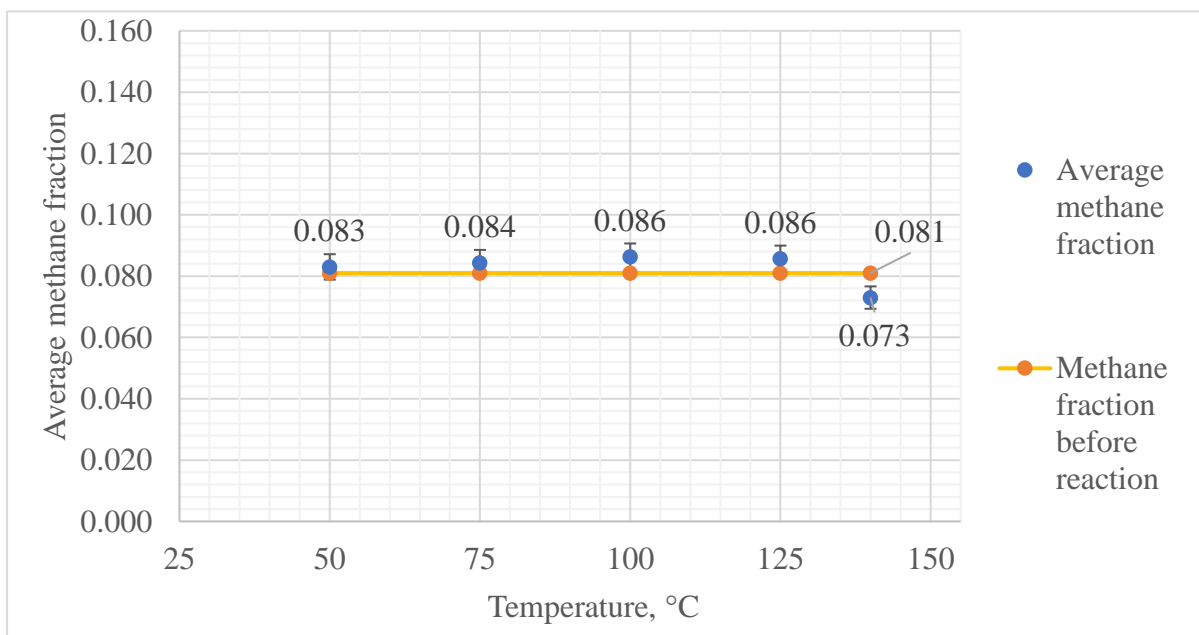
Figure 4.11: Methane fraction vs. temperature

81

4.2.4 Impact of Catalyst preparation method: room temperature and pressure, 36.7 W power, no added heat, fresh catalyst prepared 0.33 gm, uniform electric field.

Figure 4:12 compares methane fraction produced by using catalyst prepared using two different methods: that of Yamada (2020) and Manabe (2016). The variables of these experiments were catalyst preparation and time; others were constant as discussed in the baseline experiment. The methane fraction over time is identical for both catalysts. except for 60 minutes. However, the data point 0.087 and 0.092 is significantly different as determined by a T-Test only at a 59% confidence level.
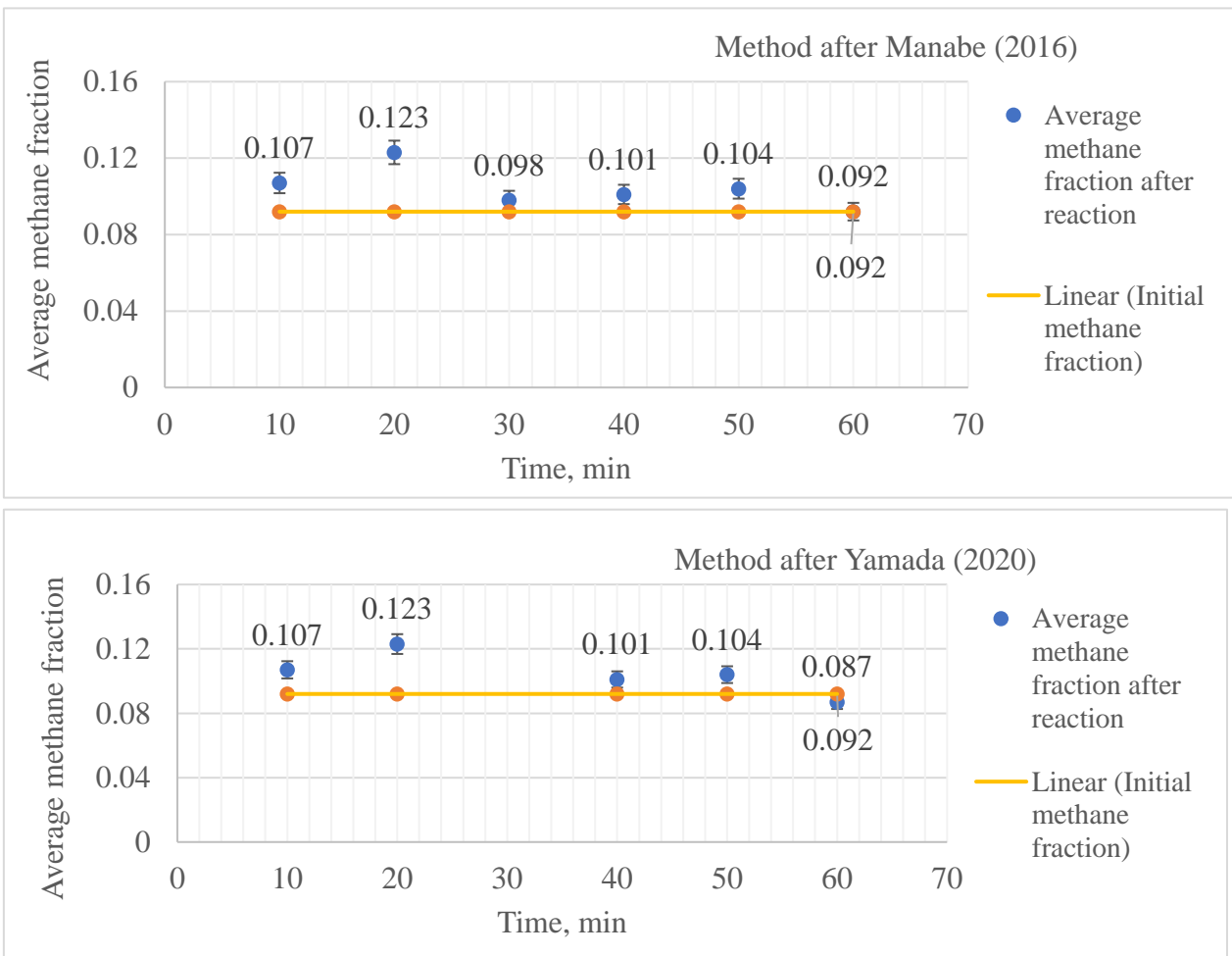
Figure 4.12: Methane fraction produced by catalysts prepared by different methods

4.2.5 Impact of electric field type: room temperature and pressure, 36.7 W power, no added heat, fresh catalyst 0.33 gm, new ununiform electric field.

Figure 4.13 shows the comparison between methane fraction produced in presence of a uniform EF and a non-uniform EF. The non-uniform EF converted less CO_2 to CH_4 than the uniform EF probably because the interruption in EF reduces the strength of the electric field and the molecule could not pass their activation barrier to form new bonds.
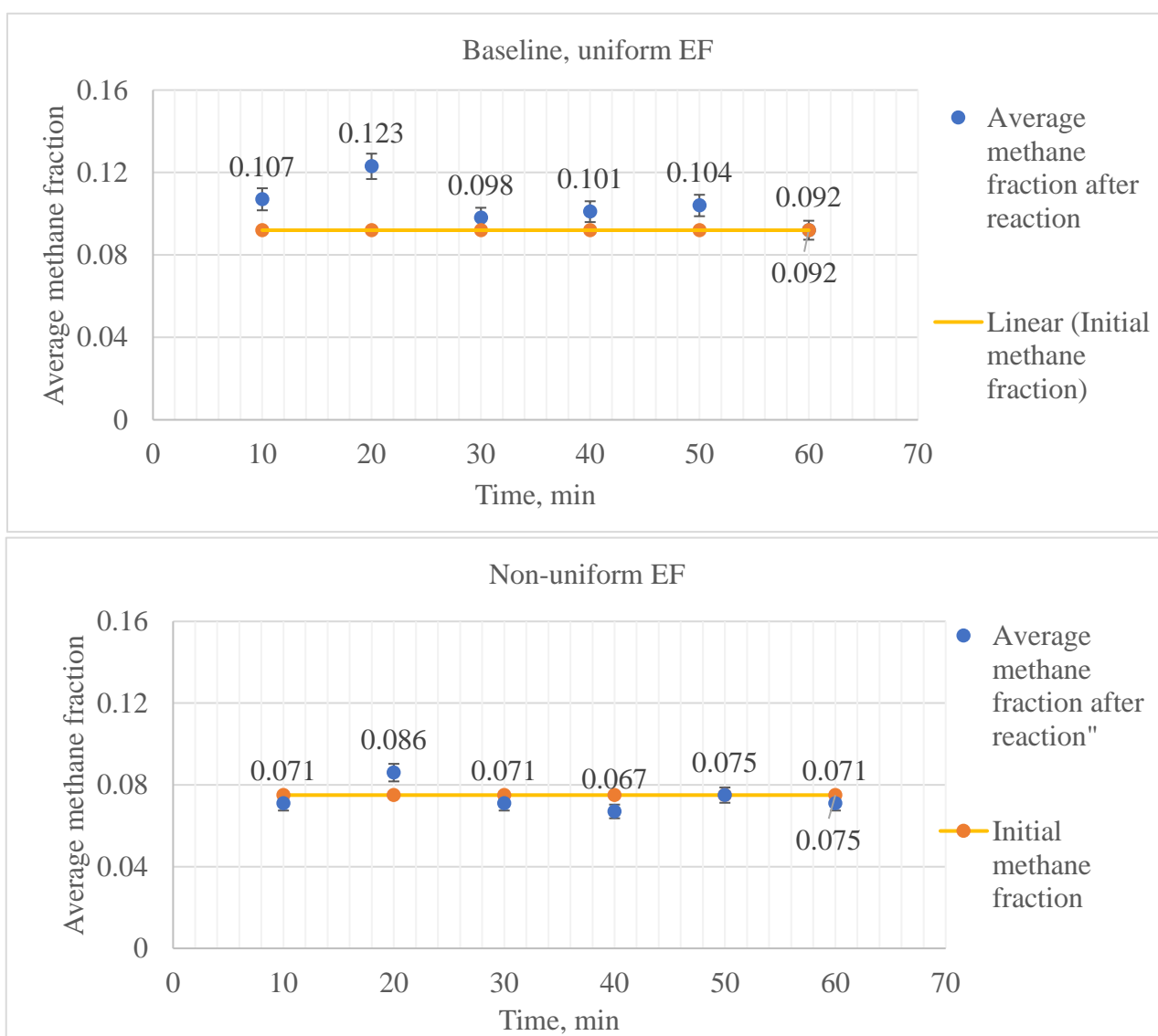
Figure 4.13: Methane fraction with uniform EF vs. non-uniform EF

The uniform EF converted significantly more methane than non-uniform EF, to at least a 98% level of confidence from the beginning of the reaction (10 min) until 40 minutes, and at a 75 & 76% confidence level at 50 and 60 minutes, respectively.

4.2.6 Degradation of Catalyst over time: room temperature and pressure, 36.7 W power, no added heat, freshly prepared catalyst 0.33 gm, uniform electric field.

The duration of this experiment was longer than the baseline experiment, to measure catalyst degradation over time. Figure 4.14 below represents the average methane fraction before (orange solid line) and after (blue data points) electrocatalysis. The highest methane fraction converted occurs at around 20 and 40 minutes. At 80 minutes, the conversion recorded is lowest, with an increase at 90 minutes. With the exception of 90 minutes, the overall conversion has a slightly decreasing trend after 40 minutes, perhaps because products fail to desorb from the catalyst, reducing the active surface area. The decrease in methane concentration from 40 minutes to 50 minutes was significant (91% confidence). Reactivating the catalyst would likely be beneficial.
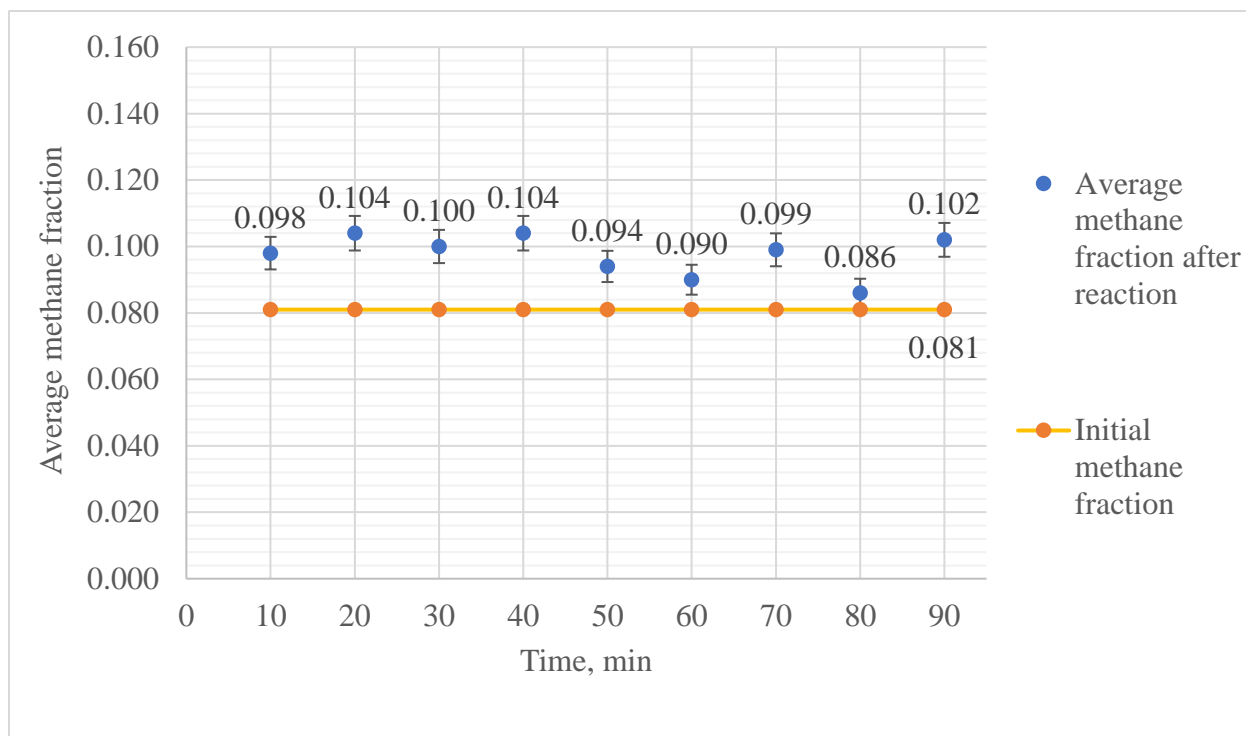
Figure 4.14: Methane fraction vs. time to assess catalyst degradation

4.2.7 Reactivating the Catalyst: room temperature and pressure, 36.7 W power, no added heat, reactivated catalyst 0.33 gm, uniform electric field.

A noticeable amount of silica was detected in the used catalyst during catalyst characterization. This silica, from the catalyst bed, could potentially block the active surface of the catalyst and reduce the catalyst activity. Figure 4.15 below shows the average methane fraction after the reaction using the reactivated catalyst. Reactivated catayst converted less methane than the freshly prepared catalyst. The difference between before and after mean values for the experiment conducted with fresh catalyst is higher at all times than the difference between the before and after mean values for the experiment conducted with reactivated catalyst. The differences with fresh catalyst and reactivtated catalyst are significantly different to a 99% level of confidence at all

times. The average difference for fresh catalyst was 6.1 and the average difference for reactivated catalyst was 2.1.
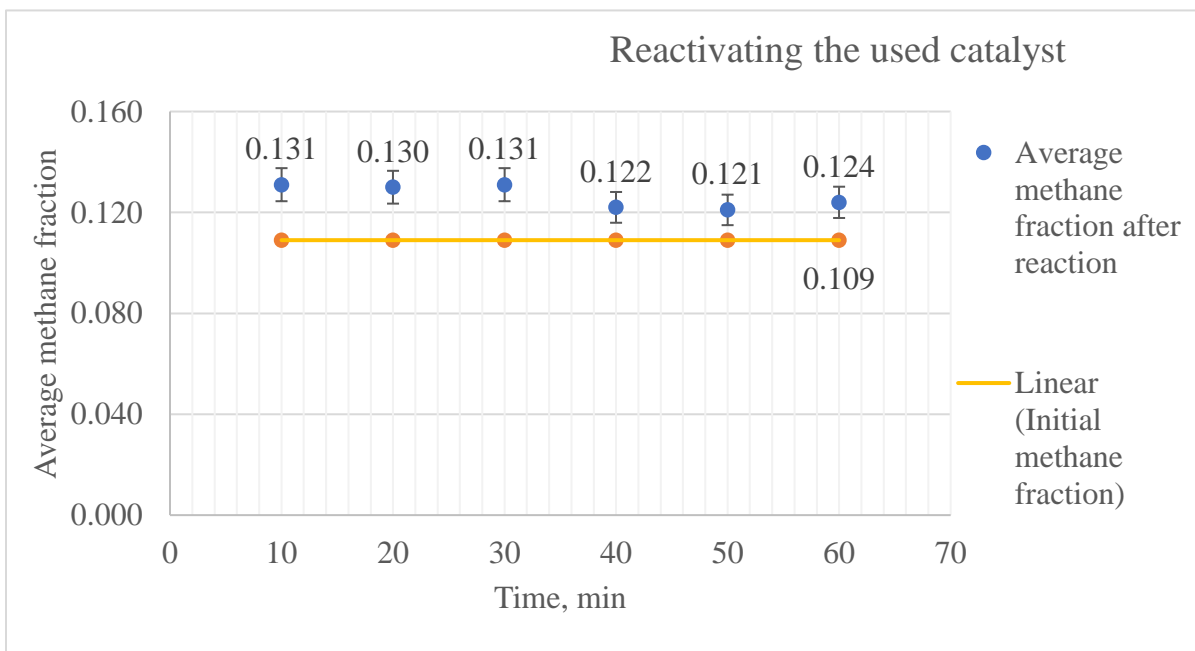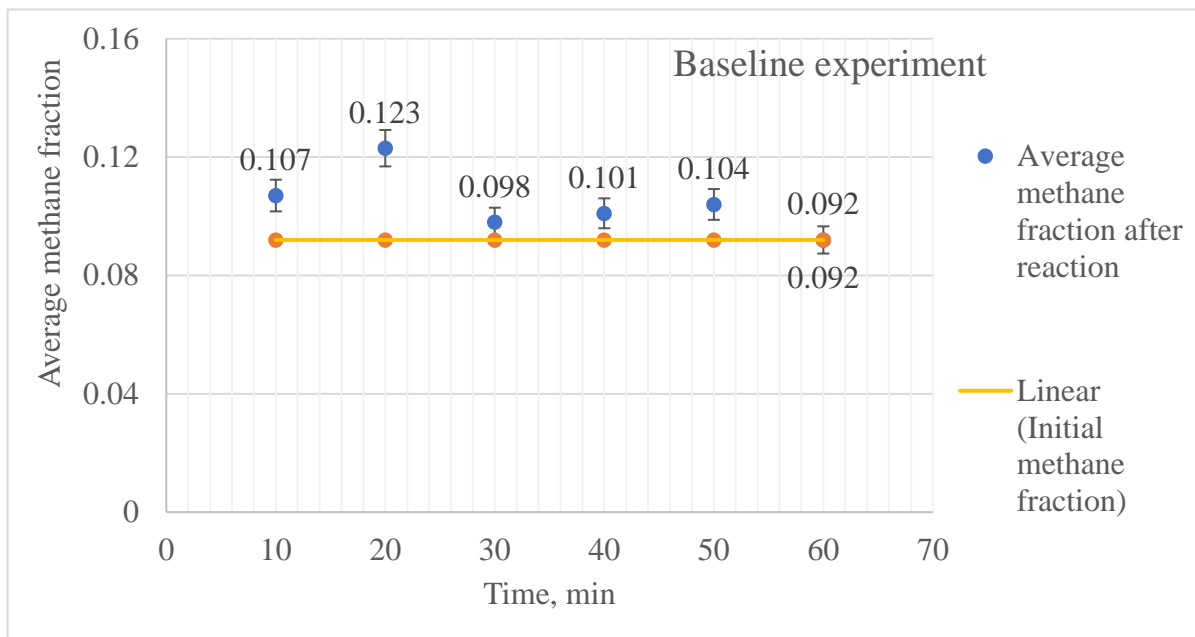
Figure 4.15: Methane fraction produced with new catalyst vs. reactivated catalyst

4.8 Results of Objective 2: Using the best values of process variables determined in Obj. 1, test the Waseda process with real landfill gas (54.43 W, uniform EF, and 0.33 gm new catalyst)

The landfill gas was collected in Tedlar gas sampler bags from a landfill in Texas. The gas was collected from a header before flaring. The name and the exact location of the landfill are not released due to the owner's request. Using a Landtec Gem 5000, the landfill gas constituents were measured as follows: hydrogen sulfide (H_2S) 16 parts per million (ppm), carbon monoxide (CO) 48 ppm, methane 39.5 %, and CO_2 21.3 %, oxygen 6.7 %, and the balance (likely nitrogen) was 31.5%. This allows us to test the impact of the common landfill gas impurity H_2S on the Waseda process.

Figure 4.16 below illustrates the methane fraction before and after electrocatalysis on the real landfill gas. The average methane fraction after reaction shows an increasing trend apart from one data point at 30 minutes. The data points fluctuate until 30 minutes and at this point, the methane fraction is below the initial methane fraction by 3.5%. However, the T-Test showed a low confidence level for this decrease (53%). From 40 to 60 minutes, the fraction of methane increases over time and the highest conversion occurs at 60 minutes. The percent increase in methane fraction at 60 minutes was 43% and this increase is significant to a 97% level of confidence according to the T-Test. The experiment could not be continued after 60 minutes because there was not enough landfill gas.
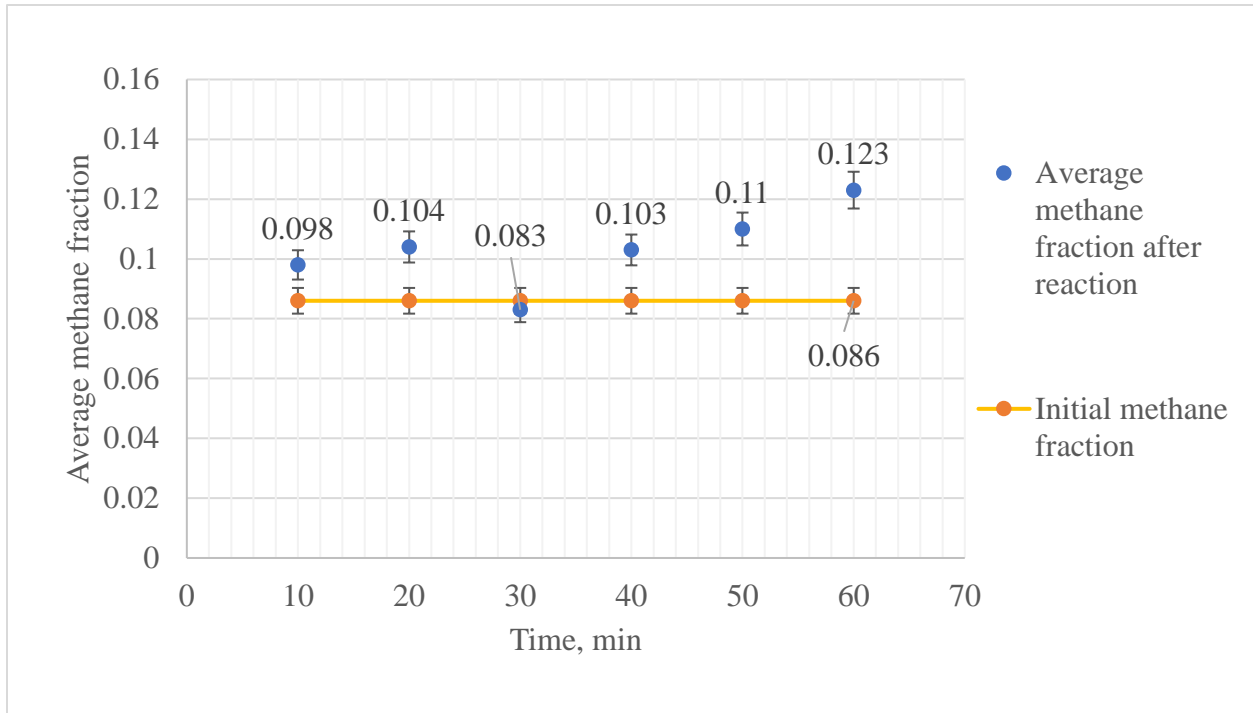
Figure 4.16: Methane fraction vs. time for real landfill gas

4.9 Results of Objective 3: Conduct a life cycle environmental and economic analyses of the Waseda process, as applied to landfill gas.

4.9.1 Life Cycle Environmental Analysis

Figure 4.17 and Figure 4.18 show the environmental impacts and CO_2-equivalent emissions from the Waseda process powered by hydropower and solar power, respectively, without considering the emissions benefit of burning the renewable methane generated.

The maximum amount of CO_2-equivalents was produced by the use phase due to the energy consumption. However, the source of the power had a critical impact. The impact of methane conversion was 7.6 mPts for hydropower and 66 mPts for solar power. The estimated carbon footprint was 1.6 kg CO_2-equivalents/ kg of methane for hydropower and 13 kg CO_2-equivalents/

kg of methane for solar. The emission savings from burning the renewable methane generated is

considered below.
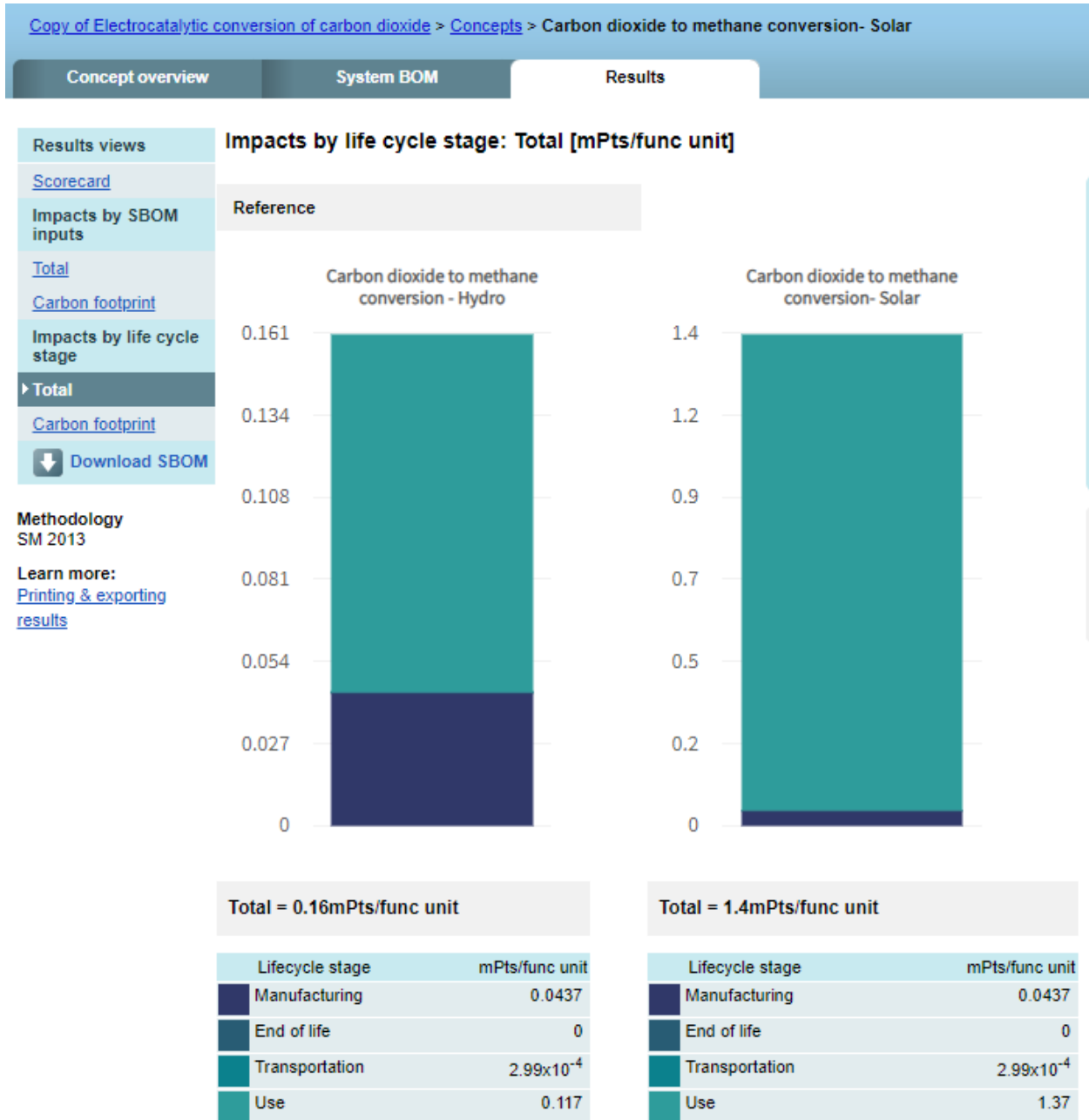
Figure 4.17: Comparison of environmental impacts of the Waseda process powered by

hydropower vs. solar power, not including benefit of burning renewable methane produced
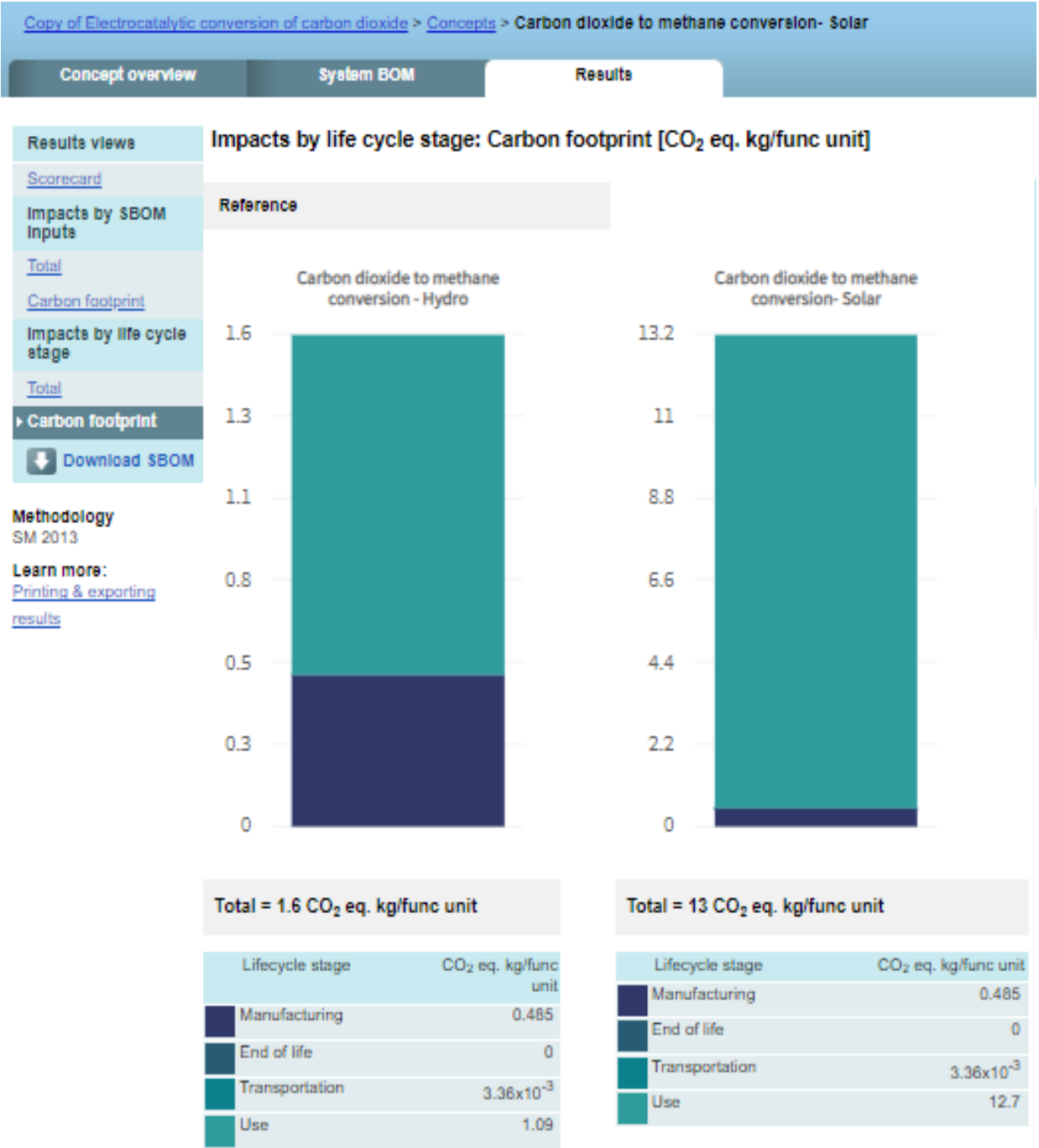
Figure 4.18: Comparison of carbon footprint of the Waseda process powered by hydropower vs. solar power, not including benefit of burning renewable methane produced

Table 4-2 summarizes the net environmental impact of the lab-scale Waseda process powered by hydropower and solar power, including the benefit associated with using the renewable methane, assuming that the electricity produced displaces that of the standard US power grid. It can be seen that the process has a net benefit in terms of environmental impact and carbon footprint only when hydropower is used to power the process (benefit of 51.5 mPts and 20.4 kg CO_2-equivalents, respectively, indicated by the negative numbers on Table 4-2). When solar power is used to power the lab-scale process, there is a net environmental impact of 7 mPts, not a benefit. An industrial-scale version of the equipment would have lesser environmental and CO_2 impact per kg of methane generated, due to efficiencies of scale, and using solar power to power the process might become feasible.

Table 4-2: Net impact of the lab-scale Waseda process, including benefit of burning methane produced

Source of Power for the Waseda Process	Impact of the Waseda Process, not including burning of methane produced		Benefit of burning methane produced		Net impact of the Waseda process, including benefit of burning methane produced	
	mPts	kg CO_2-Equiv.	mPts	kg CO_2-Equiv.	mPts	kg CO_2-Equiv.
Hydropower	7.6	1.6	59	22	-51.5	-20.4
Solar power	66	13	59	22	7	-9

4.9.2 Life Cycle Cost Analysis:

For the life cycle cost analysis of the project, a list of items was created with their current price, quantity, expected lifespan, and reference. Some items were considered buying in bulk quantity at the initial stage of the project. For the thermocouple, DC power supply, and pyrometer, present worth has been calculated as follows:

Item 1: Thermocouple

The estimated average life span of a thermocouple is 10 years [Homedepot]. Two will be needed in a 20-year time. The present worth/cost of the thermocouple is $63. After 10 years, there will be a need to purchase another and the future cost will be, $P = F (P/F, i, n)$, where F is the future worth, P is the present value, and i is the interest rate = 2.00% and n is time = 10 years. The value of (P/F, i, n) = 0.8203 from the interest rate factor table. Therefore, $P = \$63 * 0.8203 = \$51.68$.

Item 2: DC power supply

The estimated average life span of a DC power supply is 10 years [Bravoelectro]. A total of six will be needed in a 20-year time. The present worth/cost of each DC power supply is $70. After 10 years, there will be a need to purchase three more. Therefore, $P = \$70 * 0.8203 = \$57.42$.

Item 3: Pyrometer

The estimated average life span of a Pyrometer is 10 years [Yika.us]. The present worth/cost of three Pyrometer is $320. After 10 years, there will be a need to purchase one more and the future cost will be, $P = \$320 * 0.8203 = \$262.5$

The present worth of operating cost will be P = A (P/A, $i\%$, n) where annual operating cost is -$ 477.6. At a 2% interest rate, the factor (P/A, $i\%$, n) is 0.0612. Therefore, P = -$ 477.6 × 0.0612 = -$ 29.2. The total expense that includes maintenance cost of the project for 20 years has been added in Table 4-3 below.

Table 4-3: Life cycle cost analysis of the lab-scale Waseda process

Materials acquisition cost						
Item no	Name	Unit price	Life span (yrs.)	Quantity	Total price	Reference (Lifespan of items)
1	Ruthenium (III) acetylacetonate	-$ 157.95	20	1	-$ 157.95	VWR, 2023
2	Cerium (iv) oxide	-$ 53.00	20	1	-$ 53.00	VWR, 2023
3	Tee fittings	-$ 1.00	100	10	-$ 10.00	The guardian, 2023
4	Plastic tube	-$ 5.00	10	5	-$ 25.00	The guardian, 2023
5	Electrodes	-$ 6.00	50	2	-$ 12.00	Repipenow, 2023
6	Rubber stopper	-$ 2.50	7	56	-$ 140.00	Stangnet, 2023
7	Quartz glass tube	-$ 22.00	10	2	-$ 44.00	Wastewater center, 2023
8	Silica bed	-$ 23.00	20	1	-$ 23.00	Fanryntech, 2023
9	Thermocouple	-$ 63.00	10	1	-$ 63.00	Home Depot, 2023

10	Tedlar bags	-$ 12.00	5	10	-$ 120.00	VWR, 2023
11	DC power supply	-$ 70.00	10	3	-$ 210.00	Bravo electro, 2023
12	Multimeter	-$ 40.00	20	1	-$ 40.00	VWR, 2023
13	Wire for DC	-$ 11.00	50	1	-$ 11.00	Edelmaninc, 2023
14	Flow meter	-$ 373.82	25	3	-$ 1121.46	Pumps and systems, 2023
15	Landfill gas	-$ 300.00		1	-$ 300.00	N/A
16	Argon gas	-$ 300.00		1	-$ 300.00	N/A
17	Hydrogen gas	-$ 300.00		1	-$ 300.00	N/A
18	AAA batteries	-$ 1.00	20	40	-$ 40.00	Energizer, 2023
19	Pyrometer	-$ 320.00	10	1	-$ 320.00	Wika, 2023
20	Heating pads	-$ 20.00	5	2	-$ 40.00	Amazon, 2023
Maintenance cost						
21	Thermocouple	-$ 51.68	10	1	-$ 51.68[*]	Home Depot, 2023
22	DC power supply	-$ 57.42	10	3	-$ 172.26[*]	Bravo electro, 2023
23	Pyrometer	-$ 262.50	10	1	-$ 262.50[*]	Wika, 2023
Operating cost						
24	Hydropower	-$0.05	20	9553.66	-$ 29.20[+]	Hydro Review, 2023
Total cost					-$ 3846.05	

Note: * sign in the table represents future value converted to present worth and [+] sign represents annual cost converted to present worth.

Total methane mass produced in 1 hour in the power reaction = 274.77 kg. Therefore, per kg methane production cost = \$ 3846.05/ 274.77 = \$13.99. 1 kg of methane can produce 53940 kJ of energy [World-neuclear.org]. The average efficiency of a turbine is 29% [U.S. EPA, 2016]. Therefore, $\frac{53940}{3600} * 29\% = 4.35$ kWh /kg CH_4. Total energy produced $= \frac{4.35\ KW-hr*274.77\ kg}{kg} =$ 1195.25 kWh Per kilowatt-hour cost $= \frac{\$\ 3846.05}{1195.25\ kW-hr} = \$\ 3.21/$ kWh.

Chapter 5
Conclusions and Recommendations

This chapter discusses conclusions of the research finding as well as recommendations for future research.

5.1 Conclusions

5.1.1 Catalyst characterization

- Field Emission Scanning Electron Microscope (FE-SEM) showed the surface topography, conductivity, particle size, and microstructure of all three samples to be visually similar to each other.

- The sieve analysis showed the particle size of the catalyst prepared using the method of Manabe (2016), catalyst prepared using the method of Yamada (2020), and used catalyst were less than 75 microns.

- Energy Dispersive Spectroscopy (EDS) showed the chemical composition of catalyst prepared in a muffle furnace and a tube furnace were the same, containing Ru, C, O_2, and Ce. In the used catalyst, 18.74 wt.% Si was detected.

5.1.2 Objective 1:

In Objective 1, seven sets of experiments were conducted. The results are listed below.

- Baseline: the highest methane fraction was recorded as 0.123 at around 20 minutes, which represented a 35% increase in methane over the initial concentration at room temperature.

- Impact of power: The methane fraction of the gas collected at 54.53 watts was the highest and accounts for a 3% increase over baseline. A linear correlation was found between power applied and methane fraction.

- Impact of heat in the presence of EF: Applied heat in the presence of the EF did not substantially improve the methane conversion compared to the baseline experiment.

- Impact of catalyst preparation method: the method of catalyst preparation did not impact the conversion substantially.

- Impact of electric field type: using a non-uniform electric field reduced the conversion compared to a uniform electric field.

- Degradation of catalyst over time: the overall conversion has a slightly decreasing trend after 40 minutes, perhaps because products fail to desorb from the catalyst, reducing the active surface area.

- Using reactivated catalyst reduces the conversion rate due likely to the presence of silica that blocks the active surface of the catalyst.

5.1.3 Objective 2

During the experiment for Objective 2, 54.53 W was applied to impose a strong electric field in the presence of 0.33 gm of catalyst evenly spread on the catalyst bed. It was found that electrocatalysis increased the methane fraction of real landfill gas by up to 43% compared to the initial inlet gas composition measured.

5.1.4 Objective 3

Life cycle environmental analysis

The overall environmental impact of the lab-scale Waseda process is -51.5 mPts and -20.4 kg CO_2-equivalents/kg of methane produced. This assumes that hydropower is used to provide electricity needed for the Waseda process, and that the methane generated is used to generate power that replaces power from the standard US grid. Using the lab-scale apparatus, this assumption is

necessary for the process to yield environmental benefits. An industrial-scale version of the equipment would have lesser environmental, and CO_2 impact per kg of methane generated, due to efficiencies of scale.

Life cycle cost analysis

- The total cost of the process was estimated to be $14.86/kg of methane.
- The cost of producing 1 kWh of electrical energy from the methane generated was estimated to be $3.42. This cost would be reduced considerably if the small lab-scale apparatus were scaled up to commercial size.

5.2 Recommendations for future research

- Determine why visual color difference occurred for the fresh catalyst prepared via the method of Manabe (2016) and that prepared via the method of Yamada (2020).
- Explore the impact of increasing the gas flow rate on the reaction rate and process cost.
- Explore the impact of the weight of the catalyst used on the conversion rate.
- Scale the process up to determine the impact on conversion efficiency, environmental impacts, and cost.
- Test the number of regeneration cycles possible for the catalyst.
- Quantify the other gases produced besides methane and CO_2.
- Test other catalysts to find one that is less expensive.
- Use other life cycle environmental software because Sustainable Minds has a limited variety of materials to choose from.

References:

Amazon. "Film Heater Plate Adhesive Pad, Icstation PI Heating Elements Film 12V 7W Strip Heater Adhesive Polyimide Heater Plate." https://www.amazon.com/dp/B07P2RJDPL/ref=sspa_dk_detail_1?pd_rd_i=B07P2RJDPL&pd_rd_w=Fo23W&content-id=amzn1.sym.f734d1a2-0bf9-4a26-ad34-2e1b969a5a75&pf_rd_p=f734d1a2-0bf9-4a26-ad34-2e1b969a5a75&pf_rd_r=G0QX6T4TJCN6WCGWG810&pd_rd_wg=yd3vO&pd_rd_r=7ea27d45-950a-45b3-8ceb-7301989c6648&s=industrial&sp_csd=d2lkZ2V0TmFtZT1zcF9kZXRhaWw&th=1, date accessed: December 2023.

Bravo Electro Components. "How to Prolong the Life of Your Power Supply?" https://www.bravoelectro.com/blog/post/how-to-prolong-the-life-of-your-power-supply, date published: April 2023, date accessed: December 2023.

Chandler, David L. MIT News Office. "A dirt-cheap solution? Common clay materials may help curb methane emissions." https://news.mit.edu/2022/dirt-cheap-solution-common-clay-materials-may-help-curb-methane-emissions, date published: January 2022, date accessed: February 2023.

Chemtalk. "What is catalyst?" https://chemistrytalk.org/catalysts-activation-energy/, date accessed: November 2023.

Edelman. "How Long Does Electrical Wiring Last?" https://www.edelmaninc.com/blog/how-long-does-electrical-wiring-last/, date accessed: December 2023.

Engineering ToolBox (2003). "Solids, Liquids and Gases - Thermal Conductivities" https://www.engineeringtoolbox.com/thermal-conductivity-d_429.html, date accessed: December 2023.

Energizer, "How long will my Energizer batteries last in their packaging?" https://www.energizer.com/about-batteries/battery-faq/lists/battery-faqs/how-long-will-my-em-energizer-em-sub-reg-sub-batteries-last-in-their-packaging#:~:text=Energizer%C2%AE%20Ultimate%20Lithium%E2%84%A2%20AA%20and%20AAA%20last%20up,for%20AA%20and%20AAA%20batteries, date accessed: December 2023.

Environment and Climate Change, Canada. "Understanding the shared socio-economic pathways (SSPs)." https://climatedata.ca/resource/understanding-shared-socio-economic-pathways-ssps/#:~:text=Meanwhile%2C%20the%20%E2%80%9C8.5%E2%80%9D%20describes,different%20levels%20of%20Radiative%20Forcing, date accessed: May 2023.

Environment-clean-generations. "Greenhouse Effect." http://environment-clean-generations.blogspot.com/2011/07/greenhouse-effect.html, date accessed: January 2023.

Fanryntech. "Life Expectancy of Glass Wool Insulation." https://www.fanryntech.com/info/life-expectancy-of-glass-wool-insulation-38641138.html, date published: September 2019, date accessed: December 2023.

Home Depot "How to replace a thermocouple?" https://www.homedepot.com/c/ah/how-to-replace-a-thermocouple/9ba683603be9fa5395fab901ced3a679, date accessed: December 2023.

Hydro Review, "Hydropower remains the lowest-cost source of electricity globally" https://www.hydroreview.com/business-finance/business/hydropower-remains-the-lowest-cost-source-of-electricity-globally/#gref, date accessed: December 2023.

Kaiterra. "Is Carbon Dioxide Harmful to People?" https://learn.kaiterra.com/en/air-academy/is-carbon-dioxide-harmful-to-people, date published: July 2019, date accessed: October 2023.

Lindsey, Rebecca; "Climate Change: Atmospheric Carbon Dioxide." publisher: climate.gov. https://www.climate.gov/news-features/understanding-climate/climate-change-atmospheric-carbon-dioxide, date published: June 2022, date accessed: February 2023.

Macrotrends. "10 Year Treasury Rate – Historical Chart." https://www.macrotrends.net/charts/interest-rates, date accessed: August 2020.

Manabe, R.; Okada, S.; Inagaki, R.; Oshima, K.; Ogo, S.; & Sekine, Y. " Surface Protonics Promotes Catalysis" Scientific Reports volume 6, Article number: 38007 date published: December 2016.

National Aeronautics and Space Administration. "What is the Greenhouse effect?" Climate Kids, https://climatekids.nasa.gov/greenhouse-effect/#:~:text=The%20greenhouse%20effect%20is%20a,a%20comfortable%20place%20to%20live, date published: March 2023, date accessed: May 2023.

Petroleum Processing. "Natural gas composition and specifications." Penn State College of Earth and Mineral Sciences, https://www.e-education.psu.edu/fsc432/content/natural-gas-composition-and-specifications, date accessed: May 2023.

Pumps & Systems. "Considerations for Choosing a Flow Meter." https://www.pumpsandsystems.com/considerations-choosing-flow-meter#:~:text=including%20flow%20meters.-,Life%20Cycle,with%20no%20possibility%20for%20maintenance, date published: September 2010, date accessed: December 2023.

Repiping Professionals. "How Long Do Copper Pipes Last?" https://www.repipenow.com/blog/how-long-do-copper-pipes-last/, date published: December 2021, date accessed: December 2023.

Science Business. "Removing methane from the atmosphere could significantly slow temperature increase." https://sciencebusiness.net/climate-news/news/removing-methane-atmosphere-could-significantly-slow-temperature-increase#:~:text=One%20method%20to%20directly%20remove,naturally%20removed%20from%20the%20atmosphere, date published: November 2021, Date accessed: February 2023.

Scientific American. Bond, Camelli; "Why capturing methane is so difficult?" https://www.scientificamerican.com/article/why-capturing-methane-is-so-difficult/#:~:text=But%20methane%20is%20200%20times,unfeasibly%20large%20amount%20of%20energy, date published: January 2023, date accessed: February 2023.

Stanford Earth Matters Magazine. "Removing methane from the atmosphere." https://earth.stanford.edu/news/removing-methane-atmosphere, date Published: September 2021, date accessed: February 2023.

Stangnet. "Rubber expansion plugs expected life span." https://stangnet.com/mustang-forums/threads/rubber-expansion-plugs-expected-lifespan.780038/, date published: May 2009, date accessed: December 2023.

Sustainable Minds. "Learn about SM Single Score results." http://www.sustainableminds.com/showroom/shared/learn-single-score.html, date accessed: December 2023.

Taras Blog "A short History of Solid Waste Management." https://taras.org/2020/10/10/a-short-history-of-solid-waste-management/, updated on: October 2020, date access: July 2022.

The Guardian. "Plastic can take hundreds of years to break down – and we keep making more." https://www.theguardian.com/commentisfree/2022/aug/08/plastics-climate-crisis-environment-pollution-kim-heacox, date published: August 2022, date accessed: December 2023.

The Institution of Engineering and Technology (IET). "Six ideas for CO_2 reuse: a pollutant or a resource." https://eandt.theiet.org/content/articles/2019/02/six-ideas-for-co2-reuse-a-pollutant-or-a-resource/, date published: February 2019; date accessed: October 2023.

U.S Energy Information Administration (EIA). "Natural gas explained: How much natural gas is left?" https://www.eia.gov/energyexplained/natural-gas/how-much-gas-is-left.php, updated: January 2022; date accessed: January 2023.

U.S. Environmental Protection Agency (US EPA). (2016). "Evaluating the Air Quality, Climate & Economic Impacts of Biogas Management Technologies." EPA 600/R-16/099, www.epa.gov/research, date: September 2016.

U.S. Environmental Protection Agency (US EPA). (2016). "Landfill methane outreach program (LMOP); Basic information about Landfill Gas." https://www.epa.gov/lmop/basic-information-about-landfill-gas, date: January 2023.

VWR. "Gas sampling bags, Tedlar." https://uk.vwr.com/store/product/20306861/null, date accessed: December 2023.

Wastewater Center. "Quartz Glass Tube." https://www.wastewatercenter.com/our-products/uv-purification/quartz-glass-tube/, date accessed: December 2023.

Wika. "Pyrometer or Surface Thermocouples: Which Is Better for Tube Wall Temperature Monitoring?" https://blog.wika.us/products/temperature-products/pyrometer-or-surface-thermocouples-which-is-better-for-tube-wall-temperature-monitoring/?doing_wp_cron=1701130957.8431379795074462890625, date accessed: December 2023.

World Bank. "Population growth: annual."

https://data.worldbank.org/indicator/SP.POP.GROW?view=bar, date accessed: January 2023.

Worldometer. "Natural gas left in the world (BOE)." https://www.worldometers.info/gas/#:~:text=The%20world%20has%20proven%20reserves,levels%20and%20excluding%20unproven%20reserves, date accessed: December 2023.

World Nuclear Association. "Heat values of various fuels." https://world-nuclear.org/information-library/facts-and-figures/heat-values-of-various-fuels.aspx, date accessed: December 2023.

Yamada, Kensei; Ogo, Shuhei; Yamano, Ryota; Higo, Takuma; and Sekine, Yasushi. "*Low-temperature Conversion of Carbon Dioxide to Methane in an Electric Field*" Waseda University, date published: January 22, 2020.

Zhang, Xiaolong; Guo, Si-Xuan; Gandionco, Karl A.; Bond, Alan M.; Zhang, Jie. "*Electrocatalytic carbon dioxide reduction: from fundamental principles to catalyst design.*" Science Direct, date published: 26 May 2020, date accessed: November 2023.

Appendix

Figure below shows the net counts, intensity ZAF value, weight %, weight % error (+/- 1 signa), normalized weight %, and atomic percentage. ZAF is a correction method in EDS that accounts for atomic number (Z) effect, absorption (A) effect, and fluorescence excitation (F) effect during elemental composition analysis through EDS.

Net Counts

	C-K	O-K	Ru-L	Ce-L
Base(2)_pt1	60	1085	1263	6822

Intensity

	C-K	O-K	Ru-L	Ce-L
Base(2)_pt1	0.015	0.271	0.316	1.706

ZAF Value

	C-K	O-K	Ru-L	Ce-L
Base(2)_pt1	1.53	1.91	1.24	1.06

Weight %

	C-K	O-K	Ru-L	Ce-L
Base(2)_pt1	0.70	7.45	7.09	84.76

Weight % Error (+/- 1 Sigma)

	C-K	O-K	Ru-L	Ce-L
Base(2)_pt1	±0.28	±0.35	±0.70	±2.15

Normalized Wt. %

	C-K	O-K	Ru-L	Ce-L
Base(2)_pt1	0.70	7.45	7.09	84.76

Atom %

	C-K	O-K	Ru-L	Ce-L
Base(2)_pt1	4.89	38.81	5.85	50.45

Figure A. 1: EDS analysis for the catalyst prepared in a tube furnace following the method of Yamada (2020).

Net Counts

	O-K	Ru-L	Ce-L
Base(7)_pt1	3373	2636	12118

Intensity

	O-K	Ru-L	Ce-L
Base(7)_pt1	0.865	0.676	3.107

ZAF Value

	O-K	Ru-L	Ce-L
Base(7)_pt1	2.29	1.32	1.11

Weight %

	O-K	Ru-L	Ce-L
Base(7)_pt1	18.64	8.80	72.55

Weight % Error (+/- 1 Sigma)

	O-K	Ru-L	Ce-L
Base(7)_pt1	±0.48	±0.60	±1.39

Normalized Wt. %

	O-K	Ru-L	Ce-L
Base(7)_pt1	18.64	8.80	72.55

Atom %

	O-K	Ru-L	Ce-L
Base(7)_pt1	65.83	4.92	29.25

Figure A. 2: EDS analysis for the catalyst prepared in a muffle furnace following the method of Manabe (2016).

Net Counts

	O-K	Si-K	Ru-L	Ce-L
Base(3)_pt1	2020	2127		1800
Base(3)_pt2	3213		4034	7172

Intensity

	O-K	Si-K	Ru-L	Ce-L
Base(3)_pt1	1.036	1.091		0.923
Base(3)_pt2	0.803		1.009	1.793

ZAF Value

	O-K	Si-K	Ru-L	Ce-L
Base(3)_pt1	1.91	1.63		1.24
Base(3)_pt2	2.35		1.24	1.14

Weight %

	O-K	Si-K	Ru-L	Ce-L
Base(3)_pt1	28.11	18.74		53.15
Base(3)_pt2	18.64		15.65	65.72

Weight % Error (+/- 1 Sigma)

	O-K	Si-K	Ru-L	Ce-L
Base(3)_pt1	±0.72	±0.54		±2.81
Base(3)_pt2	±0.53		±0.77	±1.73

Normalized Wt. %

	O-K	Si-K	Ru-L	Ce-L
Base(3)_pt1	28.11	18.74		53.15
Base(3)_pt2	18.64		15.65	65.72

Atom %

	O-K	Si-K	Ru-L	Ce-L
Base(3)_pt1	62.67	23.80		13.53
Base(3)_pt2	65.12		8.66	26.22

Figure A. 3: EDS analysis for the use catalyst

Table A.1: Experiment Component table

No.	Component	Material	Max. Temp. °F	Max. Pressure	Description	Catalog link
1	Tee fittings	Plastic	280	150 psi	Tight-Seal Moisture-Resistant Plastic Barbed Tube Fittings for Air and Water Temperature Range: -20° to 280° F Tubing: Use with firm or soft (Durometer 50A-90A) polyurethane rubber or PVC plastic Specifications Met: FDA Compliant 21 CFR 177.2470 Fittings have a single barb that creates a smooth clamping surface for extra-tight connections that minimize leaks. Made of acetal, they won't absorb water and lose strength, even in high-humidity environments.	https://www.mcmaster.com/fittings/tight-seal-moisture-resistant-plastic-barbed-tube-fittings-for-air-and-water/number-of-barbs~single/shape~tee/for-tube-id~3-16/
2.	Tube for hydrogen	TEFLON	600	160 psi @ 72° F	Semi-Flexible Compatible with Compression Tube Fittings Hard (Durometer 60D) Temperature Range: -450° to 500° F Run acids, coolant, and other harsh chemicals through this PTFE tubing over a wide range of temperatures. It has a smooth interior for unrestricted flow and easy cleaning. Tubing is semi-flexible, so it is good for gradual bends. Not for use in medical applications. PTFE tubing can be used in vacuum applications. Teflon® PTFE tubing meets UL 94 V-0 for flame retardance, so it delays the spread of flames to valuable equipment.	https://www.mcmaster.com/high-temperature-plastic-tubes/maximum-temperature~range~~-1604304526747/sterilize-with~gas/system-of-measurement~inch/od~1-4/wall-thickness~1-32/flexibility~semi-flexible/color~white/

3.	Welding Electrodes	Flux coated. E6013	Variable	60000 psi	Industrial 6013 welding sticks are used for alternating and direct current applications where the maximum tensile strength is 60,000 psi. The 6013 electrode is best used for light to medium penetration on thin or sheet metal pieces. 6013 electrodes are commonly used in manufacturing truck frame bodies, metal furniture, storage tanks, farm implementations, or where aesthetics are of grave importance.	https://www.mcmaster.com/stick-electrodes/aws-material-code~e6013/
4.	Rubber Stopper	Rubber	570 for 20 minutes	N/A	Good for electroplating, paint baking, and powder-coating applications, these plugs withstand temperatures up to 570° F for 20 minutes. All are tapered to fit a range of hole diameters.	https://www.mcmaster.com/high-temperature-plugs/
5.	Quartz Glass Tube	quartz	2000	7000 psi 1000 psi is recommended	• Color: Clear • Max. Temperature: 2000° F • Fabrication: Annealed Blistering temperatures won't melt these quartz tubes, and rapid temperature shifts won't cause them to crack. Even tougher than borosilicate, they can be used in furnaces and ovens heated up to 2000° F. These highly pure tubes are often used in laboratories because they won't leach impurities into samples or contaminate chemical reactions. Quartz tubes are optically clear and have excellent UV transmission, making them ideal for UV purification systems.	https://www.mcmaster.com/quartz-glass-tube/material~quartz-glass/
6.	Catalyst Bed	Silica	2000	N/A	• Temperature Range: 0° to 2000° F • Heat Flow Rate: 0.78 Btu @ 800° F • Density: 10 lbs./cu. ft. • Color: White	https://www.mcmaster.com/wool/material~silica-fiber/

					Commonly used in furnaces and engine compartments, these flexible silica fiber sheets resist corrosive acids. They perform best at temperatures above 1000° F.	
7.	Thermo couple	Stainless steel	500	N/A	To monitor the internal temperature of soft solids in humid conditions and harsh environments, these thermocouple probes have an armored stainless-steel cable that protects wiring from corrosion and damage.	https://www.mcmaster.com/thermocouples/probe-diameter~1-8/probe-length~12/
8.	Tedlar bag	Avail-able in the lab				
9.	Cold trap	ICE				
10.	DC power supply				Dual adjustable outputs: 0-30V and 0-3A Fixed output: 5V and 3A Input voltage: 110V Line regulation: CV <= 0.01% + 1 mV, CC <= 0.2% + 1 mA Load Regulation: CV <= 0.01% + 3mV, CC <= 0.2% + 3 mA Ripple noise: CV <= 0.5 mV RMS, CC <= 3 mA RMS Protection: constant current and short-circuit protection LCD reading accuracy: +/-1% for voltage and +/-2% for current Environment: 0-40C, relative humidity < 90% Size: 14" x 10" x 8" HY3003D Triple Output Adjustable Variable 0-30V 0-3A Lab Grade Pro DC Power Supply	

| 11 | Multim eter | N/A | K type | | Product Features:
Dual displays permit simultaneous reading of amps and volts
Measurement ranges include:
AC current to 600A
AC and DC voltage to 600V
Capacitance to 3000 µF
Resistance to 40MΩ
Frequency to 40kHz
Measures temperature with included K-type thermocouple probe
Includes micro amps measurement for testing flame sensors
Diode test quickly finds voltage drops
Continuity beeper detects opens and shorts
Autoranging feature instantly selects correct range
Hold and maximum reading functions
Thin jaws make it easier to access conductors in tight spaces
Accommodates conductors up to 25 mm (1.0") in diameter
Auto power off and low battery indication help extend battery life
Rubber, over-molded case absorbs shock | Fbeyond |
| 12. | Tube sleevin g | silicone rubber blend | 2100 | N/A | A mica and silicone rubber blend allows this sleeving to withstand temperatures up to 2100° F and creates a fire barrier around its contents. A good option for emergency patches, it can be quickly applied to hose or cable like tape. When wrapping, sleeving should overlap itself by half its width. | https://www.mcmaster.co m/tubing/performance-properties~high-temperature/high-temperature-wrap-sleeving/ |

13.	Wire for DC power supply				The male quick-action connector on these cables gives your welding set-up greater versatility by allowing quick changes.	https://www.mcmaster.com/welding-cable/
14.	Flow meter	Mathe-son 1000 both will work	Unit is SCCM		We are ordering FM 1000 series, Range 10 to 130 SCCM	https://store.mathesongas.com/fm-1000-series-high-accuracy-flowmeter-direct-read-brass/